Real-time monitoring and control of an aquaponic system to ensure sustainability

Chris Adriaan van Beukering

Dissertation submitted in fulfilment of the requirements for the degree

MASTER OF ENGINEERING: ENGINEERING: ELECTRICAL

in the

Department of Electrical, Electronic and Computer Engineering
Faculty of Engineering, Built Environment and Information Technology

at the

Central University of Technology, Free State

Supervisor: Professor Pierre Hertzog

Co-supervisor: Professor James Swart

Bloemfontein

2021

Declaration

I, Chris Adriaan van Beukering, student number __________, do hereby declare that this research project which has been submitted to the Central University of Technology Free State for the degree: Master of Engineering in Electrical Engineering, is my own independent work and complies with the code of academic integrity, as well as other relevant policies, procedures, rules, and regulations of the Central University of Technology, Free State. This project has not been submitted before by any person in fulfilment (or partial fulfilment) of the requirements for the attainment of any qualification.

CA van Beukering
June 2021

Acknowledgement

I thank my parents who instilled an unceasing curiosity in me and allowed me the leeway to explore and experiment. I cannot emphasise enough the appreciation I have for the freedom to set things on fire, take expensive machinery and equipment apart, build and break things, and restore them to functional condition. Without the motivation to explore and an accompanying exposure to a liberal view of the world, my drive to comprehend would be much curtailed. In addition, the discipline applied as consequence of many of these unwise choices instilled an appreciation of always considering the consequences of my choices and actions. I find that these qualities have shaped my growth and illuminated my future path.

I wish to convey my thanks and gratitude to my main supervisor, Professor Pierre Hertzog, for input regarding the selection of the study topic, as well as technical guidance on the subject of aquaponics. His continued counsel and support throughout the research period ensured my focus and success. I also wish to thank my co-supervisor, Professor James Swart, for his diligent and exacting attention to my progress during the review process. His attention to detail and structure and his incisive commentary was most helpful and an example to follow in my future endeavours. I have a great respect for his ability to elicit the maximum response from a few well-placed words of constructive criticism in his capacity as professional educator.

In addition, the financial contribution of the Central University of Technology towards both student fees and the physical installation of the system, and the Centre for Sustainable Smart Cities, Department of Electrical-, Electronics-, and Computer Engineering, deserves special mention.

Abstract

In recent years, climate change awareness, with resultant potential dwindling water resources and strain on existing food production infrastructure, has grown. Establishing a sound scientific basis for the creation, operation, and maintenance of alternative sustainable food production methodologies is thus essential. The ‘closed system’ nature of aquaponics promises high yield versus surface area as compared to traditional agriculture and is inherently sustainable.

Since aquaponics systems may be set up in cities and suburbs, there is potential to establish food ‘cells’ that benefit the population in the immediate area. Such benefits include fresh produce, reduced storage, pollution and transportation costs, and increased employment and food security. In a climate that features freezing winter temperatures (such as in Bloemfontein, South Africa), sustainable thermal supplementation is required to maintain the viability of aquaponics systems. Monitoring and controlling thermal supplementation in real-time is necessary to mitigate thermal losses and prevent bio-filter micro-biota mortality related to extreme cold winter temperatures and to ensure sustainability.

The dynamic interrelated nature of thermal interaction between aquaponics subsystems and the large volume of water typically present in main aquaponics reservoirs further inform the necessity of implementing such a monitoring and control system. Presenting the aquaponics system and subsystems’ thermal interaction in a conceptually simplified manner, which may be applied to other aquaponics systems and topologies, also promotes integration of aquaponics into the African agricultural paradigm. The subsystem contributions, as conceptually described via water mass-flow energy transfer, may be readily quantified by differential temperature measurement and volumetric flow determination.

Furthermore, presenting a grid-equivalent energy- purchase estimation methodology to maintain sustainability potentially motivates entrepreneurs and investors by offering investment confidence, thus further incentivising adoption of aquaponics as technology. This study was conducted during an unusually severe 2020 winter season in Bloemfontein, South Africa, and fortuitous occurrence of uncommonly closely spaced cold fronts enables challenging the hypothesis expounded in the presented

methodology. Offsetting midwinter temperature loss in the 42 kl main aquaponic reservoir, as further detailed in Annexure F, a 1.3°C temperature loss mitigation over a period of three days was realised. Employing the daily temperature recovery slope metric (as more examined in Annexure G), an average positive temperature recovery slope of 0.278°C was noted. The real-time nature of the online data as collected by the monitoring and control system additionally promotes adoption of such electronically enhanced aquaponics systems into the concept of ‘Sustainable Smart Cities’.

The method presented, utilising the concept of mass-flow energy transfer to quantify the subsystem energy contribution to the main aquaponics reservoir, is inherently scalable and may be readily incorporated for use in different aquaponics system topologies. As such, it represents a useful tool for further research in the field and compares favourably against the established epistemological approach of using a thermodynamic description, which is complex and computationally taxing, and can be difficult to realise for systems also containing a biological component.

Keywords: Aquaponics, Solar, Supplementation, Evacuated Tube Collector, Sustainability, Wi-Fi, Climate Change, Cloud Data, Smart Cities

Table of Contents

List of Figures

List of Tables

List of Abbreviations

AD	Anno Domini
AWS	Automatic Weather Station
Bi	Biot index
DC	Direct Current
ESCOM	Electricity Supply Commission (South Africa)
ETC	Evacuated Tube Collector
GHI	Global Horizontal Insolation
HTTP	Hypertext Transfer Protocol
I2C	Inter-Integrated Circuit
IO	Input/Output
IPCC	Intergovernmental Panel on Climate Change
GHI	Global Horizontal Insolation
GPRS	General Packet Radio Service
GSM	Global System for Mobile Communications
LoRa	Long Range (low power, wide-area-network radio frequency modulation scheme by Semtech)
LSB	Least-Significant Bit
MODBUS	(Modicon) Schneider data communications protocol
PC	Personal Computer
PCB	Printed Circuit Board
PV	Photo Voltaic
PVC	Polyvinyl Chloride
RTC	Real-time Clock
SCADA	Supervisory Control and Data Acquisition
SD	Secure Digital (memory card)
SPI	Serial Peripheral Interface
SSL	Secure Sockets Layer
UN	United Nations
URL	Uniform Resource Locator
USB	Universal Serial Bus
Wi-Fi	Wireless Fidelity
XBee	Brand name of Digi International radio modules
ZigBee	Zonal Intercommunication Global standard, long Battery life, Economical, Efficient (paraphrased)

Chapter 1 - Overview

1.1 Background

In recent years, public awareness of climate change along with dwindling water resources and strain on existing food production infrastructure, has grown (Stocker et al, 2018). It is becoming imperative to establish a sound scientific basis for the establishment, operation, and maintenance of *sustainable alternative food production methodologies* (Phyllis et al, 2018). The inherently sustainable ‘closed system’ nature of aquaponics promises high yield versus surface area compared to traditional agriculture.

These systems may be set up in cities and suburbs (Proksch, Ianchenko and Kotzen, 2019) resulting in the potential to establish food ‘cells’ that benefit the population in the immediate area (Chunjie Li et al, 2018). Benefits include reduced cost, pollution, and production near point-of-use (reduced delivery-, storage-, transport -and packaging costs) (Goddek et al, 2015). Local jobs generated lead to community involvement and better support and ownership of such projects. This is especially relevant considering recent unemployment statistics (Statistics South Africa, 2019).

Nomenclature referencing size varies widely with no set size boundaries for small, medium, or large systems. However, implementation seems to be universally grouped as follows (based on a cross section of various informational web pages, commercial aquaponics web pages and books):

- Small systems, for home or hobby use, commonly several hundred to about 5 kl for the main water reservoir;
- Medium systems, for commercial implementation, typically 10 kl to about 100 kl; and
- Large systems, typically covering up to several hectares of grow beds with no specific upper limit to water reservoir size.

An example of a South African business scaling up from commercial to large scale production is (Sishuba, 2019).

This type of technology is potentially disruptive, becoming a crucial part of future food security planning. However, local implementation also means that each system has unique challenges, as system layout, climate, solar radiation, water availability, and budgetary constraints are among the relevant factors. To maintain biological viability of an aquaponics system, the temperature of the fish reservoir must be maintained to the requirements of the specific fish species (a wide range of cold-water to tropical species may be catered for) and importantly, the bio-filter component should operate between 7˚C and 34˚C to ensure the sustainability of the system (Sugita, Nakamura, Shimada, 2005). Such systems require some form of monitoring and control if they are to be integrated into a Sustainable Smart City via wireless communication to the internet.

1.2 Problem Statement

In an aquaponics system where a local climate includes temperatures below freezing and/or summer temperatures higher than the optimal cultivation temperature, it is necessary to have real-time monitoring and control of such a system to mitigate the losses and ensure the sustainability of the fish stock and micro-organisms in the bio-filters. The problem is the large energy input required to control many thousands of litres of water in the main reservoir tank within an acceptable temperature range, while also maintaining bio-filter acceptable temperature and water flow required through the filter(s) and grow bed(s). Quantifying the relationships between available solar radiation, required temperatures of the subsystem components (such as the bio-filters, grow beds and main fish reservoir), and environmental aspects pertaining to thermal management, is a requisite.

The problem is further exacerbated by the interrelated nature of the ambient temperature, water flow rate within the system (and system sub-components), and varying subsystem thermal loss coefficients. A further issue is that the potentially large solar collector thermal input requires heat-exchange into the bulk system, which raises the concern that localised overheating might occur, leading to organism mortality. Thus, the problem of monitoring and controlling a medium-sized aquaponic system to ensure its biological sustainability must be addressed.

1.3 Aim and Objectives

The main aim of the research is to actively monitor and control the main aquaponics reservoir and bio-filter water temperature to prevent organism mortality, thereby ensuring sustainability. As such, the objectives are:

- Modelling the thermal coefficients of the aquaponics system and subsystems to establish criteria for the sustainable control of the system;
- Implementation of an electronic monitoring and control system to actively exchange thermal energy with the system as required;
- Continuous monitoring of the system performance via internet-enabled data; and
- Comparison of the modelled system and collected data to assess the level of sustainability.

1.4 Methodology

Figure 1 shows a block diagram of a typical aquaponics system. For clarity, the system example includes simplified thermal loops as well as the solar collector indicated. To maintain biological viability of the bio-filters, their temperature must be maintained above 7˚C, and therefore needs to be supplemented in environments where the temperature can fall to below 0˚C. This necessitates the sizing of a suitable thermal collector and quantifying the lumped thermal characteristics of the subsystems.

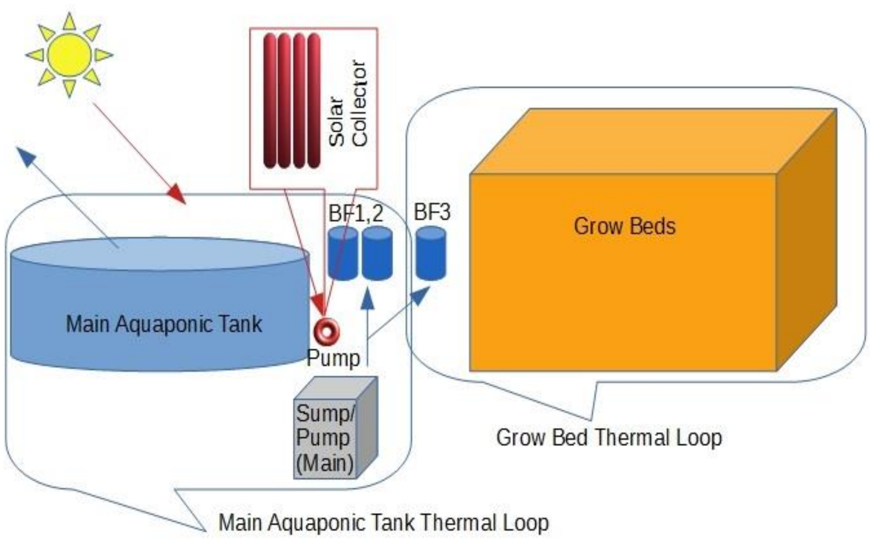

Figure 1.1: Block diagram of a typical aquaponics system

To initially model the thermal coefficients of the aquaponics system, historical temperature data from 2018 will be used in conjunction with the system main pump flow rate, and the heat capacity of the main reservoir. This will be used as a baseline for comparison of the collected data and further evaluated in the model to be compiled.

To evaluate the efficacy of thermal supplementation via evacuated tube solar collectors (and ensure viability of the biological component), an established biological system with stable interaction of the fish, micro-organisms, and plants, was identified for this research. The system is of medium size (such as might be implemented in the Bloemfontein area, in a distributed cultivation scheme) with a 42 kl main reservoir tank and multiple grow beds.

The electronic monitoring and control system must log the relevant data to a web client via Wi-Fi in real-time to enable real-time evaluation of any significant deviations in temperature. This record will be especially relevant for the winter period that runs from the middle of May to the middle of August, when critically low temperatures may be expected in Bloemfontein. The system thermal response should be slow due to the large main reservoir; therefore, temperature measurements that are logged every half-hour should be sufficient.

The monitoring and control system will be implemented to actively switch the various pumps on or off, as per identified energy supplementation demand and based on various temperature measurements within the subsystems. The collected data for the May to August period will be compared to the records of 2018 in conjunction with the simplified lumped-thermal model to evaluate the viability of the proposed solution.

1.5 Overview

To facilitate a rapid grasp of the structure of this dissertation, the chapters cover the following:

- Chapter 1 illustrates the study background, problem statement and aims of the project, and lists the proposed methodology to be implemented;
- Chapter 2 will discuss relevant literature relating to the main components of an aquaponics system, as well as the importance of determining a lumped model that can be used to describe the mathematical relationships of the system's thermal behaviour;
- Chapter 3 will present the proposed system design, including details of the lumped thermal model used, the electronic control system to be implemented, and the proposed heat exchange mechanism;
- Chapter 4 will list the results obtained from the study, presenting them in figures and tables; and

- Chapter 5 will draw conclusions and present plausible recommendations.

1.6 Delimitations

The study does not aim to provide a detailed thermal model of every system component of the aquaponic system. This has been done by Dongellini et al, 2015, Coetzee, Mwesigiye and Huan, 2017 and Sabiha et al, 2015. The study does not aim to optimise the aquaponic environment in terms of temperature, but rather to investigate the viability of implementing thermal supplementation using an Evacuated Tube Collector (ETC) to ensure sustainability. The study does not aim to present various heat exchange mechanisms as a direct-flow method is envisaged.

1.7 Summary

In this chapter, a short overview of the background pertaining to aquaponics was illustrated. The problem of sustainably maintaining a thermally viable aquaponics system in the Bloemfontein area was examined, and four research objectives were identified. The proposed methodology was briefly examined, and an overview of further chapter content provided. The study delimitations were also listed.

In Chapter 2, a literature review of the main system components (i.e. the evacuated tube solar collector system, main aquaponics subsystems, and the monitoring and control system, as well as the heat exchange mechanism) will be examined more closely. In addition, a suitable modelling method of the thermal coefficients will be investigated.

Chapter 2 - Literature Review

2.1 Introduction

In Chapter 1, the problem statement was formulated, namely the problem of monitoring and controlling a medium-sized aquaponic system to ensure its biological sustainability. A short overview of the background pertaining to aquaponics was presented and four research objectives were identified. The proposed methodology was briefly examined and an overview of further chapter content provided. The study delimitations were also listed.

In Chapter 2, the literature review will be presented, highlighting the history and evolution of aquaponics with some examples of aquaponics systems. Furthermore, the physical subsystems of an aquaponics system will be examined. Different methods of harvesting thermal energy will be investigated and a suitable lump-modelling method presented. Monitoring and control aspects pertaining to an aquaponics system will be reviewed by examining cloud storage, Wi-Fi communication, and the application of temperature sensors to quantify the dynamic thermal behaviour of the system.

2.2 History of aquaponics

There seems to be a perception that aquaponics cultivation systems are a modern invention but this is in fact not the case. The famous Hanging Gardens of Babylon (built around 600BC) are commonly believed to have been operated on hydroponic principles (the city was built on tiers, with water manually raised from the plain to the top tier and cascading down again. Nutrients in the form of manure would have been added with some plants growing in the water medium – i.e. basic hydroponics) — and may likely have included fish which would have qualified it as an aquaponics system.

In Myanmar, the Intha tribe still cultivates produce (e.g. tomatoes) on floating gardens on the Inle lake (see Figure 2.1), and the Aztec civilization farmed on floating reed 'islands' (Chinampas, see Figure 2.2) on lake Tenochtitlan, as early as the 10th or 11th century AD. Marco Polo wrote about seeing similar floating gardens in China in the late 13th century AD (although the floating raft technique in the specific region dates as far back as the 6th century AD — see Figure 2.3a, 2.3b — and included raising ducks).

Figure 2.1: Modern-day Myanmar floating aquaculture, tomatoes

Figure 2.2: Depiction of Floating Gardens (Chinampas), Aztec 10th, 11th century AD

The method also yields itself to waste treatment, as human and animal urea (urine) and faeces were used to fertilise the plant component, breaking down the wastes and utilising them for growth. Even today, it is common for Chinese people in rural areas (according to Liu et al. 2014) to gather human and animal wastes for their aquaponics fields, and water buffalo were historically kept in and around these fields to convert unwanted plant matter back into fertiliser.

Figure 2.3: a) and b) Song Dynasty woodcut – Aquaculture

In the 1620's, Sir Francis Bacon researched soil-less gardening (published in 1627, posthumously). Berkley scientists Hoagland and Arnon (1949) first published 'The water culture method for growing plants without soil' in 1938, a seminal work laying the foundation for hydroponics. During World War 2, the technique was used to grow crops for troops on barren Pacific islands. Modern aquaponics development is commonly attributed to the various research works of McMurtry, (circa late 1980s) with various others building on this basis (Love et al, 2014).

The more recent adoption and commercial implementation of aquaponics systems is largely driven by market considerations, as altering climates have led to water scarcity, growing urbanisation, and changing agricultural cultivation methods that have caused the technique to become economically viable. Climate change predictions by the IPCC as per Stocker et al., (2018) indicate that aquaponics systems will likely become widely adopted due to their much larger yield-per-hectare and per litre of water (Goddek et al., 2015). This is especially relevant in arid southern African areas such as Namibia and the Kalahari as these are areas of water scarcity and unreliable precipitation.

Such aquaponics systems additionally yield fish protein, competing with overfished and dwindling ocean resources (Stocker et al., 2018) as well as terrestrially farmed proteins. Traditional methods of protein production typically require that larger amounts of water be used, making aquaponics preferable in arid areas. Since the system is 'closed', pest control and environmental control can be easily achieved and these systems lend themselves to implementation in urban areas (including vertical farming), thus greatly reducing packaging, transport, and refrigeration costs, and promoting local food security (Tomlinson, 2017 and Chunjie Li et al., 2018). For these reasons, it can be confidently stated that aquaponics systems may potentially be adopted worldwide in the future, and the rationale of facilitating the control, management and integration into the concept of Smart Cities is clear.

2.3 Current aquaponics systems and their benefits

Aquaponics is not limited to the common perception of holding reservoirs, tunnels and grow beds as the historical examples show (arguably the 'Smart Cities' of their time). Modern implementation of floating raft and open-air type aquaculture includes rice and fish cultivation in Nigeria (see Figure 2.4). Open-air aquaculture systems like these utilise more water than tunnel/grow beds or indoor systems (due to the added evaporative losses due to sun and wind exposure) but do not require the added thermal management and potentially expensive artificial lighting of cold-climate implementations (see UNOSSC, 2018).

Nigeria spans several climatic zones, with more arid regions in the north experiencing minimum winter temperatures of typically 10˚C but potentially falling to 0˚C (daytime temperatures can also reach 40˚C during the same season), while the more southern areas experience more tropical conditions with typical day/night variation of only a few degrees. In contrast, the minimum mid-winter temperature in Bloemfontein typically falls to below 0 ˚C, while daytime temperature maximums during the same period average about 17˚C. Temperatures have been known to reach -9˚C minimum and 8˚C maximum (data collated from freemeteo.co.za, accessed Mar 2020, for the month of July from 2004 to 2016, and daily minimums and maximums determined for the 13-year period). Knowing these cold event minimum values are critical in terms of system cool-down prediction, rather than just knowing the average minimum/maximum temperature for the month (Refer to Annexure A for detailed historical temperature data for the month of June, for Bloemfontein). Aquaponics implementation in Bloemfontein would thus require thermal supplementation and could not readily be sustained in open air throughout the year as in the Nigerian example.

Figure 2.4: Nigeria - Open-air rice/fish cultivation

The world's largest aquaponic project currently located on lake Taihu in China, was implemented to clean up the lake's algal growth in the summer of 2004 due to fertiliser and waste contamination build-up and it covers over four acres (approximately 10 hectares) of floating wetlands. It was implemented as a clean-up/restoration project to re-establish water quality in the lake. Once installed, it operates at almost zero cost, as opposed to modern mechanical/filtration systems), and at the same time serves to cultivate flowers and vegetable produce commercially. Climate conditions in the area are mild, with cold but not freezing temperatures in winter. The lake covers a large area but is only 2m deep on average, and the area is heavily populated. The lake lies on a river delta with abundant water, hence the open-air implementation.

In the region of Bloemfontein, South Africa, rainfall is limited, making open-air implementation impractical as the region is classified as semi-arid and experiences high summer temperatures (and thus high evaporation of already strained water resources). The identified system for this study consists of grow beds under shade netting, and an open-air dam, which is a more suitable method considering the climate variation in Bloemfontein.

Figure 2.5a illustrates the Lake Taihu implementation, and Figure 2.5b is an example of the clean-up effect of the implemented aquaponics floating wetlands on water quality. The beaker on the left holds water with a high algae content, while the beaker on the right is notably clear.

Managing water quality, as well as minimising the effects of effluent impact on river systems, has become achievable by adopting strategies such as the floating wetland system adopted in Nanjing, China (see Figure 2.6). The western world seems to be lagging in this area of application (note the US lack of such implementation in the Great Lakes) exemplified by the toxic algal bloom in Lake Erie during 2019.

Figure 2.5: a) and b) Lake Taihu, China. World's largest aquaponics project

Figure 2.6: Nanjing, China: Floating wetlands project

Some companies are offering a containerised solution, such as the London based GrowUp (see Figure 2.7). Note the urban setting, promoting public awareness of the technology.

Figure 2.7: Containerised Aquaponics systems: GrowUp, London

Of note is the potential re-purposing of abandoned buildings, which may be readily retrofitted to aquaponics (Tomlinson, 2017), thereby serving a local urban client-base (promoting community acceptance and adoption of the method due to food security, potential local job creation and a ready supply of healthy produce. Figure 2.8 illustrates the scale of operation possible, in New Jersey, US.

In addition, due to the recycled nature of the water and nutrients, as well as significantly reduced use of fuels and heavy machinery, aquaponics has a smaller carbon-footprint than traditional agricultural methods. Aquaponics is therefore a technology that is in line with the reduction of CO2 goals as agreed on in the Paris accord, to which South Africa is a signatory. Note that such enclosed systems typically require thermal management as well as artificial lighting. This implies high setup costs, as well as running costs (as opposed to utilising natural lighting and natural temperatures).

The identified system for the study is outdoors with shade netting and an open-air dam which fluctuates with seasonal variation. Since Bloemfontein experiences sub-zero winter temperatures, thermal supplementation is required to ensure system sustainability. In addition to ensuring the goal of sustainability, optimising main reservoir temperature potentially maximises fish growth (Clarke and Johnston, 1999).

Figure 2.8: AeroFarms, New Jersey

Figure 2.9 illustrates a South African commercial aquaponics system that was implemented at Ichtys Aquaponics, Midrand, Gauteng (photo credit, Sishuba (2019)). This implementation delivers trout, tilapia, redbreast kurper, herbs, tomatoes and baby spinach to local supermarkets and restaurants.

Figure 2.9: Ichtys Aquaponics, Midrand, Gauteng

The reservoirs at Ichtys are stocked at 25 kg per 1000 litres for tilapia, and 20 kg per 1000 litres for trout. The owners stated an implementation cost of R450 / m^2 for their aquaponics system using horizontal and vertical farming techniques. This allows them to use more than 90% of the greenhouse space for growing vegetables. Note that Figure 2.9 illustrates their initial implementation before expansion and optimisation of the space.

Various benefits of aquaponics systems are noted below (Goddek et al., 2015; Stocker et al., 2014; Tomlinson, 2017; Chunjie Li et al., 2018):

- Aquatic species food input optimised (no waste, no runoff);
- Nutrient input (trace minerals) optimal due to circular nature of system water flow (no runoff);
- Minimised water wastage (closed-loop nature of system);
- Reduced carbon footprint — does not utilise tractors or heavy farm equipment;
- Simplified pest control (pertaining to enclosed systems –however, if untreated, unidentified, or identified late, such may be fatal to the system);
- Reduced fertiliser requirement — symbiotic nature of fish/plant interaction and closed system nature ensures optimal usage;
- Improved yield — plants are closer, generally larger and can be vertically cultivated — yield potentially an order of magnitude larger than traditional outdoor agricultural methods;

- More compact production compared to traditional methods — more densely planted, may be vertically stacked;
- May be used as part of a water purification system;
- Reduced energy requirement (no heavy farm equipment, localised production potential means less transport, storage and cooling required)
- Healthy and nutritious produce; and
- Readily scalable methodology

Aside from the already noted water efficiency and improved yield-per-hectare, it is important to note that the fish stock thus farmed is a valuable commercial resource and potentially competes with traditionally accepted agricultural methods to provide protein. The reduced carbon footprint and localised food security are important factors, and the ease of scalability is perhaps the most salient feature.

In addition to raising fish and vegetables, aquaponics is also suited to cultivating aquatic snails, various species of shrimp, other crustaceans, and eels. It integrates well with poultry farming (the chicken waste is highly nutritious to fish and can be added to the aquaponics system), and worms and other insects that are fed on garden and other waste (such as mulched paper) are ideal feed stock for the fish. In addition to the benefits listed above, the following considerations apply to South Africa and the Bloemfontein area in particular:

- Unemployment is rising and aquaponics implementation (in addition to much needed localised food security) creates employment. According to Statistics SA (Statistics South Africa, 2019), the Mangaung (greater Bloemfontein area) ratio of employed persons/population had already reached 42.4% in the fourth quarter 2019. These benefits are further examined by Walraven, 2014;
- Already mentioned is the production of fish proteins, but these are also a source of amino acids considered important to adolescent cognitive development (Assissi, et al., 2006). This is especially critical in impoverished rural areas (Beveridge, et al., 2013) where inhabitants often do not have the means to secure a quality nutritive diet; and
- The long-term climate forecast for the southern-African region indicates reduced seasonal rainfall and that more arid conditions will become prevalent (IPCC, 2019).

2.4 Components of an aquaponics system

An aquaponics system may be compartmentalised into:

- A biological aspect — for example the types of plant(s), fish, additives and nutrients required, and the medium in which they are cultivated;
- The physical system — the various pumps, filters, dams, reservoirs, and pipes; and
- The control system – which integrates the operation of these various aspects into a functional whole, by monitoring and controlling its' operation continuously.

Most sources provide a clear breakdown of the aquaponics cultivation methods' physical systems, with Goddek et al. (2015) perhaps being the most comprehensive.

The biological component consists of the aquatic species cultivated (typically fish species but may also include shrimp, mussels, and snails), the plant species cultivated (typically a variety of vegetables and flowers), and the bio-filter organisms. Failure (mortality) of any of these components leads to system imbalance and toxicity and could cause the entire system to fail.

The physical system may be compartmentalised as follows:

- The main aquaponics reservoir may be one or multiple containers. Typically this contains a large amount of water and the aquatic species cultivated (note that shrimp might be kept in the sediment filter instead). The reservoir constantly overflows into the sump from where it is pumped, or it overflows into the sediment filter (typically a swirl/Coriolis-type which accretes sediment in the centre of the rotating 'swirl'), from where it is pumped to the rest of the system. Figure 2.10 illustrates the sump but for purposes of illustration it may be construed as being either the sump, or the sump and sediment filter combined;

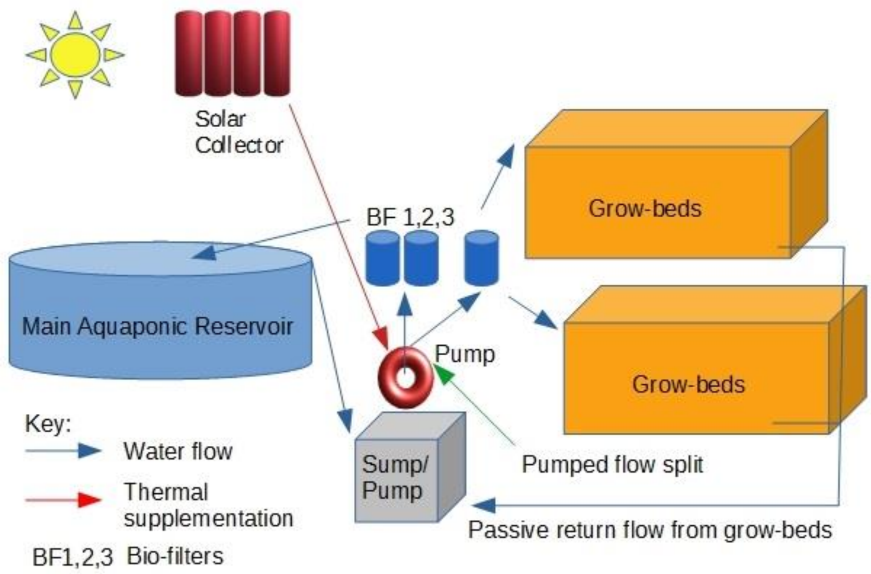

Figure 2.10: Block diagram of a typical aquaponics system, indicating water flow.

- The bio-filter(s) are supplied with pumped water from the sump. In this example there are multiple bio-filters and from here, the flow is split back into the main aquaponics reservoir and the grow bed section. The purpose of the bio-filter is to act as a medium for cultivation of the biofilm-bacteria, which convert ammonia compounds into nitrates and nitrites for use as nutrients by the plant section. It typically has a very large surface area for bio-film growth. The bio-filter requires a minimum of 7˚C to be maintained as a lower temperature may cause organism mortality, according to Sugita, Nakamura, and Shimada (2015). Not shown in Figure 2.10 is an aeration pump, which pumps air into the main reservoir (this is either an actual air pump, a Venturi-type insert into the return water flow, or the return water flow is allowed to drop into the main reservoir from a height, causing aeration via the turbulence/bubbles thus formed). This is required to ensure that sufficient dissolved oxygen is maintained for the fish to survive;
- The grow bed section consists of either horizontal or vertical grow beds, or a combination of both, with plants growing in a non-nutrient substrate and nutrients supplied by the constant water flow as pumped from the bio-filters. The plants utilise the nitrates/nitrites for growth, and the 'clean' water is returned to the main reservoir(s). The grow bed area may also be regulated for humidity in order to maximise growth. Note that the absence of fish,

bio-filters or plant populations will result in a toxic build-up within the system — the goal of aquaponics is to cultivate these various populations in balance; and

- A solar collector system is shown, supplementing either the main/bio-filter section, or the grow bed area. This requirement of thermal supplementation is only present if, during cold weather, the main water reservoir temperature falls below the temperature required for the aquatic species cultivated; -or the bio-filter temperature falls below 7˚C. Bio-filter organism mortality leads to system toxicity build-up (Goddek et al., 2015), and the organisms typically require a minimum of 7˚C (Sugita, Nakamura, and Shimada, 2005). Since the system identified for this study is in the Bloemfontein area and regularly experiences freezing winter temperatures, the requirement for such thermal supplementation in order to sustainably maintain system viability is evident. Various other thermal harvesting or supplementing methods could also be implemented and are further investigated in section 2.5. For indoor systems, the grow bed area may also require expensive artificial lighting and electricity input. It is often desirable to implement an outdoor system where possible to realise the trade-off between free (or cheap) solar energy vs. electricity costs (and capital expenditure for initial implementation).

As noted in section 2.3, aquaponics systems may also be terrestrial and open-air or floating water-borne systems. However, these systems are typically not thermally regulated, and utilise species and methodology suitable to their climate and environment. They are thus not suited for the research topic and are not discussed further. It should be stated, however, that the potential for water quality treatment in this fashion has been largely overlooked (the previously mentioned untreated Lake Erie algal blooms refer).

A system requiring thermal supplementation has been selected for the study, which aims to investigate the viability of such energy supplementation to prevent organism mortality in especially the bio-filters.

The control system may be as simple or complex as the requirements: a simple system might have no ‘control’ features as such but would implement the pumps and filters and be manually monitored for temperature and toxic build-up on an ad-hoc basis. This is more suited to the hobby user and typically applies to small systems that are easily monitored. More complex systems might monitor (and/or control) criteria such as temperatures and flow rates, air temperature and humidity, solar insolation, wind speed, water chemical stability (nitrite/nitrate levels, dissolved oxygen, water acidity, etc.) and fish feed rates, as well as temperature, humidity, and air flow in the grow bed section(s).

2.5 Thermal energy supplementation source

Aquaponics systems typically require both electrical (e.g., continuous water pumping) and thermal (water heating in wintertime) energy input. The temperature requirements may be met by electrical heating, but it often proves to be non-viable financially as the costs inflate the produce price. It is thus desirable to investigate various methods of supplementing the thermal requirement.

Karimanzira and Rauschenbach (2018) performed a comprehensive study that lists and investigates several alternatives, including photovoltaic and solar thermal modules, wind turbines, hydropower, biomass converters, heat pumps, gas boilers, and interfacing to the electrical grid. They investigated the cost-effective implementation of using these systems in conjunction with the electrical grid and presented a method for determining the least-cost alternatives.

They also highlighted the main problem that faces the use of alternative energy harvesting methods, namely the issue of energy storage. This is particularly problematic when implementing PV or wind-energy harvesting, as the energy demand is predictable, but the energy available for harvesting fluctuates with weather conditions. They highlighted the use of solar and wind energy due to its non-polluting nature and relatively low maintenance. Figure 2.11, reproduced from Karimanzira and Rauschenbach (2018), illustrates the various energy sources considered.

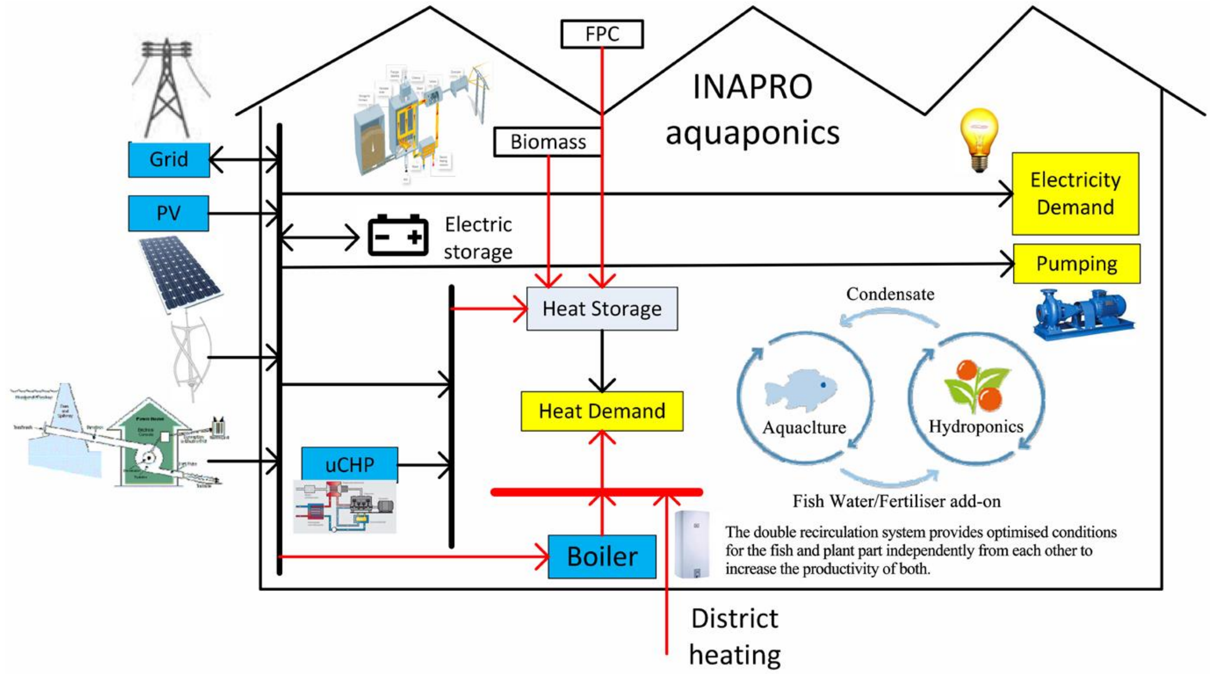

Figure 2.11: Hybrid energy illustration, reproduced from Karimanzira and Rauschenbach (2018).

The problem statement of this study relates to evaluating the viability of thermally supplementing an aquaponics system to prevent organism mortality, in the Bloemfontein area, due to extreme cold winter temperature events (see also section 3.2 and Annexure A). Rising electricity costs and increasingly unreliable grid-supplied electricity (evinced by load-shedding in South Africa) dictate the adoption of either solar- or wind energy harvesting (gas being rejected as a polluting source, and not aligned with carbon emission goals). Additionally, the requirement for the evaluation of thermal supplementation indicates the use of solar thermal collection. Biomass reactors would be a viable option in an agricultural setting, however, the study site is located in an urban environment where readily available reactive biomass (manure, plant residues, etc.) is limited. Supplementation using wind-derived energy, which by nature tends to be sporadic and unpredictable, is unsuitable to this application, in this location.

This, then, leads to the choice of a solar thermal collector, of which the solar evacuated tube system is a proven solution with high yield and desirable characteristics such as relatively low collector-to-ambient loss, efficiency over a wide angle of incidence and a predictable, stable energy input taking into consideration weather conditions and solar insolation. The study by Coetzee, Mwesigye and Huan (2017) under Southern African conditions provided quantification of the expected yield of an evacuated solar collector system, including the desired mounting angle for maximum harvesting output during winter. The period was identified using historical data as the critical time during which the bio-filters could experience sub-minimum temperatures leading to organism mortality. Their study at Pretoria, South Africa, latitude) found solar insolation to be relatively low during June, with only about 5 hours of the day yielding 400 W/m^2 or more. Note that for the period experiencing winter minimum temperatures, the study indicates a mounting angle of around 40 degrees for the ETC. This contrasts with the accepted norm for year-round best energy average of around 30 degrees.

The thermal energy harvested will be exchanged into the main reservoir or main water flow, based on demand as dictated by weather conditions and monitored by an electronic control system. Chapter 3 details this system implementing direct energy exchange and no energy storage.

2.6 Modelling

Thermal modelling is a complex science, especially of an interactive aquaponics system also containing various biological components with active thermal interaction such as solar irradiation, evaporative effects, ground and ambient cooling (and heating) of the various sub-components, and the effects of metabolic processes of these various biological components (Cannon, 2014). Typically, thermal modelling consists of a ‘ground-up’ approach which dictates individually considering the thermal input acting on each system component (and potentially, its own thermal contribution), the dynamic effects and interchange of energy incident on it, and its exchange/contribution to the system/subsequent components, in the thermal equation (Close, Frederick and Newell, 2002). This needs to be repeated for each individual component, and the many interactions thus evaluated must be quantified and summed.

This study aims to evaluate the viability of thermally supplementing the aquaponics system to maintain viability, and therefore thermal exchange will be considered as a subsystem-based variable, i.e. the model will consist of a lumped-model evaluation of the active aquaponics system energy interaction, which may be considered a ‘top-down’ approach. Close, Frederick and Newell (2002) suggest suitable methods, and the lumped system can therefore be considered as a dynamic thermal interaction of the main component subsystems. These have been identified in section 2.4, but to recap: These subsystems are the main reservoir (which represents the bulk of the thermal mass), the sump/pump (which may also include the pump heat energy as direct contribution if the pump is the submersible type), the bio-filter(s), the grow beds (which represent a more ‘active’ exchange to ambient due to the large flow component and exposed nature of the build) and any thermal supplementation, such as the evacuated solar collectors.

The lumped model needs to consider the dynamic contribution of the system components based on the thermal mass and the energy exchanged for any given time interval. The initial model is compiled and presented in Chapter 3. This simplified dynamic lumped-model approach should yield valid results to assess data gathered and reach a valid conclusion as to evaluating the ETC thermal supplementation implementation, in accordance with the goal of preventing organism mortality that also requires some form of monitoring.

2.7 Monitoring and Control

Aquaponics is by nature a dynamic agricultural method with constantly changing criteria such as water flow, temperatures, concentrations of dissolved nutrients and gasses, and varying requirements for the plant and fish component (i.e. food, sunlight, water quality and temperature). It is necessary to monitor many of these factors to ensure sustainability. An automated monitoring system is thus required as it vastly reduces the burden of physical checks and bookkeeping. Various options exist to interface a client remotely with a system (and system parameters), including:

- Direct-cable-connected data transmission (such as serial RS232/RS485 to a PC monitor);
- Industrial-type control systems such as a MODBUS or SCADA system (Odema, et al., 2017);
- GSM/GPRS systems (such as noted by Nagayo, et al., 2017), and
- Radio links such as
    - Wi-Fi (as illustrated by Vernandhes et al., 2017);
    - ZigBee and XBee (as informed by Dasig, 2019);
    - Bluetooth (Kjellby, et al., 2019) ; and
    - LoRa (as illustrated by Allbright-Borden, Wang, and Thomson, 2019).

Client requirements and specific site implementation would dictate the applicable choice of communication device and stratagem. The site under investigation has an existing Wi-Fi node available. A suitable example of this implementation (specific to an aquaponic system) was used by Vernandhes et al., (2017). The requirement is also to have data available on the internet. This, and the relatively short communication distance required on site, make it the correct choice for this particular implementation.

To evaluate system performance, the various system measurements need to be logged to a web-client via Wi-Fi and be available in real-time for monitoring purposes. The electronic control system (described in Chapter 3) must measure the various system temperatures and the pump/heat exchange status and should send this data via a site-installed Wi-Fi access point to the web client. Control of the pumps reside in the embedded system rather than through web-based communication (which might be interrupted, potentially resulting in organism mortality).

Cloud storage options are many and varied and some basic options are listed here along with typical selection criteria of relevance identified for the purpose of this study, namely: difficulty of implementation, cost, encrypted transit/storage, and two-step verification. The survey by Alamri et al., (2013) highlights some of the aspects considered.

Numerous options are available for online data storage, or ‘cloud’ storage (referring to the online ‘cloud’ of distributed services), with varying degrees of ease-of-implementation. Some services are suited to storage of files, some are suited to dynamic data (or both, such as Google Drive as implemented in Google Sheets). Table 2.1 lists a small selection of the many options available, and the criteria by which a suitable service was selected.

For instance, Dropbox, a well-known utility service, is well-suited to storing files. Other services expand on the functionality of file storage service by offering additional capability — Google Drive arguably being the most comprehensive and well known. It notably includes the support for online spread-sheet data, which may be accessed by a secure connection data exchange using SSL (Secure Sockets Layer). Most importantly, Google Drive makes these services available for free to all clients, subject to a data storage capacity limit (but a paid option to extend the size is available).

Table 2.1: Some cloud storage service options

Service vendor	Dropbox	Google Drive (Google documents)	OneDrive	Tresorit
Difficulty of implementation	Medium – not ideally suited to dynamic data	Low – Data may be readily dynamically added to various document types	Medium – not ideally suited to dynamic data	Medium – not ideally suited to dynamic data
Cost	*Free	*Free	*Free	Cost varies. Business orientated
Encrypted transit/storage available	Yes	Yes	Yes	Yes
Two-step verification available	Yes	Yes	Yes	Yes

* Size limitations are usually the determining criteria for costs

The reason for selecting Google Documents as the cloud storage medium of choice is readily apparent – the service is free (assuming maximum storage limit is not exceeded). Google also has an excellent record of reliability, as Izraelevski and Bell (2018) state. As a relevant example, a blog post (by a software engineer Olga Belomestnykh, posted in April 2010 and stored in Google Drive itself) was found during the literature review process, discussing the various new Google Documents features Google had just implemented (Belomestnykh, 2010). Google Documents being fairly new at the time (an outgrowth of a 2009 initiative), it is relevant that the post is still available on Google Drive ten years later.

Google access is ubiquitous, wherever internet connectivity is present. Data will thus be readily available, data retention is indefinite, and the available data set storage size is large (at time of writing, June 2020, Google allocates 15 GB of free space per account). Figure 2.12 illustrates the proposed data collection, control, and communication to be implemented as a functional block diagram.

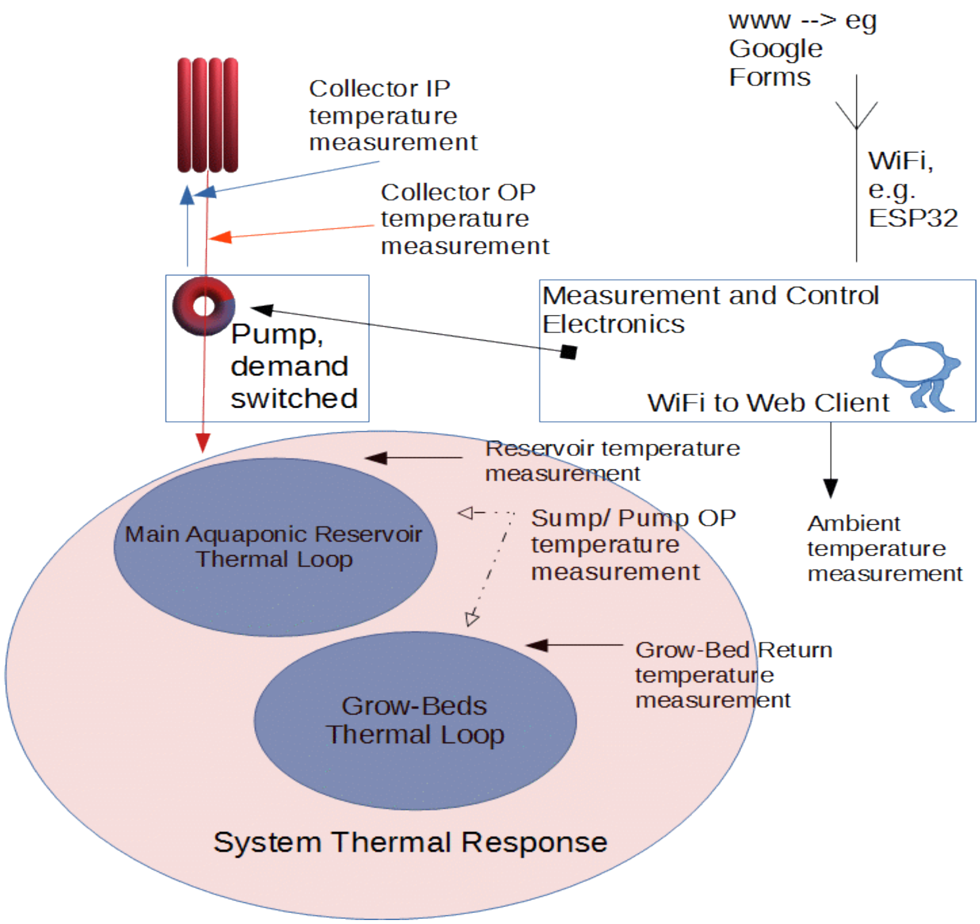

Figure 2.12: Functional block diagram of system interaction.

The data set needs to allow real-time monitoring and control of the system, as well as evaluation of the implementation corresponding with research goals as stated in Chapter 1. Further details of the system are provided in Chapter 3.

2.8 Chapter summary

In this chapter, a short overview of the history and evolution of aquaponics systems were presented. Several current aquaponics installations were listed, and the distinction between open-air and enclosed systems visually illustrated. The basic structure of an aquaponics system was reviewed, and the various subsystems identified and listed. Some thermal collection methods were reviewed and the choice of evacuated tube solar collector system relevant to this study was justified. The modelling approach to be adopted was briefly highlighted, and the monitoring and control aspect, along with data collection and storage, was introduced.

In Chapter 3, the physical control system to be implemented will be detailed, including details of the evacuated solar tube collector system, pumps, and heat-exchange methodology. The modelling method will be further examined and a suitable lumped model presented.

Chapter 3 – Design and methodology

3.1 Introduction

Chapter 2 reviewed the history and evolution of aquaponics systems, listing some examples and presenting distinguishing characteristics visually. The basic structure of an aquaponics system and the various subsystems were identified and listed and thermal collection methods examined. The choice of evacuated tube solar collector system relevant to this study was justified. The modelling approach to be adopted was briefly highlighted, and the monitoring and control aspect, along with data collection and storage, was introduced.

In Chapter 3 the physical system under study will be detailed, including details of the evacuated solar tube collector system, pumps, and heat-exchange methodology. The modelling method will be further examined and a suitable lumped model presented. The monitoring and control system will also be detailed.

3.2 Aquaponics system under investigation

As seen from Chapters 1 and 2, a generic aquaponics system has several functional components, namely the main aquaponic reservoir, the bio-filter(s), the sump, the grow beds, and the circulation system (such as pumps, channels, pipes, valves, filters, and so on). The system may include a control system for these various components. Figure 3.1 illustrates the additional system components required to evaluate the feasibility of thermally supplementing a physical aquaponic system under study, to ensure viability. Indicated are the evacuated tube collector (ETC) panels, a circulation pump, and the various measurement points deemed important, as warm water flow returns into the main aquaponic reservoir.

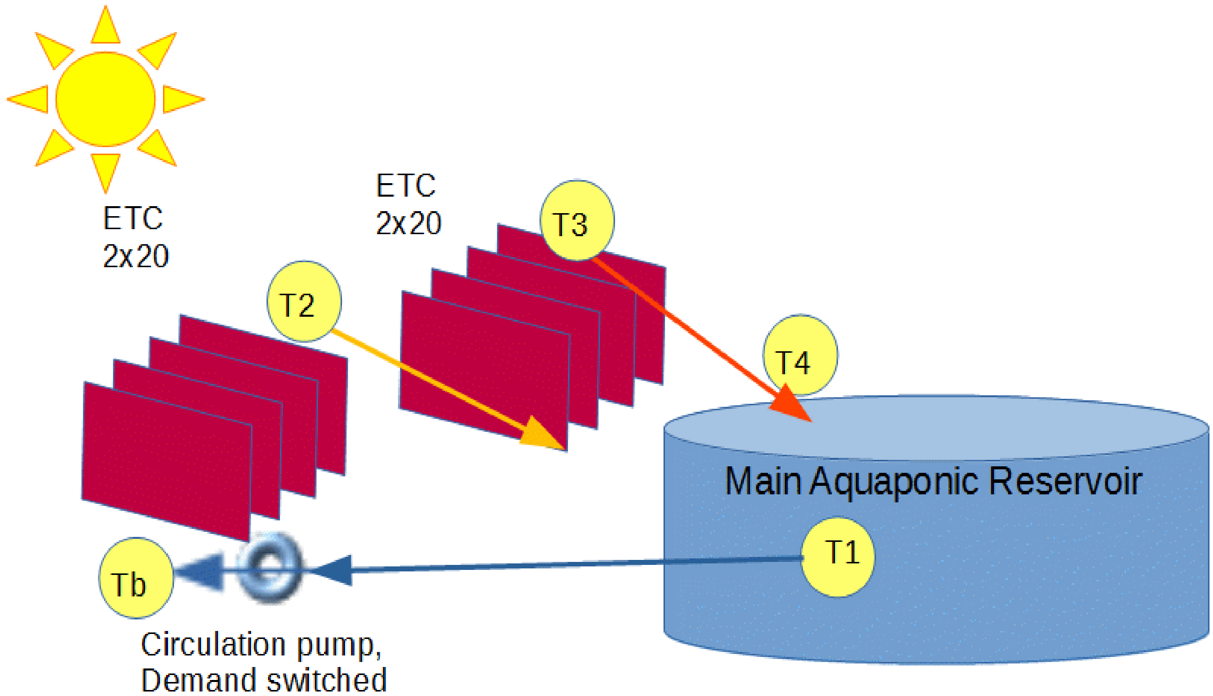

Figure 3.1: Additional equipment installed to realise study goals

3.2.1 Evacuated solar thermal collector determination

As mentioned in Chapter 2, evacuated-tube thermal collectors (ETC) possess attributes making them a desirable choice for implementation as part of a thermal supplementation system. Some of these attributes include:

- Low tube-to-ambient thermal loss;
- Tolerance of non-north facing orientation due to tubular construction;
- Efficient over a wide angle of incidence;
- Stable and predictable energy input for given solar insolation;
- No operating costs, except a small circulation pump; and
- Maintenance-free or low maintenance.

To maintain a cost-effective and efficient implementation, the thermal supplementation utilising an ETC must be designed to suit the specific application. As such, the following steps were considered:

- Step 1: Evaluation of historical data logs taken at the site during winter 2019 and determination of a suitable temperature buffer considering historical weather conditions in Bloemfontein, in conjunction with system thermal losses. Establishing such a buffer would mitigate temperature loss and the resultant danger of exceeding the 7˚C bio-filter minimum temperature, as examined in Chapter 2;
- Step 2: Determination of the pre-existing equivalent active system (i.e. as implemented and already operational) thermal capacitance with some initial assumptions; and
- Step 3: Compilation and evaluation of historical weather data for the month of June to determine the frequency of occurrence of extreme weather sequences (see Annexure A). Note that this data is a historical listing for the Bloemfontein area, and not to be confused with the 2019 site actual data log, as utilised in Step 1.

Step 1: Evaluation of the site data logs as captured in 2019 indicated that the system temperature changes vary daily and consistently within 0.5˚C (and mostly less), with some exceptions. Figures 3.2 and 3.3 graphically illustrate the available data set. It is important to note that this was evaluated as an active system, i.e. the positive or negative contributions of the bio-filter and grow bed subsystems as described in Chapter 2 are conceptually identified as part of the main aquaponics reservoir for initial evaluation purposes. This assumption was justified based on the much larger physical capacity of the main aquaponics reservoir, as compared to these flow components (as well as any holding tanks and the sump) tidal volumetric capacity.

Figure 3.2 graphically represents the available data logged on site during 2019. The red arrow indicates the key value, namely the maximum negative temperature gradient of the measured dam temperature. Note that the 2019 winter season had slightly higher than average temperatures. The normal winter overnight minimum temperatures are about 2-3˚C lower than one might infer by inspection of the graphical data represented in Figure 3.2, as Annexure A further informs.

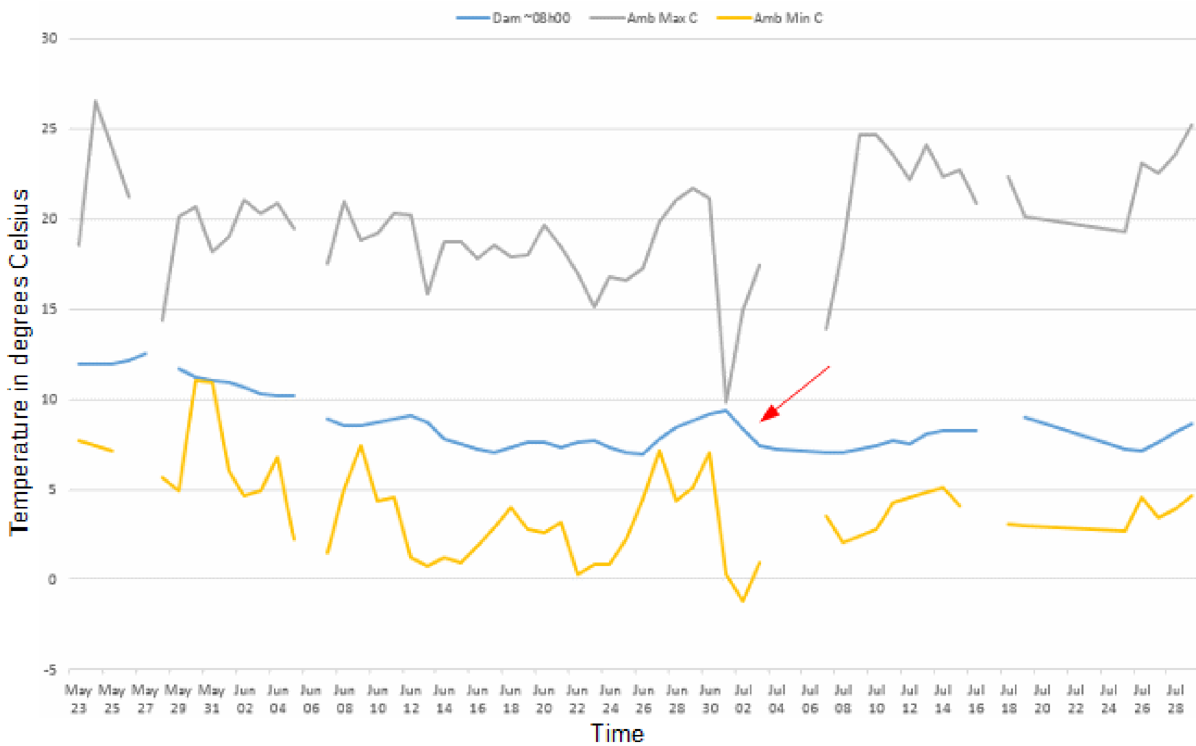

Figure 3.2: Historical site data, period 24 May 2019 to 28 July 2019

The dam data is separately represented in Figure 3.3, clearly illustrating the relevant temperature points. The gradient of interest is represented by the Celsius temperature value of 9.38˚C minus 7.44˚C over two days, or 0.97˚C per day. Note that these dates are close to the winter solstice, the time of critical interest, as potential solar ETC supplementation will thus be at a minimum also. This datum point is serendipitous as the daily maximum fell to about 10˚C and the daily minimum to 0˚C (and -2˚C the following night as shown in Figure 3.2), establishing a viable baseline for expected system temperature loss during such conditions. The buffer estimation of 3˚C is arrived at by using the figure of maximum decrease in dam temperature of 0.97˚C per day, and assuming that similar conditions (but with cloud cover and thus minimal solar ETC supplementation available) persist for no longer than three consecutive days. The goal is thus to establish this 3˚C buffer during average winter conditions to offset losses during the sporadic temperature extremes that may be experienced.

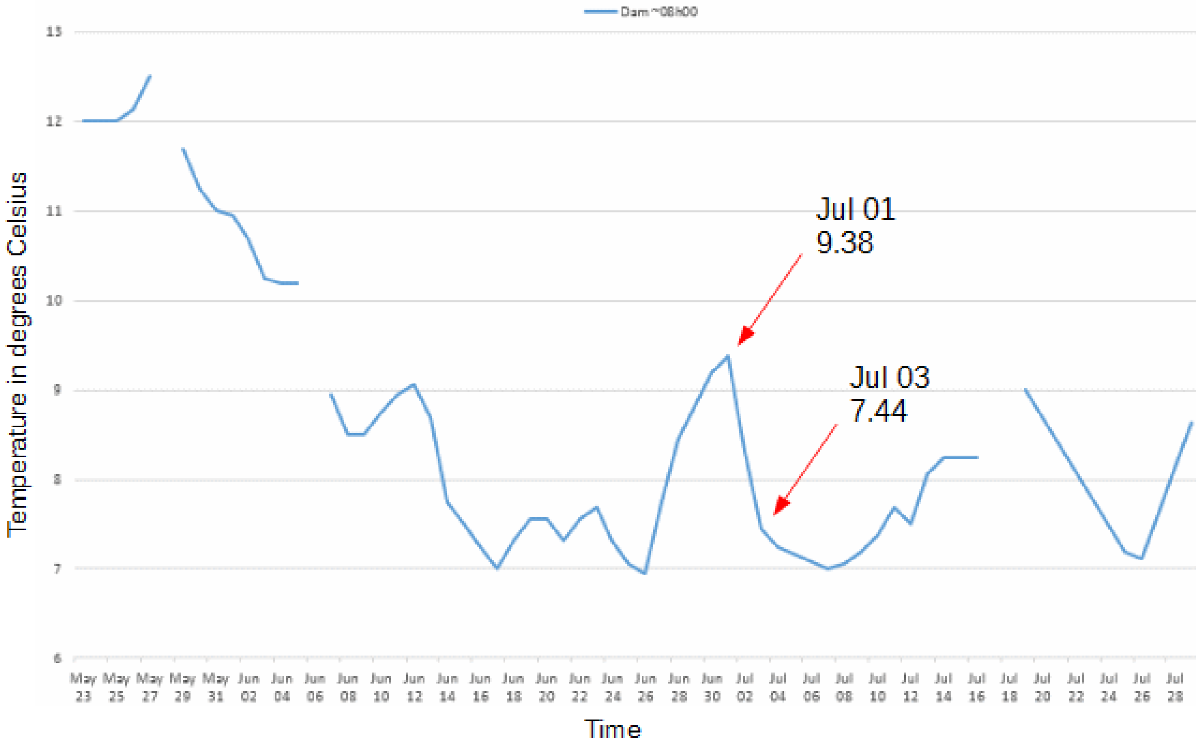

Figure 3.3: Historical site data, dam temperature variation, 2019 log data.

The daily supplementation minimum required (i.e. on 21/22 June, the date of the southern hemisphere winter solstice in Bloemfontein which is at ≈29˚ South latitude) assuming maximal insolation was determined to be ≈0.5˚C. This estimation is arrived at by examining the average temperature loss ≈0.25˚C (taken around the critical 7˚C bio-filter minimum temperature value) and establishing a daily positive recovery slope (i.e. the 0.25˚C difference between the estimated 0.5˚C ETC supplementation requirement and the ≈0.25˚C loss slope). This approach would allow for about a one-week requirement for the system temperature buffer to recover following any adverse extreme weather sequence, i.e. it is assumed there is at least one week of average weather following any extreme weather event.

Step 2: To determine the ETC output requirement (as acting on the main aquaponic reservoir as thermal storage in conjunction with the specific heat of water), the required main reservoir degree rise in Centigrade and water volume to be heated were calculated. The minimum potential harvesting of solar energy occurs during a winter solstice when the sun's angle of incidence is at its lowest (illustrated by the Coetzee, Mwesigye and Huan study, 2017). The ETC size determination was arrived at as outlined next.

The thermal coefficient of water (and hence the energy gain or loss required to heat or cool any given amount) is ≈4.184 $J.g^{-1}.K^{-1}$ as indicated by Close, Frederick and Newell (2002). The power required to heat any given water mass, therefore, is the water thermal coefficient multiplied by its mass and temperature rise required, divided by the time over which the energy input is applied:

$$P = (K * T * M)/t \qquad (1)$$

Where:

P = the power required in kWh

K = water thermal coefficient, in $J.g^{-1}.K^{-1}$

T = the required temperature increase in degrees Kelvin or Celsius, K or C

M = water mass, in g

t = the time over which the energy is applied, in s

Over a 1-hour period, heating a 42 000-litre water tank by 1˚C, therefore requires:

P = (4.184 $J.g^{-1}.K^{-1}$) x (1ºC) x (42 000 kg) / (3600 s)

= 48,813 kWh

Note that the above assumes no other system thermal losses during this period. It thus represents a method for estimation of the total additional thermal gain required by the system when other thermal changes over the period have been accounted for. Similarly, the loss of energy from the active, un-supplemented system can be calculated (as for instance illustrated by a system temperature loss of 0.5˚C), using equation (1), thus:

Power loss = (4.184 $J.g^{-1}.K^{-1}$) x (0.5˚C) x (42 000 kg) / (3600 s)

≈ 24,406… kWh

Where T, as in equation (1), represents a day-on-day pre-existing system temperature change as may be similarly calculated for every day. As noted, Figures 3.2 and 3.3 graphically illustrate the thermal variation of the active aquaponic system (as per the historical data gathered at the site in 2019). Of relevance is the system temperature trend following the ambient average temperature trend, and the magnitude of the system day-on-day changes, typically a third of a degree Celsius or less, with sharper peaks during more acute ambient temperature variation for the period. The identified solar collector energy requirement is thus to lift the main aquaponic reservoir to around 10˚C (representing the identified temperature buffer) and maintain the bio-filter minimum temperature (this is 7˚C as outlined in Chapter 2) to prevent organism mortality.

As outlined above, the estimated thermal input needs to account for about a three-day buffer supplemented by solar harvesting to maintain viability. The South African study by Coetzee *et al.*, (2017) indicated that a 33-tube x 1.6 m collector averages about 13.2 kWh per day during the winter solstice, i.e. each tube thus potentially produces 400 Wh per day. Their study latitude (-25.75˚ (NASA GISS)) indicates an average insolation of 241.45 W.m^2 for June, while the corresponding average insolation for Bloemfontein is 219.76 W.m^2. This represents a ~9% relative decrease in terms of available insolation at the Bloemfontein study site which enables a baseline comparison for calculating the minimum required ETC output, ETC_{min}. Assuming a 24.4 kWh total requirement with 400 Wh per day per tube and a factor of 91% (accounting for the 9% relative decrease) yields the following result:

$$ETC_{min} = \frac{24400}{400*0.91} = 67\ tubes\ minimum \qquad (2)$$

However, this allows no margin for sub-optimal thermal harvesting and assumes 100% sunny weather. The tubes are locally commercially available in sets of 20, supplied with a frame, and thus the minimum required installed tube amount is 80 tubes. An ETC capacity of 80 x 1.6 m tubes thus equals (13.2 kWh / 33 tubes x 80 tubes) or 32 kWh under optimal harvesting conditions. Rearranging equation (1):

$$P.t/(K * M) = T \tag{3}$$

- yields: 32 kWh x 3600 s / 4.184 J.g^{-1}.K^{-1} / 42000 kg = 0.655…˚C

This represents the optimal thermal supplementation at the winter solstice, achievable by the 80-tube setup. This was deemed adequate, as the figure allows for sub-optimal harvesting losses including mounting considerations, site layout and potential occlusion by surrounding trees (see Figure 3.6), when compared to the figure of 0.5˚C minimum thermal supplementation arrived at as per Step 1.

Step 3: To appraise the incidence of extreme weather sequence events (see Annexure A, also note the sequential 3-day critical daily minimum chosen as -3˚C and critical daily maximum chosen as 15˚C), and thus evaluate the reliability of the system maintaining the minimum temperature, yearly historical data was compiled for the month of June. Assuming the 3˚C temperature buffer was established, it would nominally require three or more days of sequential extreme temperature (see criteria chosen above) to lose the buffer, typically associated with much reduced insolation, i.e. much reduced ETC supplementation potential.

The 'perfect storm' of such extreme weather does not occur frequently, thus mitigation options will be addressed separately in a later chapter. The determination of an installed ETC at 32 kWh daily (optimally, during the winter solstice) is thus judged to be adequate, considering the reasoning as outlined in Steps 1 and 2 above. Summarising the calculations and justification provided in steps 1 and 2:

- Potential optimal winter solstice supplementation = 32 kWh;
- 32 kWh x 3600s / 42 000 kg / 4.184J.g^{-1}.K^{-1} ≈ 0.65… ˚C as per Step 2; and
- (0.65˚C / 0.5˚C) = 1.3 potential harvesting ratio above absolute requirement as per Step 1.

These values compare quite favourably with the historical data collected during 2019 and will be further examined in Chapter 4. The considerations for non-optimal harvesting are outlined below.3.2.2 ETC physical description.

The ETC consists of four banks of 20 evacuated tubes, arranged as two sets per mounting frame. They are mounted at an orientation angle of ~20˚NW and at a ~30˚ inclination which is the optimal average for year-round harvesting of energy, at the study site location, as the study by Hertzog and Swart (2018) details. Note that the optimal angle for the period during which critically low temperatures occur in winter in the Bloemfontein area, as indicated in the study by Coetzee, Mwesigye and Huan (2017) and outlined in the literature review, would be around 39˚. The actual mounting angle energy output difference during the critical period is about 6-7%. Note that the northwest-offset mounting direction has minimal effect on the ETC efficiency as the ETC tubes are by design tolerant of this (by virtue of their tubular construction). Figure 3.4 illustrates the mounting method for the two ETC banks. Note the mounting angle indicated.

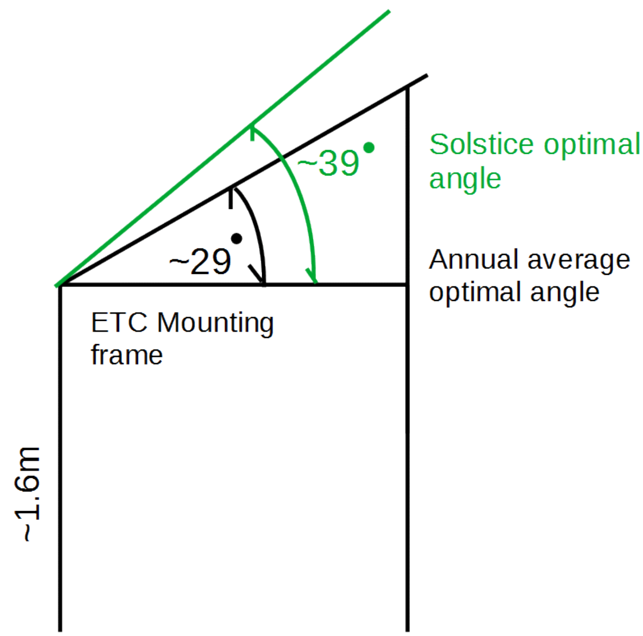

Figure 3.4: ETC mounting frame illustration, indicating winter solstice optimal angle and year-average optimal angle, at the site location in Bloemfontein

Figure 3.5 illustrates the expected June ETC inclination angle energy harvesting difference, reproduced from Coetzee, Mwesigye and Huan (2017). From visual inspection, the approximately 6-7% yield reduction between the solstice optimal angle and year-round optimal angle is apparent. The figure illustrates the various rates of useful heat (i.e. the energy in Watt), Q'u_xx, as plotted for the various mounting angles examined (xx representing 25˚, 30˚, 35˚ and 40˚ inclination for the ETC system). To_xx in the figure similarly represents the outlet temperatures at the various inclination angles. The coloured ovals and arrows in Figure 3.5 indicate the applicable criteria for 30˚ vs. 40˚ mounting angle yield.

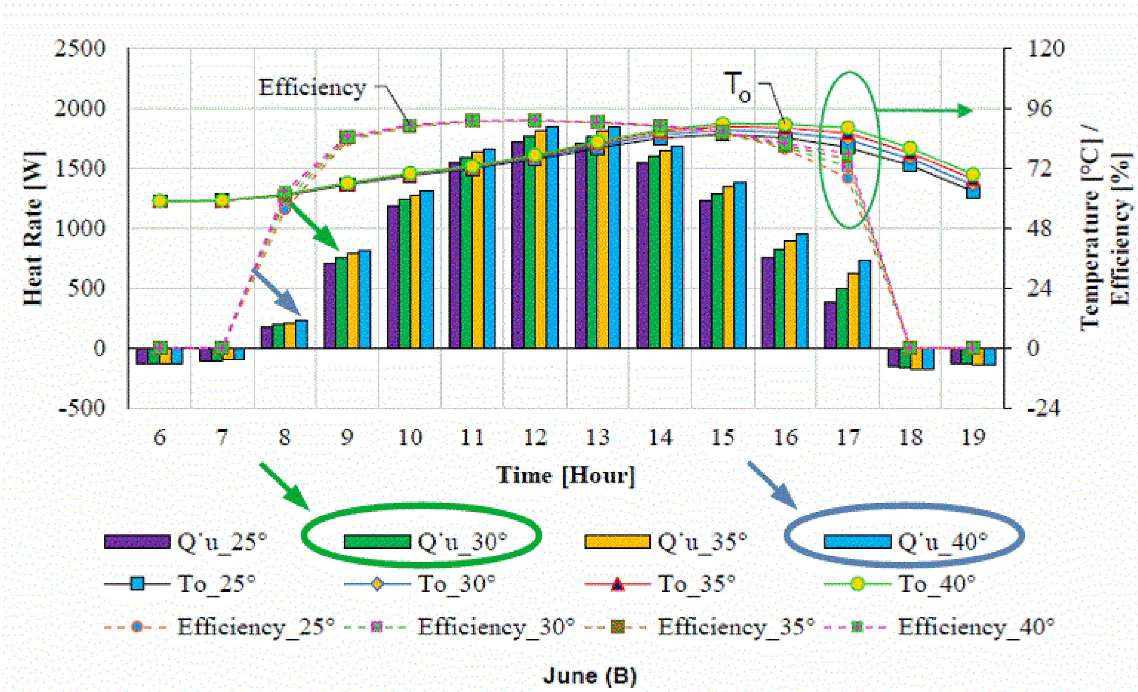

Figure 3.5: ETC mounting angle energy harvesting difference, June. Reproduced from Coetzee, Mwesigye and Huan (2017).

The site layout was constrained by the pre-existing aquaponics system, required insolation and surrounding environment. Neighbouring trees (see Figure 3.6) partially occlude the northern ETC bank (N ETC) in the early mornings and the southern ETC bank (S ETC) in the late afternoons (during the winter solstice, when the sun is lowest above the horizon). Observations made on 19 June (winter solstice is 21/22 June in Bloemfontein) indicate that the S ETC is fully illuminated at 09h02, while the N ETC is fully shaded (the orange arrow indicates full sun and the blue arrow indicates occlusion or fully shaded). The N ETC receives 50% at 09H25, rising to 100% in approximately 20 minutes.

In a similar fashion, as the sun sets along the solar arc indicated on the right in Figure 3.6, the ETC panels are occluded by the taller tree to the North-West. This occurs first for the S ETC followed by the N ETC about 25 minutes later. The occlusion by neighbouring trees, as well as the inclination mounting angle, inform the maximum achievable winter solstice daily ETC harvesting capability for the site.

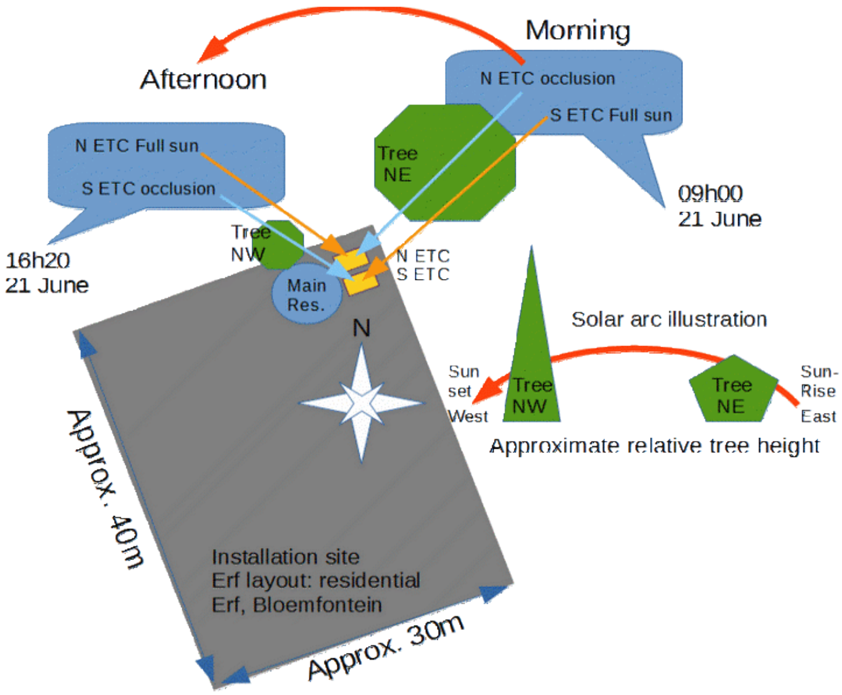

Figure 3.6: Site layout illustrating occlusion of ETC panels by neighbouring trees. Note the solar arc illustration and relative tree height as depicted on the right.

Figures 3.7a and 3.7b illustrate the ETC installed, in two sections of two panels each. The early morning shade occlusion is evident in Fig 3.7a, a well as the frost (ice) present on the ETC.

Figure 3.7: a) and b) ETC panels. Note main reservoir in rear, right, Fig 3.7b.

Connections were made using 22mm PEX (cross-linked polyethylene) piping, connecting to the 1' fittings of the ETC panels. The circulation pump is mounted in an enclosure below the N ETC. Note that the system is not under pressure if the pump is not running and may freely vent positively to the dam return point or drain via fitted vacuum-breaker attachments. There is no danger of over-pressure and at system shut-off, the residual water in the pipes immediately drains to equalised levels due to the vacuum breakers attached to the high ends of each ETC panel. Figures 3.8a and 3.8b illustrate the ETC hot-end sensor-mount method, showing the construction of the removable temperature sensor mounts.

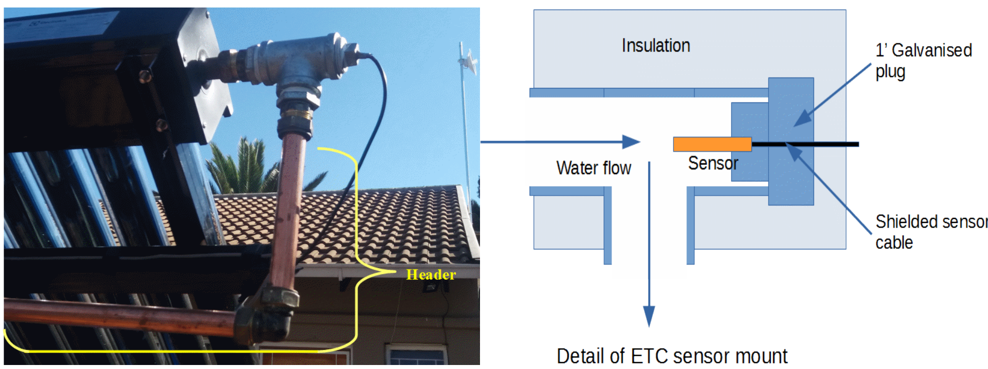

Figure 3.8: a) and b) Actual- and cutaway sensor mount on ETC hot ends. Note copper header (not yet insulated in photo).

Note the (approximately 800mm) copper header section, highlighted in the figure, as high temperatures may be present during static or fault conditions (during commissioning a 121˚C peak temperature was noted). The shielded sensor cable protrudes on the right, Figure 3.8a. The ETC hot-end sensor mounts were manufactured as screw-in to facilitate replacement. To interface the electronic control system to the pumps, an electrical panel was built. The layout is illustrated later in this chapter.

3.2.3 Circulation pumps and water flow loops

Figure 3.9 illustrates the actual aquaponics system under investigation, particularly highlighting the various water flow loops. To promote brevity during description of these various loops and their interaction, the abbreviated forms may be used in text, as illustrated in the figure, 'GB loop' denoting the grow bed flow loop, 'BF loop' denoting the bio-filter flow loop, and 'ETC loop' denoting the evacuated thermal collector flow loop, and the 'Sump loop' denoting the sump flow.

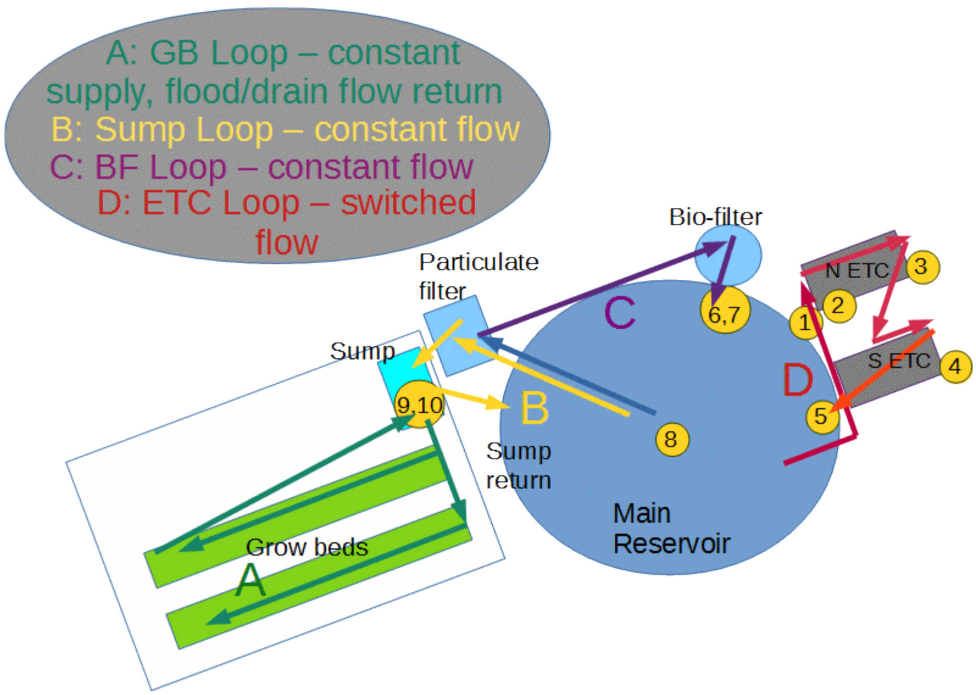

Figure 3.9: Water flow loops and relevant points of interest/sensor locations.

In Figure 3.9 the added equipment needed for this study is depicted on the right of the main reservoir, namely 'D: ETC Loop'. The numbered points further indicate various points of relevance with respect to temperature monitoring. The various flow loops and flow rates are further explored below.

3.2.4 Water flow loop descriptions

The coloured arrows in Figure 3.9 indicate water flow through the system in terms of flow loops. Important to note is that the ETC loop is closed with respect to the main reservoir, i.e. the heat exchange is a direct exchange of energy-supplemented water, as depicted in Figure 3.1. It is convenient to express this as a power transfer in terms of a kWh gain (or loss). The existing main aquaponic reservoir nominal capacity is 42 kl.

The use of flow loops presents an alternative method of quantifying heat exchange through the system. This subsystem approach eliminates the complex application of a mathematically rigorous ground-up detailed thermodynamic approach which requires specialist knowledge and is computationally intensive. The method adopted is further explored later in this chapter. Flow rates were determined experimentally, by using a stopwatch and known container size and measuring the container fill-up time when interrupting the loop flow.

The flow loop flow rates and expected temperature returns may be summarised as follows (note that the descriptions describe loop differential temperature inflow and return, as pertaining to each loop specifically):

- The GB loop flow was experimentally determined to be 1 630 litres per hour, and the return water temperature to the sump is affected by the grow bed enclosure temperature (i.e. weather conditions play a varying role). The enclosed GB space tends to retain solar heat and the return may thus add energy to the system, i.e. expected return temperature is normally slightly higher than the inflow on average during nominal midwinter conditions;
- The sump loop flow was experimentally determined to be 1 848 litres an hour, and as the sump temperature is affected by the (semi-detached) GB loop, the sump return temperature is variable. During normal winter conditions, however, the sump return temperature is expected to be slightly higher than the inflow;
- The Bio-filter loop flow was experimentally determined to be 8 092 litres an hour, and during winter months, this loop is expected to return colder water to the main aquaponic reservoir; and
- The ETC loop water flow rate was experimentally determined to be 630 litres per hour, and the flow pump switched based on potential energy gain in the ETC. The return flow temperature will therefore be higher than the inflow temperature.

The ETC loop (loop 'D' figure 3.9) pump is switched based on temperature difference between the dam and the ETC hot side temperature measurement by the implemented electronic control system. The circulation pump is a type Wilo Star RS25/4, suitable for use in ETC systems. Differential temperature measurement points (refer to Figure 3.9) are point 8 (main reservoir temperature, base reference for measurements) and point 5 (ETC return). The increase in water temperature coupled with the flow rate determines the thermal energy supplementation.

The main pump extracts water from the main reservoir (8) and pumps it through a particulate filter. From here, the majority flow is to the bio-filter (loop 'C' figure 3.9), but the sump (9) also has a float-valve type supply from the particulate filter, i.e. it fills on demand. The sump return flows to the main reservoir (loop 'B' Figure 3.9). This return-flow temperature is assumed to be the same as the sump temperature measured at point 9. The temperature contribution to the main aquaponic reservoir is dynamic over any given period and may typically add or subtract thermal energy with respect to the main reservoir for any given day.

The grow bed return (flow and temperature measurement at point 10) to the sump (loop 'A' in figure 3.9) is intermittent as the individual bed-compartments have a flood-drain type water reticulation. This means that for any calculations involving the grow beds, that flow must be aggregated over time using an average temperature. The grow bed calculations are not relevant at this stage and will be re-examined in Chapter 4.

The sump temperature is partially dependent on the grow bed return flow, which is largely weather dependent (the grow bed area is under protective shade netting and generally heats up during the day but doesn't fall to ambient minimums at night). This may be factored into the post-experimental model component for the existing system parameters — i.e. non-ETC-supplementation energy addition, which will be further explored in Chapter 4. Recall that the grow bed return flow (to the sump) is intermittent as the various individual grow bed compartments are of the flood-drain type, and that the sump flow from the dam (via the particulate filter) is controlled by a float-valve type arrangement. However, the sump return flow to the main reservoir is consistent, as is the flow supply to the grow beds.

The energy flow in these water flow loops is directly derived from the water flow rate in each loop, and the relevant measured temperature differentials. This is further discussed later in this chapter, and more explicitly discussed with the control system implementation presentation.

Note that the sump- and bio-filter detailed specification, as well as the grow bed detailed specification, have been intentionally omitted. This is directly relevant to the method adopted in this study which is applicable to generic systems that implement an electronic monitoring and control system. This is a generalised approach portraying the aquaponic system in terms of water flow and temperature differentials (and thus the required system thermal supplementation dependent on energy exchange via mass-flow). The method is expected to be more readily adopted into the concept of 'Sustainable Smart Cities', due to the potential for generic application. It is readily applicable by virtue of its relative simplicity — an additional expected benefit of the implemented method.

The aquaponics system under investigation is thus detailed and established in terms of the relevant flow loops present, with important temperature measuring points noted. The main aquaponic reservoir nominal capacity is 42 kl and is assumed to remain constant. Main reservoir thermal losses due to mechanisms such as direct conduction and radiant loss are reflected in the measured temperature changes.

3.3 System thermal exchange model

To derive a workable yet simple as possible system model, some prior discussion of the relevant criteria is warranted. 'Bottom up' thermal modelling can be a taxingly complex task, especially for systems containing a biological component (Cannon, 2014) entailing the description of every aspect of each system component, expressed as a dynamic contribution. A simpler method applicable to the problem is highly desirable: a workable model that sufficiently approximates the system under study is ideal, but some assumptions need to be clarified and justified. The main aquaponic reservoir is assumed to be uniform in temperature (experimental verification justifies this assumption) with the system having been detailed as stated. The system thermal interaction is examined later in this chapter.

3.3.1 Biot index

To consider any given system component as a 'lump' (and analyse it as part of a lumped model), it must be assumed that the temperature difference across that component is low (i.e. that the component is of fairly uniform temperature), as noted by Esfandiari and Lu (2014). Dynamically speaking, as temperature changes are introduced at some point within such a system component (for example, the main aquaponic reservoir as heated by the ETC return flow), temperature gradients are caused by the heat propagating through the medium (water) until equilibrium is reached. If such temperature differences are small, compared to the difference from the surrounding medium (i.e. the water temperature distribution in the main reservoir compared to the air temperature distribution around it), then these small differences may be ignored (or assumed to not exist for calculation purposes). The rate of heat transfer within a medium is a function of the conductivity of the medium (or its resistance to conductive heat transfer). If the resistance to conductivity is low, then the temperature variation is low.

This leads to the formulation of a ratio that indicates a measure of the validity of the assumption of the system component being a valid 'lumped model' component: the Biot number (abbreviated as Bi) or Biot index. It expresses the ratio of internal to external (i.e. water vs air in the example mentioned above) resistance to conductivity (how much better the lumped component is at distributing internal energy compared to the surrounding medium), and by convention the system component may be assumed to be a lumped component if this ratio is much less than 1, as Esfandiari and Lu (2014) clarify. Typically, lumped models assume Bi of less than 0.1 as validation criterion. Note that this is a dimensionless quantity.

Experimentally verified, the main aquaponic reservoir temperature distribution is very even. Variation was typically found to be within 1 to 2 bits of sensor resolution, i.e. less than 0.13˚C, based on experimentally obtained main reservoir temperature (as evident in the Google Sheets live temperature log). Ambient air temperature measurements, as obtained experimentally (two different types of ambient sensors were implemented), and night-time 'inactive' observations of the ETC temperatures (i.e. internal pipe sensors, with exposed-to-atmosphere mounting location) indicated a relatively low conductivity of the surrounding air. A randomly selected log-set data point, for 16 July 2020 at 04h21 indicates the values for the SHT21 ambient sensor, DS18B20 ambient sensor, and DS18B20 South ETC hot side sensor to be:

- SHT21 ambient air temperature measurement -3.03˚C;
- DS18B20 ambient air temperature measurement -2.31 ˚C; and
- DS18B20 South ETC hot side sensor (exposed to ambient conditions overnight as pumps are inactive) measurement -4.75˚C.

This spatial ambient difference in measurement of 1.72˚C is indicative of the air surround thermal conductivity. Compared to the main reservoir difference of 0.13˚C or less, this satisfies the BIOT index 0.1 relative requirement (i.e. 0.13˚C / 1.72˚C < 0.1) and justifies utilising the main aquaponics reservoir as a lumped component in a thermal model.

The air temperature distribution around the main reservoir thus notably varied by up to more than an order of magnitude compared to the main reservoir. This is also indicative of a 'heat island' effect around the main reservoir (further discussed in the following chapter) and illustrates the low thermal conductivity of the surrounding atmosphere.

3.3.2 Evaporative effects

Not yet explicitly addressed is the phase-change energy inherent in water evaporation — approximately 2.2 MJ per litre. If only considering the main aquaponics reservoir, this might still be feasible to at least estimate but evaporative surfaces rapidly change in surface area as grow bed pebble media alternately floods and dries. Added to this are the plant respiration water losses (which are also dependent on relative humidity, plant size, and physiology), varying as new plants are added or existing ones harvested, and it becomes apparent that the problem cannot be reasonably solved in this way. Thus, evaporative effects will not be included as a separate thermal influence, as neither historically relevant main reservoir water refill data nor current refill data are reliable, nor can they both be reliably estimated or extrapolated. This study nonetheless aims to incorporate a simplified but workable solution to crafting a mathematical description of the aquaponics system under study, as supplemented by the added components that deliver thermal supplementation.

3.3.3 Further assumptions

As noted, the main aquaponic reservoir is assumed throughout to be at capacity (42 kl). The heat-capacity of water is assumed to be 4.184 $J.g^{-1}K^{-1}$. This 'constant' is marginally variable, depending on the water density and impurities within it. Furthermore, evaporative effects are not reflected in the historical log data and are not reflected in the current study. The extensive system log data set gathered during the research data collection phase contains atmospheric relative humidity data not directly indicated by the study requirements, which may be of future use.

In addition, in the system under study, the main reservoir capacity is much larger than the volume of water contained in the grow beds and the bio-filter. This provides justification for the assumption of the system being of the same water mass as the main reservoir capacity, hence this capacity (nominally 42 kl) can be used in initial calculations. Furthermore, the grow beds and bio-filter are conceptually dealt with as energy contribution loops, via mass-flow transfer. Their specific size and layout are thus of less interest than the dynamic contribution they make to the system power transfer sum. Experimental results should yield quantification of their effect and will be further examined in Chapter 4.

Of import is the similarly lumped treatment of the aspect of heat loss via radiation. It is treated as a subsystem component subsumed into the thermal response as examined via the method of mass-flow transfer. Simply put, this aspect is assumed to be consistent in terms of the historically gathered temperature data as contrasted to the temperature data gathered during the study.

3.3.4 System exchange description

Incorporating the flow components into the system exchange is therefore a matter of expressing them as the summed components of the main un-supplemented system. The ETC supplementation loop further sums into the integrated supplemented system. Expressing this mathematically:

$$P_{us} = P_{bfr} + P_{sr} + P_{main} \qquad (4)$$

Where:

P_{us} = the sum of the un-supplemented system power gains, in Wh

P_{bfr} = the power transfer inherent in the bio-filter return loop, in Wh

P_{sr} = the power transferred via the sump return flow, in Wh

P_{main} = the main reservoir power change, in Wh

Note that the quantity P_{main} is only inferred using equation (4), not measured (recalling that both the historical data and the system logs obtained during the research period are of the active system, i.e. P_{us}). This is because an aquaponic system is by nature interactive and the bio-filter and grow beds are an integral part of the system function. The relationship expressed in equation (4) will be further examined in later chapters. As previously mentioned, initial estimations and calculations assume P_{us} and P_{main} to be the same. However, the study (through experimental results) will be separating the individual contributions to determine subsystem impact on the total system power change. Therefore, equation 5 denotes the supplemented system power change as the sum of the un-supplemented system and the ETC supplementation installation:

$$P_{sup} = P_{us} + P_{etc} \qquad (5)$$

Where:

P_{sup} = the supplemented system power gain in Wh

P_{us} = the sum of the un-supplemented system power gains, in Wh

P_{etc} = the power gained from the ETC panel loop, in Wh

The historical data did not include the energy loop log data, which the current study does, and which may be directly used to quantify these contributions after the data gathering phase. The un-supplemented power change is approached as the equivalent of the entire system power change, as historically determined from the main reservoir temperature change coupled with the main reservoir capacity of 42 kl and using the value of water heat capacity of 4.184 $J.g^{-1}.K^{-1}$

Equation 5 describes the system power exchange considering the additional energy supplementation by the implemented ETC system. However, as an additional benefit of the approach, and using equation 4, the subsystem contributions can be quantified, as will be further examined. This has the implied benefit of potential energy management of those loops, for instance by intervention in the flow capacity or by other means (such as added insulation).

To gain a clearer perspective on the exchange of energy, it is convenient to express the system in terms of its thermal capacitance and the transfer of energy via a thermal resistance. The thermal capacitance in units of $J.K^{-1}$ of the main aquaponic reservoir may be calculated using equation 6:

$$C = M\sigma \tag{6}$$

Where:

C = thermal capacitance of the reservoir in units $J.K^{-1}$

M = water mass in kg

σ = the specific heat of water in units $J.g^{-1}K^{-1}$

Thus, the main aquaponic reservoir thermal capacitance is:

$42x10^{6}$ kg x 4.184 $J.g^{-1}.K^{-1}$ = 175.728 $MJ.K^{-1}$

The nett heat flow rate into a body may be represented as:

$$Q = \int_{t0}^{t}[\mathrm{qin(t) - qout(t)}]\mathrm{dt} \tag{7}$$

Where:

Q	= the nett interval heat flow, in J
qin	= the heat flowing into the body, in W
qout	= the heat flowing out of the body, in W
t	= the time interval in s

Temperature change of a given body may be expressed as a function of the nett heat flow, coupled with the thermal capacitance of the body. Equation 8 thus represents the temperature change of the main aquaponic reservoir in terms of the energy flowing into and out of it:

$$Tt = Tt0 + 1/C \int_{t0}^{t} [\mathrm{qin}(t) - \mathrm{qout}(t)] \mathrm{dt} \qquad (8)$$

Where:

T = temperature of the main aquaponic reservoir in degrees Celsius

C = the main reservoir thermal capacitance, in units of $J.K^{-1}$

t = the time interval in s

The rate of heat flow from the aquaponic reservoir to the ambient surround (i.e. losses to the air via evaporation, radiation, and conduction, and losses to the ground through conduction) may also be expressed in terms of the thermal resistance between the main reservoir and the surround. Again, note that the entire aquaponic system is conceptually equated with the main reservoir for initial calculation purposes. The governing equation may be expressed as follows:

$$q(t) = \frac{1}{Req} [T1(t) - T2(t)] \qquad (9)$$

Where:

q(t) = nett heat flow from the main reservoir to the surround, in W

T1 = the main aquaponic reservoir temperature in degrees, in unit K (or °C)

T2 = the temperature of the surround in degrees, in K (or °C)

t = the time over which the flow occurs, in s

R_{eq} = the equivalent thermal resistance between the main aquaponic reservoir and the surround, in units — K/W (or °C/W)

The energy change of a given water volume temperature change may be directly calculated from the water heat capacity (as previously outlined – see equation 3 and relevant text). Using equation 9 and approximating T1 and T2 over a given interval, R_{eq} may be calculated (both using the historical data gathered in 2019 and the site experimental data gathered in 2020). This allows a method for comparing the two sets of data. For initial modelling and estimation, R_{eq} as outlined above would refer to the entire active systems' equivalent thermal resistance. This value would be of practical use only in initial estimation but may be further refined based on results obtained during data gathering.

It should be noted that the top-down approach of utilising water-loop power transfer to express the system thermally greatly simplifies the system model, as opposed to attempting to calculate the various contributions in terms of first principles. Equations 5-8 may be used to quantify the individual system aspects (assuming the assumptions regarding system simplification remain valid for the relevant element being quantified), keeping in mind that the system is always active as an integrated whole.

As experimental results would quantify power transfer for the actively circulating water aspect (the flow loops referred to in Figure 3.9), the ETC supplementation power transfer is similarly known, and therefore the main-reservoir-only losses (without the grow beds or bio-filter sub-systems) may be calculated. This is relevant in order to evaluate potential thermal loss mitigation factors specifically. Note again that doing so would inclusively reflect the conductive loss aspect, evaporative loss aspect, as well as the radiative loss aspect of the main aquaponic reservoir.

The simplified evaluation approach followed may be summarised by referring to Figures 3.10 through 3.12. Figure 3.10 represents the system thermal influence pre-study and depicts the un-supplemented system temperature input based on ambient weather conditions. The enclosed grey oval is the existing aquaponics system. The main aquaponics reservoir, bio-filter, and grow beds are represented as a combined thermal unit, as per the initial assumption and calculations:

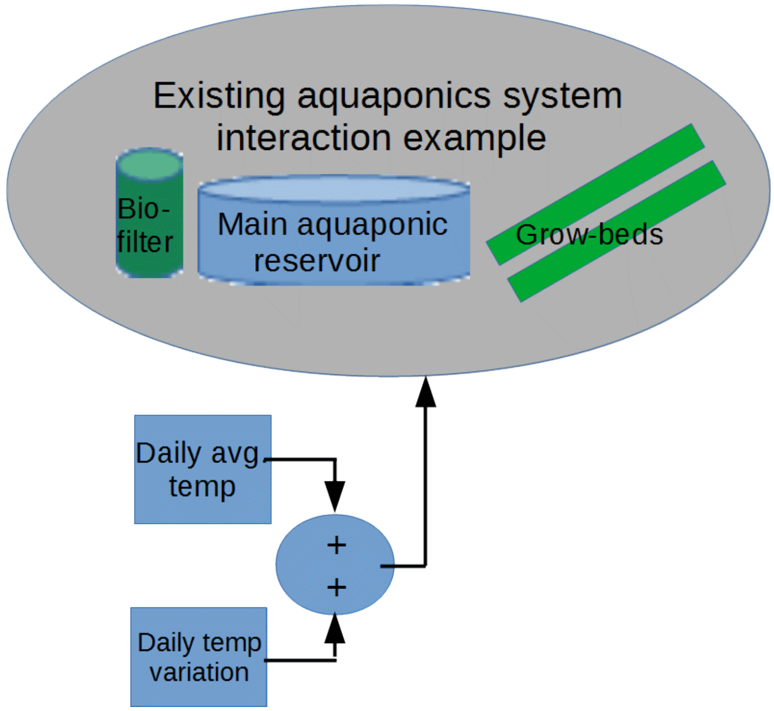

Figure 3.10: Pre-existing aquaponics system temperature interaction.

Figure 3.11 represents system interaction during the ETC supplementation evaluation phase and depicts the un-supplemented system temperature input (see Figure 3.10). It also adds the ETC supplementation temperature (i.e. active ETC water flow loop) input to the main aquaponic reservoir. The enclosed grey oval is the existing aquaponics system, again depicted as a combined thermal unit:

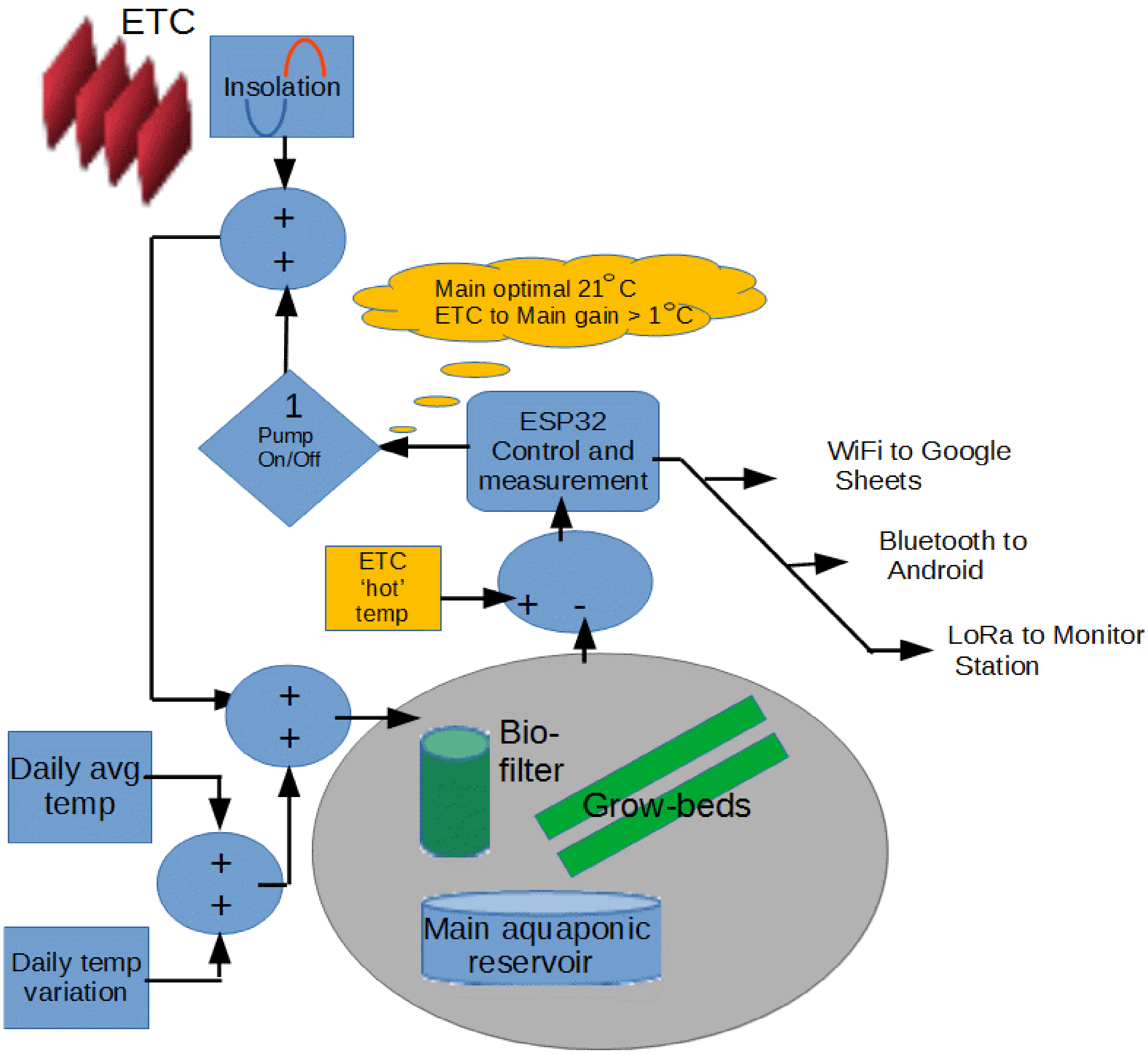

Figure 3.11: Aquaponics system including ETC supplementation.

An additional benefit due to the method implemented is represented in Figure 3.12. It graphically represents the now quantifiable individual effect of the ambient weather conditions on the grow bed and bio-filter sections as impacting the temperature of the main aquaponic reservoir.

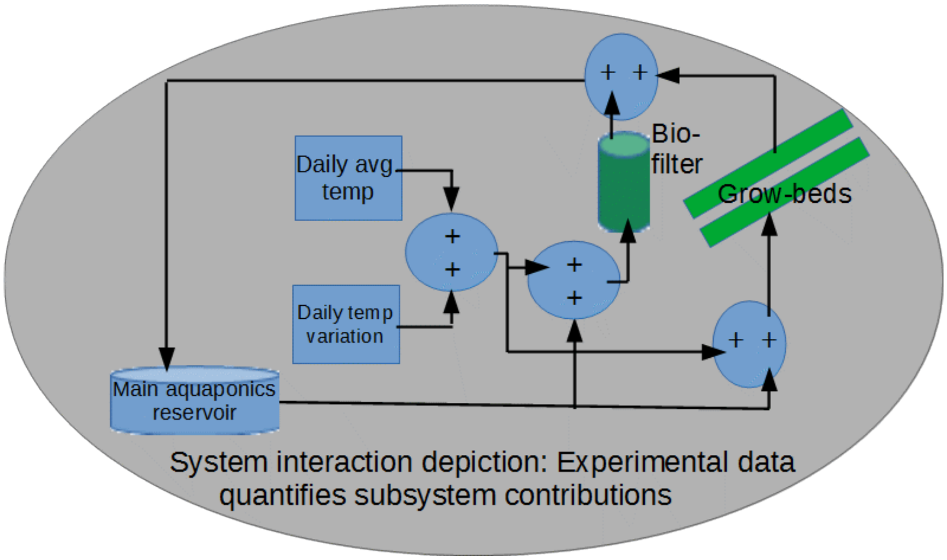

Figure 3.12: Expected experimental outcome - subsystem contributions quantified.

3.3.5 Simplified deterministic system thermal model

Modelling may now be presented, utilising the equations listed in previous sections, for the thermal interaction of the pre-existing aquaponic system (refer to Figure 3.10a). It should be noted that the nature of the model is deterministic, the assumption being that the main aquaponics reservoir and the active system are assumed to be the same, for initial calculation purposes. The model does not include direct insolation effects and considers the study delimitations. The heat capacity of water and the main reservoir capacity is assumed constant, at 4.184 $J.g^{-1}.K^{-1}$ and 42 kl respectively. The temperature change in the main reservoir and the ambient temperature at this time is known (the historical raw data from 2019 lists them).

For purposes of illustration, extracted values from the raw 2019 data set was used, values at 17h06 and 00h10, on 23 and 24 May 2019 respectively. The main reservoir measured 12.63˚C and 12.44˚C, while ambient temperatures were 16.31˚C and 9.63˚C. This yields an average main reservoir average temperature of 12.535˚C and ambient average of 12.97˚C. Main reservoir temperature change is 0.19˚C. Calculations for this interval (about 7 hours) and temperatures proceed as follows:

1) For the interval water temperature change, calculate the power change in the main reservoir, using equation (1):

$(4.184\ J.g^{-1}.K^{-1} \times 0.19^{\circ}C \times 42\ 000\ kg) / 3600\ s = 9.27453\ldots\ kWh$

2) Covert this to Joule:

$9.27453\ldots\ kWh \times 3600\ s = 33.38832\ MJ$

$= \text{‘}q\text{’}$ (the system energy change used in eq. 9)

3) Using equation 6, calculate the equivalent thermal capacitance of the main aquaponic reservoir (the previous calculation is replicated here as an example):

$42\times10^{6}\ kg \times 4.184\ J.g^{-1}.K^{-1} = 175.728\ MJ.K^{-1}$

$= \text{‘}C\text{’}$ (the system equivalent thermal capacitance)

Note that equation 8 suggests an alternative method to calculate the main reservoir equivalent thermal capacitance, rather than that of the system equivalent as used in the initial assumption. The methodology is otherwise similar.

4) Rearranging equation 9 and assuming that the main reservoir and ambient temperature over the interval is averaged and linear, determine the equivalent thermal resistance, *Req*, from the main aquaponic reservoir to the ambient surround. Substituting the calculated energy exchange (in Joule) and the interval average main reservoir temperature and interval (about 7 hours or 25560 seconds) average ambient temperature from the 2019 historical data into the equation yields the following:

$((12.535^{\circ}C \times 25560\ s) - (12.97^{\circ}C \times 25560\ s)) / 33.38832\ MJ = \text{‘}Req\text{’}$

$= -\ 333.00866\ldots \times 10^{-6}\ {^{\circ}C}.J^{-1}$

Note that the value of *Req* may be either positive or negative, depending on the relative temperatures of the main reservoir and the ambient surround. In simple terms, *Req* relates a degree Centigrade change in the main reservoir, per Joule energy gained (or lost). In this example, the main reservoir has cooled down despite the interval average main reservoir temperature (12.535˚C) being colder than the interval average ambient temperature (12.97˚C). This seems counterintuitive but is a direct result of the long interval chosen and the dynamic non-linear nature of the ambient temperature variation.

5) The resultant electrical-equivalent model may then be represented as a simple R-C circuit. Figure 13 illustrates the resulting interaction as a model.

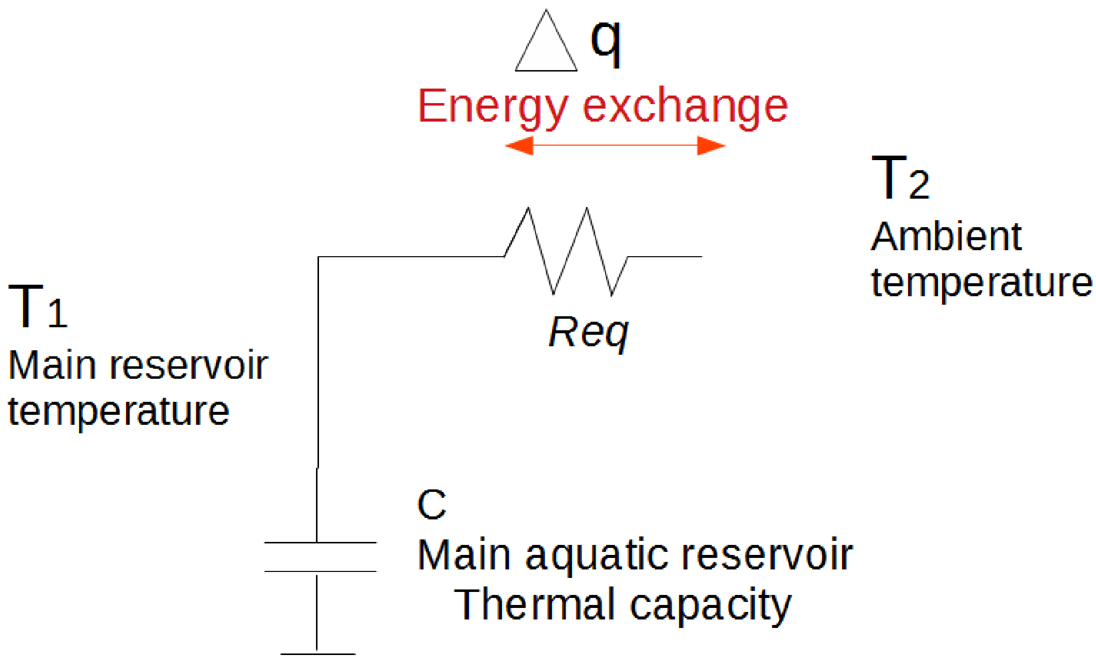

Figure 3.13: Simplified system thermal model

6) Any calculated value of *Req* is only valid for the particular circumstance, referring to equation 9. By visual inspection, it is apparent that *Req* is directly dependent on the temperature difference between the ambient surround and the main reservoir water temperature. In simple terms, the hotter something is, the quicker it loses heat. In terms of the electrical equivalency circuit, the capacitor (main reservoir) charge/discharge curve is exponential and

asymptotic (i.e. it loses temperature faster when it is colder outside, and the loss rate slows as the main reservoir and ambient temperatures start to match).

7) The system model equivalent values may be calculated for arbitrary intervals but non-linear changes in ambient temperature will introduce error. There is a trade-off between the slowly changing main reservoir temperature and rapidly changing ambient conditions which are generally not linear.

3.4 Monitoring and control system

To realise the study goal of thermally supplementing, monitoring, and controlling an aquaponic system to ensure viability, and evaluating the feasibility of thermal supplementation of such a system, the addition of the ETC and circulation pump(s) are required. Figure 3.1 is a graphic illustration of these components. To manage these components and obtain logs that are stored with a cloud data client, an electronic monitoring and control system was developed. This section details the design aspects of the system, examines, and justifies the design choices, sets out the communication strategy emplaced within the system design, and summarises system operational aspects.

3.4.1 Functional system description

This section assumes some familiarity with basic concepts and protocols generally used in embedded system design and implementation. The basic electronic system requirements to meet the research project goals are as follows:

- Temperature measurement at the various relevant points pertaining to the evaluation and monitoring requirements;
- Communication to a local wireless device (i.e. the site Wi-Fi access point) to facilitate cloud data logging;
- Logging of these measurement data to a cloud data client (Google Sheets was selected, as per criteria outlined in section 2.7, see also Table 2.1);
- Switching the circulation pump(s) on demand (see Figure 3.1); and
- Mains powered.

In addition, the following features were implemented, being deemed either sensible or useful:

- A system-local SD-card backup of all log data. The access point and/or internet connectivity might not always be available. Local SD data storage ensures contiguous data;
- Bluetooth communication broadcast of each log data set and pump status, also Wi-Fi connection failure notifications. The ability to monitor the system in real-time on an Android device while walking around the physical installation proved very useful. The full temperature data set, humidity, and Wi-Fi connection failure (if any) was broadcast every minute, enabling immediate feedback during testing, commissioning, and operation;
- A battery backup capable of extended backup periods — the anticipated grid supply failures did indeed materialise, and an inverter failure occurred. Data might have been lost if the extended battery backup power was not available;
- A solar PV module to supplement backup period energy requirements. The mains and inverter failures mentioned above did not extend over multiple days, so this feature proved unnecessary during the study period. However, the justification for the implemented PV solution remains valid;
- A custom linear regulator unit for the mains power DC supply and the PV module supply, maintaining battery charge. The 12V 7Ah backup battery must be maintained at a healthy charge level, neither over nor under charged;
- A slave PCB relay driver to interface the ESP32 control module to the electrical panel. It is good design practice to separate the computational core from the mains switchgear in this manner as it facilitates implementation, replacement, and repair. In addition it decreases the influence of electrical interference and allows third party support of the electrical system without detailed knowledge of the control hardware design. It also allows point-of-load regulation of the 12V battery supply; and
- A separate electrical panel containing switchgear (refer to the figures later in this chapter). See the reasons stated above for separation of the computational control section and mains switch gear.

Figure 3.14 lists the developed control system functionality as a block diagram and is substantiated in the following sub-sections. Functionally, the external electrical panel (which is separate from the control system, see Annexure B for further detail) feeds the unregulated, fused, filtered DC supply. This input is represented as ‘Mains supply’ in Figure 3.14. The DC supply then supplies the linear PV/Battery regulator. This regulator also receives power from a PV panel. Regulated battery charge is thus maintained via either the mains supply or the PV panel.

The battery then supplies the digital components (note the various cut-out switches to facilitate system resets, system upkeep, or battery maintenance). The ESP32 development board is mounted on a perfboard assembly, using its own point-of-load 5 V regulator. Note that this arrangement allows live-powered in-system programming via the PC USB port without either the USB port or the ESP32 module being destroyed. Similarly, the slave IO relay driver PCB has its own regulator (and is in fact an embedded system in and of itself, although only programmed here as an IO follower, i.e. the relays switch depending directly on the corresponding input voltage states as determined from the ESP32 controller via cable connection).

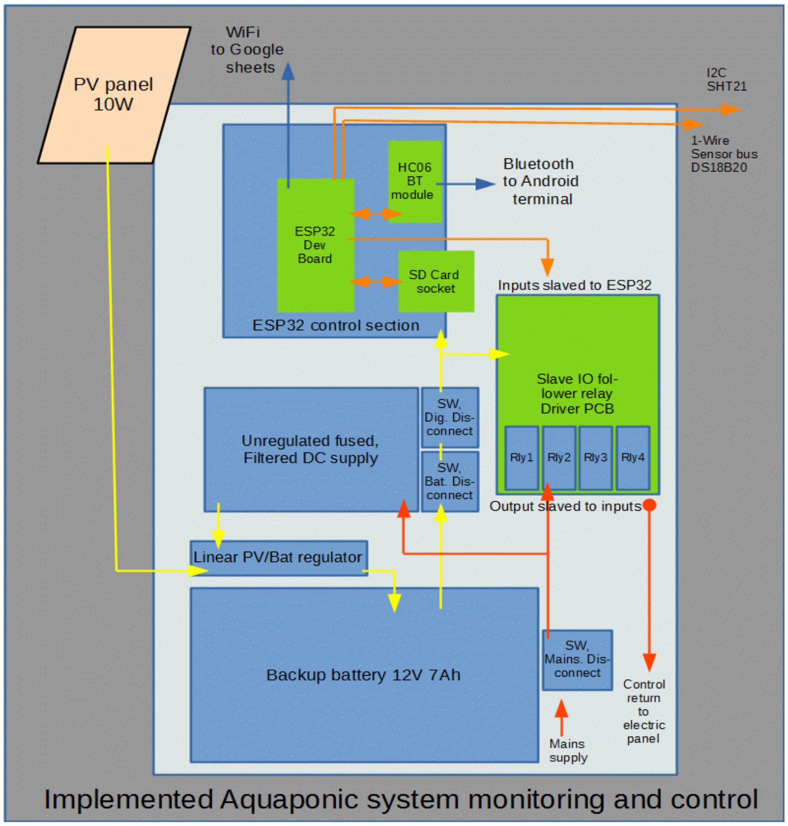

Figure 3.14: Block diagram of control system implementation functionality.

The ESP32 control section includes the SD Card socket implementation, and the HC06 Bluetooth module enabling broadcast functionality to Android serial terminal Bluetooth applications. It also interfaces to a 1-Wire sensor bus, used to read the various system temperatures from DS18B20 sensors (mounted on shielded cable, waterproofed, and submerged, or mounted internally to pipes). The I2C bus on the ESP32 is also used to interface the Sensirion SHT21 ambient sensor, which measures both temperature and relative humidity.

3.4.2 Detailed system design overview

This section explores the design choices as pertaining to the electronic control system implemented for the study. It lists the various hardware, explores powering and interfacing the hardware to the ESP32 development module, and presents the assembled system, including a field test example.

3.4.2.1 Sensor selection

The system is required to gather temperature differential data at various points in the system, referring to Figure 3.8. The numbered points are also relevant temperature log points. The DS18B20 digital temperature sensor selected may be implemented as a multiple-sensor 1-wire bus and was mounted using shielded data cable. The sensor is factory calibrated for accuracy and has a digital communications interface. These criteria made it the ideal implementation choice for the study. An SHT21 temperature/humidity sensor was also added although not specifically indicated by the study parameters. The addition provides redundancy for ambient temperature measurement (at greater accuracy and higher resolution) and adds a relative humidity measurement to the data set.

Atmospheric sensors (numbered location ‘2’ in Figure 3.9) were mounted under a 3D printed protective cover as shown in Figure 3.15. This cover is meant to provide radiant shielding (preventing the sun from directly heating the sensor). Ideally, the ambient temperature measurement is not affected by the sun heating the sensor directly, but the cover still allows free flow of air.

Figure 3.15: Example of the 3D-printed sensor radiant shield.

Communication protocols for these sensor types are completely different, as the DS18B20 types utilise proprietary 1-wire bus communication while the SHT21 utilises a standard I2C data bus. The Sensirion two-wire Clock/Data line protocol implementation is not identical to the standard I2C protocol but is compatible on the same bus.

3.4.2.2 System computational core selection

A microcontroller system is required to interface the digital sensors and collect sensor readings, store these data on an SD card, transmit data, generate control signals for the electrical panel, and send data via wireless interfaces to monitoring and cloud storage platforms. It is desirable to select a computational core that incorporates the required hardware interfacing already, to avoid excessive additional design time and complexity. Please refer to Annexure B detailing the selection of a suitable computational core.

3.4.2.3 System support hardware selection justification

The computational core described above requires additional support hardware (such as a power supply, battery backup, relay interface board, etc.). This both simplifies the design and allows ease of implementation, using already proven working hardware. Please refer to Annexure B for further detail regarding choice of supporting hardware. Motivations for their selection and implementation are documented.

3.4.2.4 Implemented control system

Figure 3.16 illustrates the electronic control system implementation. The design layout corresponds with the block diagram in Figure 3.14.

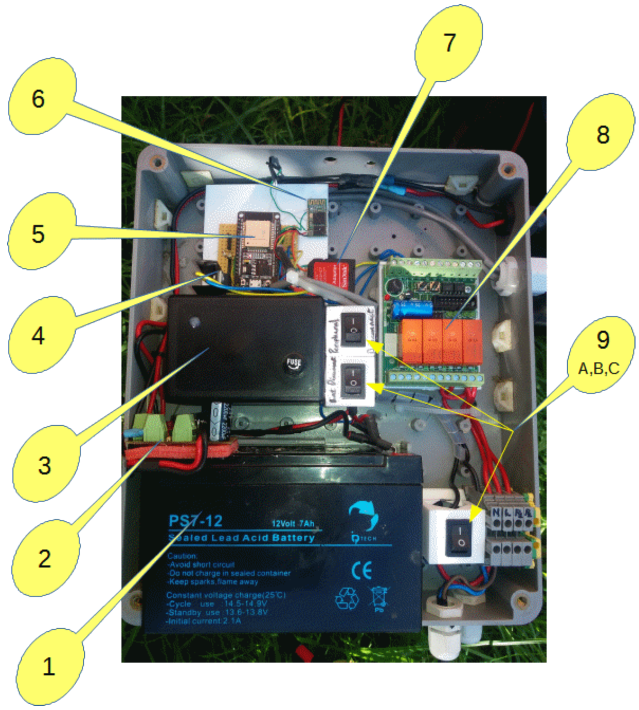

Figure 3.16: Assembled electronic monitoring and control system.

A brief description of the system functionality is provided below, with numbered references:

1) 7 Ah, 12 V backup battery is implemented to ensure data gathering during mains power outage;
2) Custom linear regulator, combining DC supply and PV input. This regulates the battery voltage;
3) Custom mains to DC supply. This provides an unregulated-, filtered-, ≈17 V DC at 3.5 VA to the regulator;
4) Project assembly on carrier perfboard, including 5 V regulator. 3D printed base. This is the control section base;
5) ESP32 development module. This is the computational core and Wi-Fi interface to facilitate data transmission;
6) HC06 Bluetooth module. This module allows Bluetooth transmission of the system criteria to any Android device with an installed Bluetooth serial terminal application;
7) SD Card. The card provides embedded data backup in the event that wireless communication is lost;

8) Relay carrier PCB. This is a slave-IO device, switching the relay outputs based on the cable connected inputs from the ESP32; and
9) Various disconnect switches (A: Mains, B: battery, C: Digital disconnect) with 3D printed mounts. The disconnect switches serve to ease system maintenance and checks.

Figure 3.17 details the digital control section and includes the ESP32 development module, SD card and HC06 Bluetooth module, mounted as served by a perfboard-mounted DC 5 V regulator (an initial design consideration was the requirement of interfacing with 5 V devices – the USB programming port, for instance). The 1-wire bus is pulled high to 5 V via 4k7 resistors, even though the devices themselves run from the 3.3 V supply. This hardens communication interference rejection considerably.

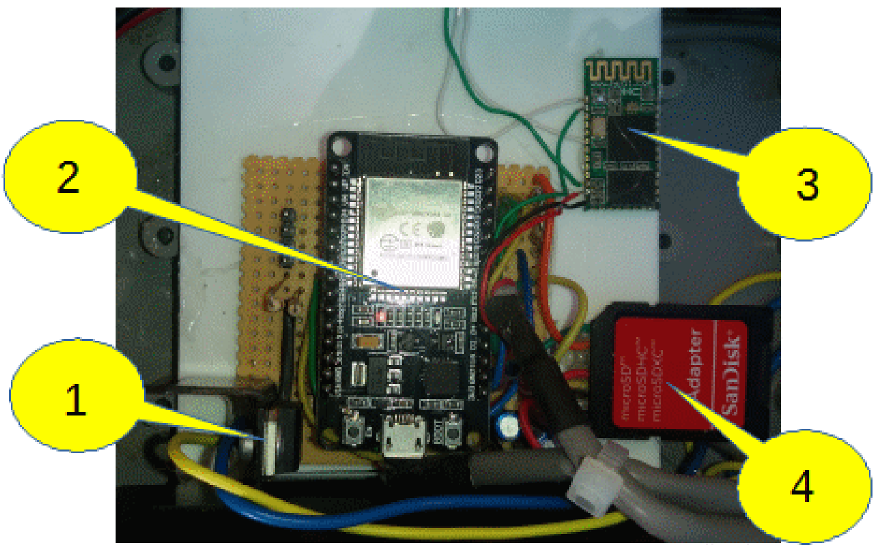

Figure 3.17: More detailed view of electronic control section.

The detailed view in Figure 3.17 allows a closer examination of the implemented solution:

1. 5 V regulator. This is a point-of-load regulation device supplying the ESP32 module, allowing better rejection of electromagnetic noise present in cabling;
2. ESP32 development module. The module incorporates Wi-Fi functionality and directly interfaces to the sensor networks and other hardware;

3. HC06 Bluetooth module. The ESP32 development module does incorporate Bluetooth functionality, but the on-board program memory is too small for implementing Wi-Fi, Bluetooth, and the application program, thus an added module was used; and
4. SD card. The SD card is of the micro-SD type, and the depicted SD card is actually the SD-to-micro-SD interface sold with some cards and used as a physical carrier.

Figure 3.18 illustrates the system on test outside, including the PV module and ambient sensor 3D printed protective covers. The test period included mostly sunny conditions, some precipitation (note control unit cover removed for photo). During the system design and test phase, the control system was deployed for several weeks to gather test data. The accompanying image refers:

1. Assembled system. Mounted in a suitable weatherproof enclosure, with battery compartment. The layout allows for easy access to the various components, and the enclosure protects the system against the elements;
2. 1-Wire sensor cluster. The actual sensors are in upright 50 mm PVC pipe for convenience;
3. Ambient sensors under protective 3D printed covers. 1 x 18B20 and 1 x SHT21; and
4. 10 W 12 V PV panel, mounted on a ladder for a more efficient solar angle.

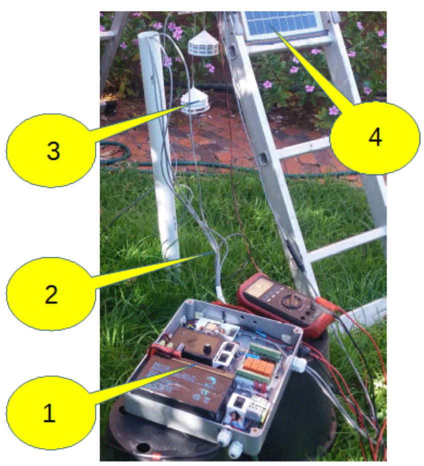

Figure 3.18: System under test.

Figure 3.19 depicts the monitoring and control system during installation. The electrical panel is also visible, and the ETC frame is shown without the evacuated tubes mounted. Figure 3.20 illustrates the site as viewed from above, with subsystem locations clearly identified. Note that the electrical panel as well as the monitoring and control system are located under the North-ETC frame, and the main reservoir is protected by a rectangular shade net mounted over it.

Figure 3.19: Monitoring and control system, and electrical panel during installation.

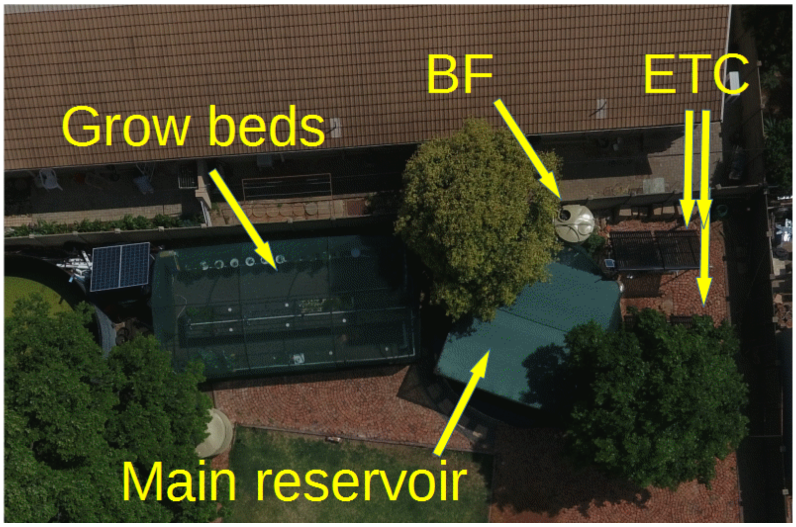

Figure 3.20: Site drone footage, showing location of subsystems.

3.4.2.5 System sensor placement considerations

To quantify the energy transfer of the various subsystem components, the flow-loop input and – return temperatures were measured and used to quantify the energy transfer by way of calculating the mass-flow thermal transfer utilising the flow rate and heat capacity of water. The equations used were previously presented, but it is now relevant to discuss some criteria pertaining to these calculations:

- Consistent (and internally consistent) temperature measurement throughout the study period is critical;
- Sensor calibration must be verified, especially for small differential measurement (such as the bio-filter loop);
- Data logs should be contiguous (i.e. any data gaps spanning temperature changing trends in measurement must be avoided); and
- Sensor placement must be such that no major conditions change around the system sensor location during the measurement period.

During the study, some challenges pertaining to maintaining a consistent temperature data log were encountered. The 2020 COVID pandemic caused delayed physical installation of the ETC, pumps, monitoring and control system, and the electric distribution panel (procuring the ETC was only possible by 30 May 2020). Some issues that were resolved included problematic pump priming, fitting vacuum breaker attachments and non-return valves, fixing leaks, and refining the sensor network and firmware programming.

Electronic logs commenced early June 2020 (logs for the month of May would also be relevant in determining trends leading up to mid-winter), with consistent logs available from the second week of June 2020. Intermittent electrical supply (load shedding) was partially circumvented by the battery back-up inverter supplying the system. However, this inverter failed during the study leading to loss of supplementation (also supplying the bio-filter pump and grow bed pump). A small fish, deceased, lodged in the ETC intake causing some confusion until the source of the deviating data was identified and removed.

The commercially available waterproof DS18B20 sensors (the sensors are supplied in a potted housing) were supplied using normal, unshielded braided wire. Using these on long sensor cable runs resulted in some erroneous readings. Replacing these sensors with custom fabricated sealed units using shielded cabling, resolved this issue. Despite these challenges, the extended log set (both the Google Sheets log set, of one system log set every 5 minutes, and the embedded SD-card system log backup, with one system log set every minute) was found to be reliable and comprehensive, over the three-and-a-half months of logs acquired during the study. There were no sensor failures for the loop-flow relevant sensors, and no notable issues pertaining to sensor reliability or accuracy during the study period.

Sensor placement to ensure consistent relevant data should be noted: The main aquaponic reservoir sensor was suspended to about half the depth of the water, about 20cm from the side wall. The loop-flow return sensors were secured directly in the water return flow, and the sump sensor placed in the sump turbulence (i.e. well mixed sump representative sample). The ambient temperature sensors were suspended at about 2m high, below the North-ETC panel, additionally protected from direct irradiance by a 3D printed ‘hat’ as detailed in a previous section. An unanticipated effect of this ambient sensor placement will be discussed in a later chapter.

3.4.3 Implementation and control strategy

To maintain real-time monitoring, system measurement logs need to be appended to the cloud data at short intervals. This requirement is excessive, as system time constants are large (i.e. system changes happen slowly). However, measurement intervals may be as low as once per second, the limiting factor being sensor self-heating (only 0.1˚C at 1 s measurement intervals) of the Sensirion SHT21 device. The other main consideration is the Google Sheets row limit, which is a maximum of 5.5 million rows of data per sheet. Considering a contiguous data log set of at least 3 months’ data is desired, and working well within these limits, a data log interval of between 1 minute and 10 minutes is perfectly acceptable.

Since the system needs to measure and control pump circulation switching on a real-time basis, however, at most a one minute switching interval seems desirable. All measurements are broadcast on the Bluetooth HC06 module (simply pairing any device using the key ‘1234’ enables system log monitoring). Annexure B illustrates an additional LoRa monitoring station, which was not implemented in the final solution. It is relevant due to the potentially large distance (>5 km in urban conditions) such a monitoring station could be situated from the aquaponics installation. The Bluetooth range and ease of connection to any Android device rendered the planned LoRa implementation superfluous for this particular site.

Desired relay status is output from the ESP32 module digitally to the slave relay carrier board, which switches the corresponding relay output (note that the ETC loop pump(s) are situated in a separate enclosure, and the slave relay carrier board outputs to switchgear mounted inside this enclosure, thus controlling pump on/off status).

SD card log backups are concurrent with actual cloud data set logs, and in the same format (this means that any missing logs may be cut/pasted from either set to complete the other). Actual implemented SD log intervals are one minute, while logs to the online Google Sheets client is approximately every five minutes.

3.4.4 Schematics and layouts

The electrical panel (with contactors switching the pumps, and implementing manual override switches, circuit breakers, and so on) is physically installed underneath the north ETC on the supporting frame. It accepts control signals generated by the monitoring and control system (also physically installed on the north ETC support frame) and switches the ETC pump accordingly. Refer to Annexure B for additional detail regarding the system schematic and electrical panel layout.

3.4.5 Firmware programming

Refer to Annexure C for detail regarding the embedded ESP32 program code. The Arduino IDE open-source programming environment and interface was used. The basic functionality to fulfil the study requirement is as follows:

1) Establish the necessary library references to interface the hardware used. These include a 1-wire library, time functions library, Wi-Fi library, HTTP client library, SPI library, SD and File System library, I2C communication library and RTC library.
2) Define global variables, including the study site Access Point (AP) security and connection detail, the Google Script URL and its Root Certificate.
3) Define various subroutines, including an initialisation for Wi-Fi setup and sensor net detection, SD file functions, Wi-Fi connection, and sensor reading.
4) Establish the main program loop. The system queries internet time from a time server (all logs are date-time stamped) and uses the on-board RTC if it fails to connect to it. It collects all the digital sensor measurement data and constructs a log data string, which is stored to the embedded SD backup, sent to the Bluetooth broadcast, and stored on Google Sheets (the Google Sheets log is every fifth measurement set). If the Google Sheets request is

unsuccessful, this is noted in the SD log. Based on the temperature measurements, it also switches the ETC pump. The system waits one minute and then repeats step (4).

3.4.6 Cloud storage

To evaluate the various aquaponics subsystem contributions, and quantify and evaluate the ETC supplementation installation, a comprehensive log of various temperature data points throughout the system is required. The system data has been logged to Google Sheets. Figure 3.21 illustrates a screen capture of a typical example (note calculation of running total of cumulative ETC power supplementation on the right).

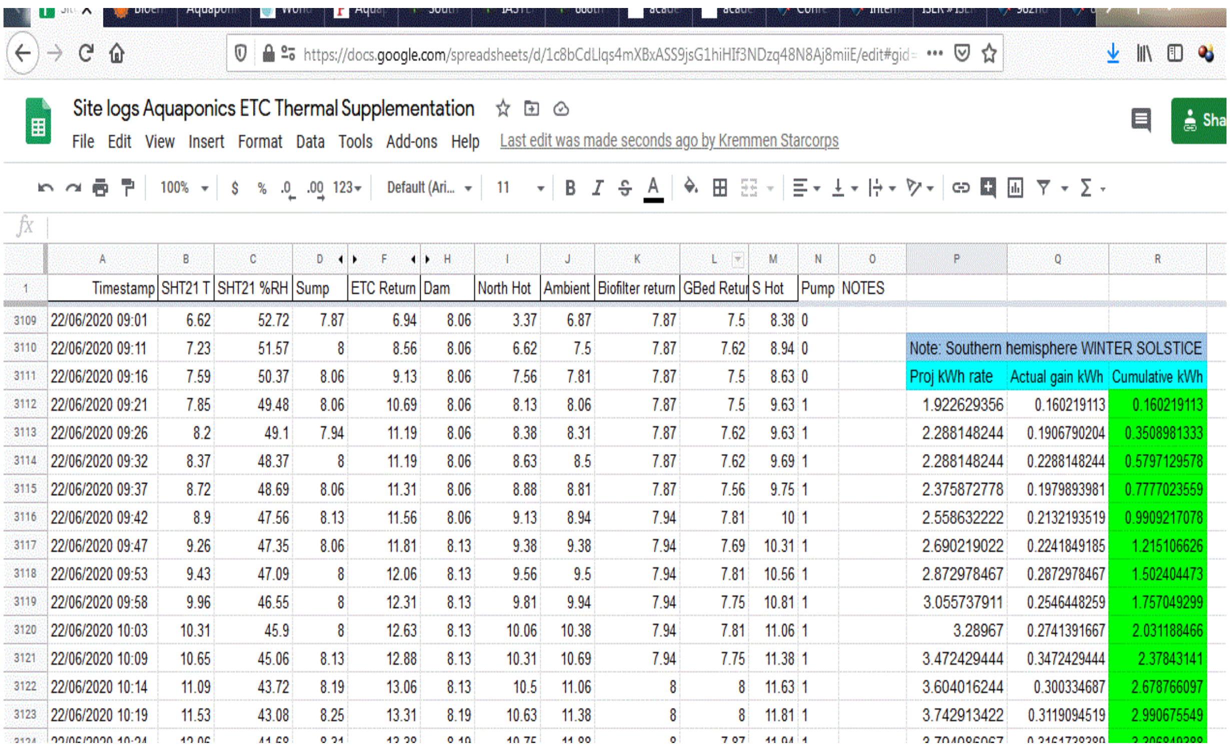

1	Timestamp	SHT21 T	SHT21 %RH	Sump	ETC Return	Dam	North Hot	Ambient	Biofilter return	GBed Retur	S Hot	Pump	NOTES			
3109	22/06/2020 09:01	6.62	52.72	7.87	6.94	8.06	3.37	6.87	7.87	7.5	8.38	0				
3110	22/06/2020 09:11	7.23	51.57	8	8.56	8.06	6.62	7.5	7.87	7.62	8.94	0		Note: Southern hemisphere WINTER SOLSTICE		
3111	22/06/2020 09:16	7.59	50.37	8.06	9.13	8.06	7.56	7.81	7.87	7.5	8.63	0		Proj kWh rate	Actual gain kWh	Cumulative kWh
3112	22/06/2020 09:21	7.85	49.48	8.06	10.69	8.06	8.13	8.06	7.87	7.5	9.63	1		1.922629356	0.160219113	0.160219113
3113	22/06/2020 09:26	8.2	49.1	7.94	11.19	8.06	8.38	8.31	7.87	7.62	9.63	1		2.288148244	0.1906790204	0.3508981333
3114	22/06/2020 09:32	8.37	48.37	8	11.19	8.06	8.63	8.5	7.87	7.62	9.69	1		2.288148244	0.2288148244	0.5797129578
3115	22/06/2020 09:37	8.72	48.69	8.06	11.31	8.06	8.88	8.81	7.87	7.56	9.75	1		2.375872778	0.1979893981	0.7777023559
3116	22/06/2020 09:42	8.9	47.56	8.13	11.56	8.06	9.13	8.94	7.94	7.81	10	1		2.558632222	0.2132193519	0.9909217078
3117	22/06/2020 09:47	9.26	47.35	8.06	11.81	8.13	9.38	9.38	7.94	7.69	10.31	1		2.690219022	0.2241849185	1.215106626
3118	22/06/2020 09:53	9.43	47.09	8	12.06	8.13	9.56	9.5	7.94	7.81	10.56	1		2.872978467	0.2872978467	1.502404473
3119	22/06/2020 09:58	9.96	46.55	8	12.31	8.13	9.81	9.94	7.94	7.75	10.81	1		3.055737911	0.2546448259	1.757049299
3120	22/06/2020 10:03	10.31	45.9	8	12.63	8.13	10.06	10.38	7.94	7.81	11.06	1		3.28967	0.2741391667	2.031188466
3121	22/06/2020 10:09	10.65	45.06	8.13	12.88	8.13	10.31	10.69	7.94	7.75	11.38	1		3.472429444	0.3472429444	2.37843141
3122	22/06/2020 10:14	11.09	43.72	8.19	13.06	8.13	10.5	11.06	8	8	11.63	1		3.604016244	0.300334687	2.678766097
3123	22/06/2020 10:19	11.53	43.08	8.25	13.31	8.19	10.63	11.38	8	8	11.81	1		3.742913422	0.3119094519	2.990675549

Figure 3.21: Google Sheet screen capture example of system data logs, 22 June 2020.

The ETC power contribution calculations (projected kWh rate, actual kWh contribution over the log interval, and running total of the actual contribution) are shown on the right-hand side. Refer to Annexure C for further detail regarding the access to Google Sheets.

3.4.7 Sensor accuracy

Achieving internally consistent temperature measurements is achieved by using a digital electronic sensor, the venerable DS18B20, which features a 0.0625°C measurement resolution (at 12bits). These sensors are factory calibrated for accuracy, but this is only guaranteed within ±0.5°C. Practically, the sensors were found to vary from one another by less than 0.2°C – this satisfies the desired 'internal consistency' criterion, but the actual sensor accuracy must still be determined.

To verify the loop-specific temperature sensors, a true-RMS Brymen TBM829 multi-meter with a thermocouple attachment was used. The multi-meter features 0.5°C resolution on the centigrade scale but is also capable of Fahrenheit measurement which was used because of the finer granularity of measurement. During the study, the monitoring system temperature sensors were checked for accuracy by using a submerged ice-bath technique. The relevant sensor and thermocouple were submerged, and multiple measurements averaged after sensor thermal adjustment.

A custom-built digital type J-K thermocouple interface was used to display and measure the main reservoir temperature distribution (with a resolution of 0.125°C) and it was noted that the main reservoir had remarkably even temperature distribution, to within ±0.125°C. This is ascribed to the continuous nature of the reservoir- and sump-return flow, which induces a rotating flow in the main reservoir with the sump-return and bio-filter return flow causing vertical thermal mixing of the main aquaponic reservoir.

The unit was constructed using the digital cold-junction-compensated MAX31850, and allowed a physically extended (3.5 m, mounted on a pole) thermocouple measurement throughout the main reservoir. It serves as a necessary indication of the temperature distribution of the main reservoir, which pertains to the Biot index as mentioned in a previous section.

3.5 Chapter summary

In this chapter, the physical system under study was detailed, including details of the evacuated solar tube collector system and the calculation of the required ETC input. The installation of the

ETC panels was detailed, the modelling method was further examined, and a model presented. The monitoring and control system implemented was detailed, including the physical layout and functional block diagram describing basic functionality. The cloud storage on Google Sheets was briefly described, with an example. In Chapter 4, the data gathered from the monitoring and control system will be presented, with a view to further establishing the performance of the system.

Chapter 4 – Results

4.1 Introduction

In Chapter 3, the physical system under study was detailed, including details of the evacuated solar tube collector system and the calculation of the required ETC input. The ETC installation was detailed, and the initial lump model presented. The implemented monitoring and control system was detailed, and the physical layout and functional block diagram presented. The Google Sheets cloud storage was described, with an example of the log data.

In Chapter 4, the data gathered from the monitoring and control system is presented with a view to further establishing the performance of the system. Data subsets are presented by way of illuminating relevant discussion.

Firstly, the sensor accuracy is discussed, along with the results of electronic sensor factory calibration validation. Secondly, the concepts of temperature recovery slope and temperature buffer establishment are revisited as pertaining to initial assumptions and the actual 2020 winter period, referring to extracted cold-front data. Thirdly, some implications of the gathered data set structure and calculation methodology is briefly discussed.

This is followed by the presentation of the data log summaries, highlighting the 2020 cold fronts and recovery periods, relative severity of the 2020 winter period and further discussion of the viability of the method adopted to describe and quantify the system thermal interaction. Correlation of gathered data is then examined with a view to validating the monitoring and control system implementation, and an unanticipated effect pertaining to the choice of ambient temperature sensor placement discussed.

4.2 Results of system sensor accuracy assessment

All temperature sensors were found to be within 2LSB of the sensor resolution, i.e. accurate to within ±0.125°C or better, referenced to the thermocouple measurements. As the bio-filter flow-loop temperature change with respect to the main aquaponic reservoir was very small, coupled with a large flow volume, it was deemed necessary to perform an extended check on this sensor.

The bio-filter loop temperature sensor offset was determined to be -0.16°C as referenced to the main aquaponic reservoir sensor. This value is used in calculations for this flow-loop.

4.3 Logged data by month: Revisiting thermal recovery slope and buffer determination

In Chapter 3, a method and model were presented to mathematically determine the required thermal supplementation required to maintain a positive temperature recovery slope in the main aquaponic reservoir during inter-cold-front periods. The magnitude of the required positive slope was bound to the determination of a temperature buffer and re-establishing this buffer within a specific period. The buffer and slope determination were, in turn, based on a multi-year evaluation of site-specific temperature data, used to determine the severity and duration of cold fronts expected during the winter period. Since the winter of 2020 proved unusually severe (according to AfriWX 2020a; AfriWX 2020b), it was necessary to re-evaluate the relevant criteria to ensure that the initial assumptions regarding determination of the recovery slope and temperature buffer remain suitable.

Figure 4.1 graphically illustrates the compiled minimum and maximum recorded temperatures obtained from AccuWeather for the Bloemfontein area in June 2020, as well as the monthly averages. Note the under-average temperatures for the month, as well as the period 12–16 June which coincides with a cold front passing. The AccuWeather data serves as comparison reference to the logged system data and visually contrasts the Bloemfontein 2020 winter season weather severity to the recorded monthly average.

In determining nominal inter-cold-front period and cold front severity, the collated multi-year temperature record for the area (Annexure A) indicated that the typical cold front was found to pass over the area in 2-3 days, typically followed by a period of 10–14 days of high insolation (i.e. high potential thermal supplementation via the ETC method as implemented for the study). The inter-cold-front period (i.e. recovery period) would still feature cold weather, but relatively high insolation. The criteria selected for such unusually cold periods, as identified in Annexure A, was chosen as multiple consecutive days with minimum temperatures below -3°C and daytime highs of less than 15°C, or multiple consecutive days with significantly lower minimum temperatures (-4°C or lower).

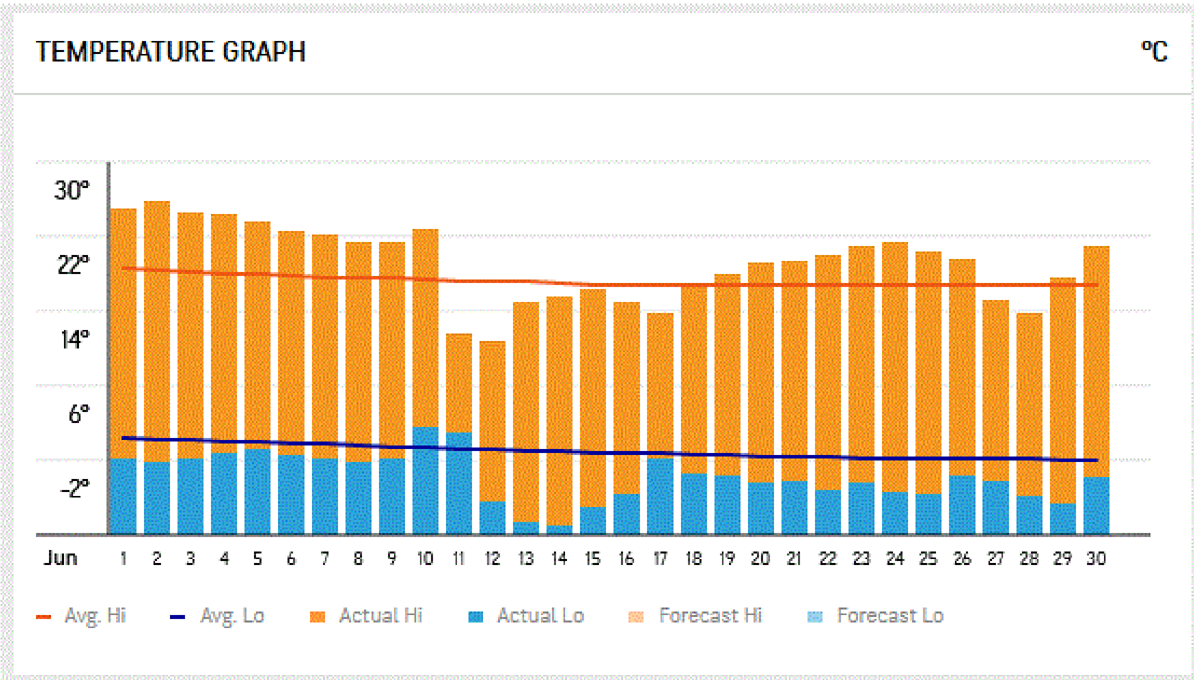

Figure 4.1: Graphic depiction of 2020 minimum and maximum temperatures, and historical averages for the month of June, for Bloemfontein. Reproduced from AccuWeather, 2020.

Referring to Figure 4.1, the front reaches the Free State on 10 of June, and after the initial cloud cover passes, temperatures plummet to consecutive overnight minimums of -7°C, -9°C, -9°C° and -6°C. Daytime maximum temperatures during this period are also low, with 6 of the 7 days from 11-17 June featuring daytime maximum temperatures below 15°C. Referring to Annexure A, the multi-year collated temperature data for the Bloemfontein area, it can be seen that this is both an unusually long-lasting and below-average cold front temperature set. Some system setup and hardware issues were still being addressed at this time, so that no ETC supplementation was added to the main reservoir on 15 and 16 June. Figure 4.2 graphically illustrates the cold front passing across southern Africa, with the image extracted from the animated graphic sourced from EUMETSAT, 2019.

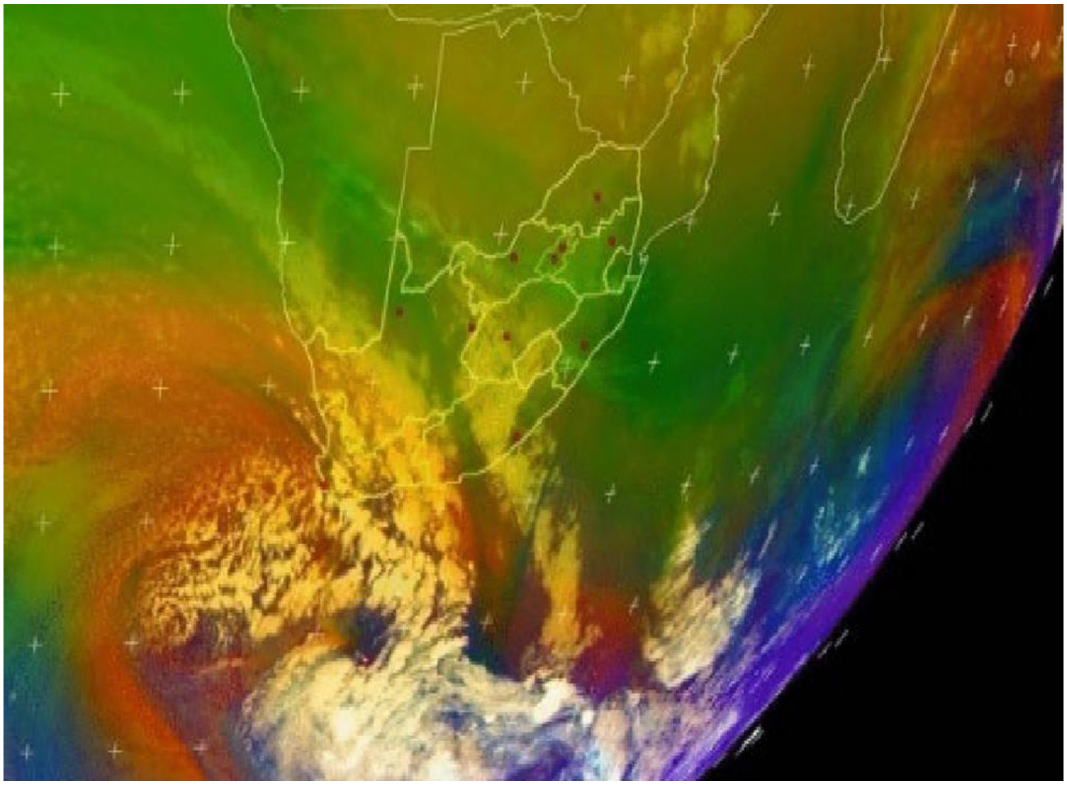

Figure 4.2: Graphic representation of cold front crossing southern Africa. Reproduced from SAWX website.

The cold front conditions coinciding with the system improvements proved unfortunate, as the main reservoir average temperate fell to 6.375°C. With the resumption of supplementation on 17 June, the main reservoir temperature recovery progressed normally, and by 18 June, the main reservoir average temperature was restored to acceptable temperature levels at 7.245°C. Figure 4.3 visually represents the temperature average as obtained from the implemented monitoring system from 10-30 June 2020. The averages are calculated as the arithmetic mean of the daily maximum and minimum as reported.

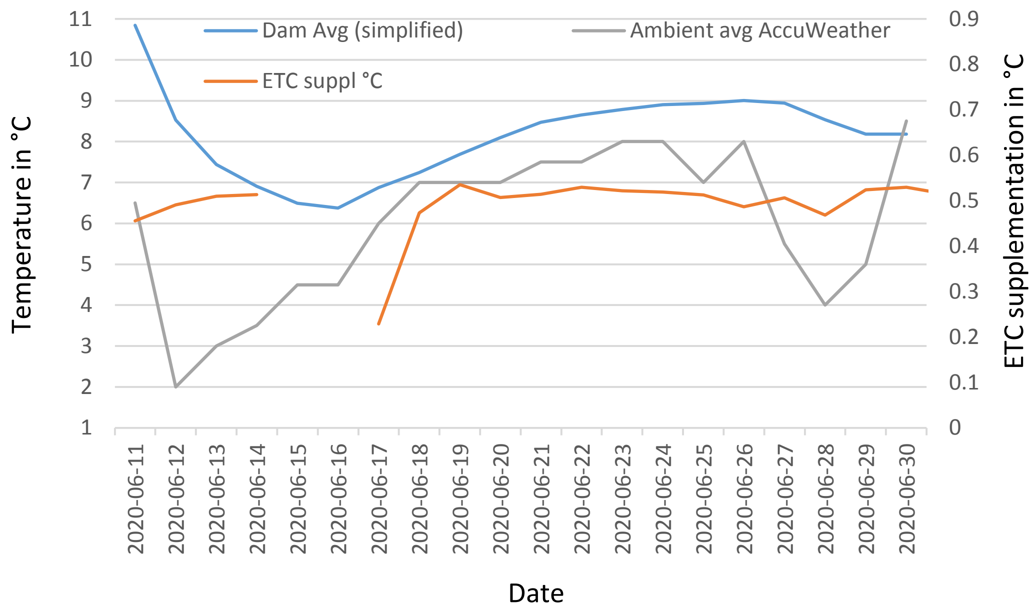

Figure 4.3: Visual representation of thermal supplementation and temperature of main reservoir, and measured ambient average for the region, June 2020.

Referring to Figure 4.3, the main reservoir average temperature (taken as the daily mean between inflection points) is represented by the blue trace. Note the gradient of the recovery slope between 18 and 26 June (asymptotically trending towards the buffer value), again falling as a second cold front reaches the site on 26 June. The 9-day inter-front-period being less than the identified 10-14 day recovery time, the main reservoir (average) maximum during the period is 9.005°C. The ETC supplementation contribution in °C is indicated by the orange trace on the secondary axis.

The average ambient reported by AccuWeather for the region (and again calculated as the mean between inflection points) is indicated by the grey trace. The AccuWeather source data are obtained from measurements taken at the Braam Fischer International Airport where an automatic weather station (AWS) is maintained by the South African Weather Services.

Figure 4.4 illustrates the compiled minimum and maximum recorded temperatures obtained from AccuWeather for the Bloemfontein area in July 2020, as well as the monthly averages. Almost the entire month of July 2020 featured minimum temperatures well below average.

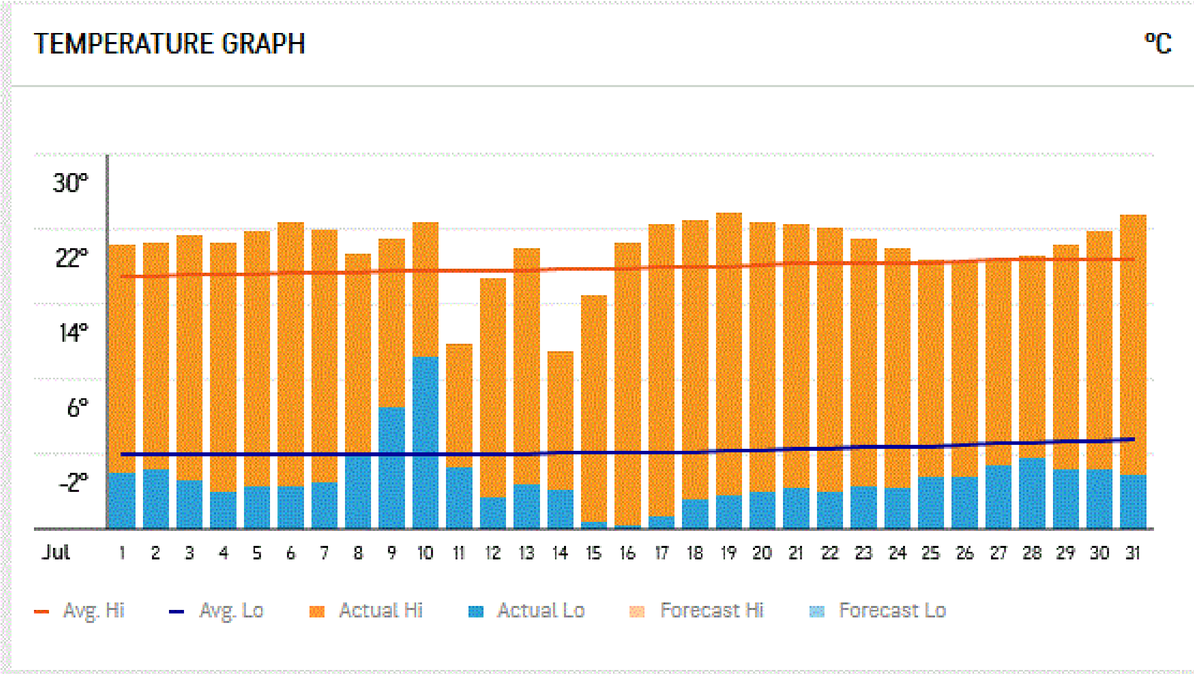

Figure 4.4: Graphic depiction of 2020 minimum and maximum temperatures, and averages for July in Bloemfontein. Reproduced from AccuWeather (2020).

July 2020 featured a particularly unusual weather pattern with three consecutive cold fronts crossing southern Africa (AfriWX, 2020b), impacting the study site location from 11 July. Figure 4.4 visually represents the temperature average as obtained from the implemented monitoring system from 1 to 31 July 2020. Note the gradient and value of the main reservoir recovery slope up until 10 July 2020 where the main reservoir (average) maximum peaks at 11.125°C, established from 8.185°C on 30 June 2020 — almost exactly the identified 3°C buffer amount within a 10-day period. This is partly due to slightly higher available insolation. The ETC daily supplementation is marginally higher by approximately 20% at the end of the July period depicted, compared to the start of June.

On 11 July, the first of the three consecutive cold fronts directly affect the study site location, with severe cold and an extended duration noted. This is evident from the grey trace (Figure 4.5) indicating the average measured daily temperature for the region. Referring to Figure 4.4, the extended below-average cold minimums are evident, with 20 consecutive days below the average yearly minimum, and the chosen ‘extreme cold’ (referring to Annexure A) criteria only returning to ‘normal’ winter minimum temperature (-3°C) by 27 July. The averages are calculated as the arithmetic mean of the daily maximum and minimum as reported.

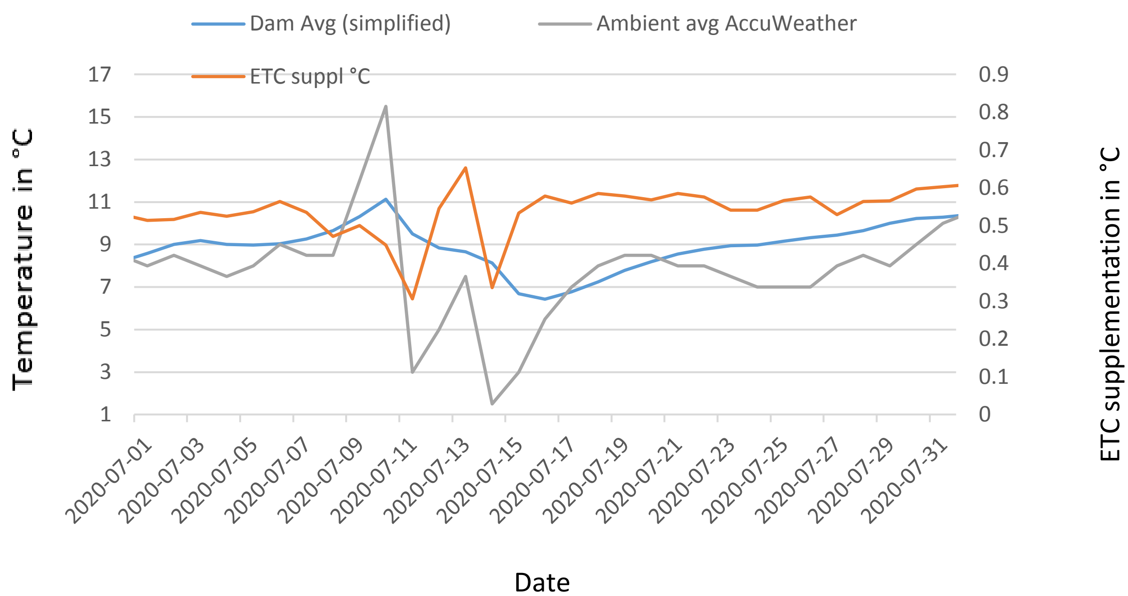

Figure 4.5: Visual representation of thermal supplementation and temperature of main reservoir and measured ambient average for the region, July 2020.

The severe conditions caused the main reservoir average minimum temperature to drop to 6.435°C on 16 July (with 15-17 July being below the identified 7°C bio-filter minimum), coinciding with the third cold front passing. This is also evident by the three dips in the orange trace (the ETC main reservoir supplementation in °C), caused by reduced insolation due to cloud cover as each cold front passes. Subsequent temperature recovery was steady, and by 31 July, the main reservoir (average) maximum temperature was at 10.28°C, despite the continued inclement weather (note the steady ETC supplementation shown by the orange trace (Figure 4.5) with the secondary axis peaking at 0.6028°C on 31 July).

Figure 4.6 depicts the compiled minimum and maximum recorded temperatures obtained from AccuWeather for Bloemfontein in August 2020, as well as the monthly averages. Like July 2020, August 2020 featured almost an entire month of below average temperature minimums. From 10-20 August, minimum temperatures were below -3°C. A cold front affected the study site from 17 August. Figure 4.7 shows the temperature average as obtained from the implemented monitoring system from 1-31 August 2020. Referring to the figure, low-insolation events occurred on 6, 16, 26 and 27 August. The first instance on the 6th represents a one-day cold front and as such did not impact the system greatly (the system recovered to approximately previous levels by 9 August).

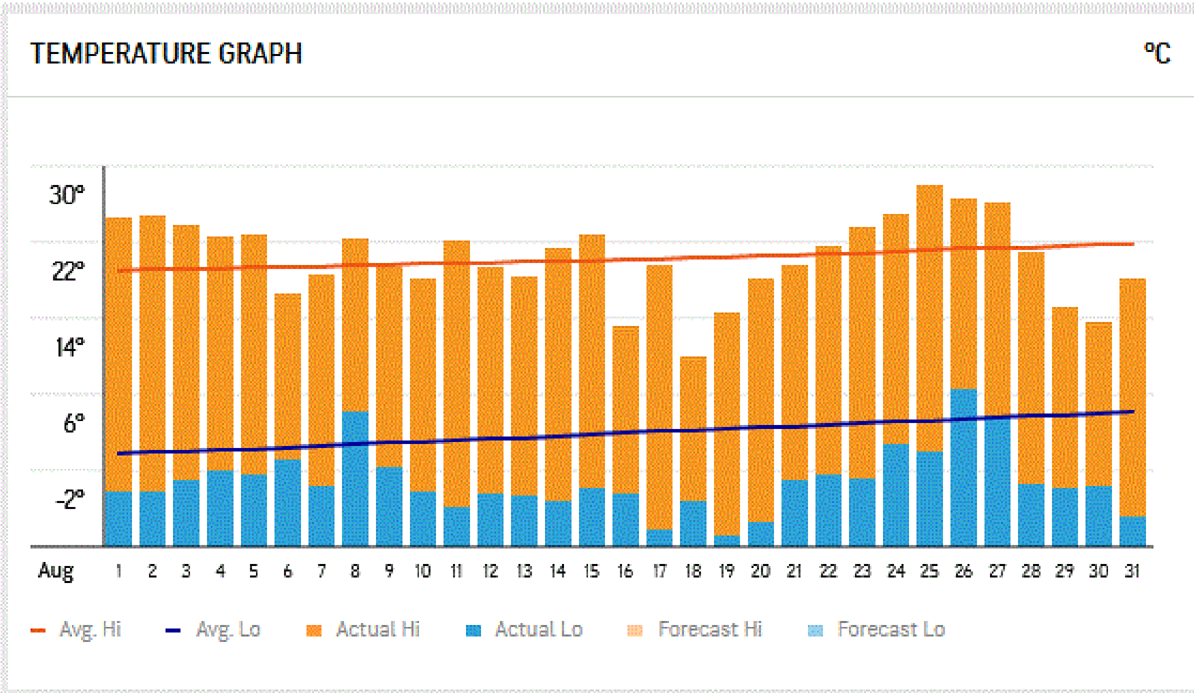

Figure 4. 6 Graphic depiction of 2020 minimum and maximum temperatures, and averages for Bloemfontein in August. Reproduced from AccuWeather (2020).

From 10-15 August, temperatures are low, but not sufficiently to cause the supplemented main reservoir temperature to drop much further. Note the low slope angle during this period (blue trace, Figure 4.7). An additional trough may be noted at the extreme right of ETC supplementation (orange trace, Figure 4.7). This is indicative of another cold front that started to affect the study site.

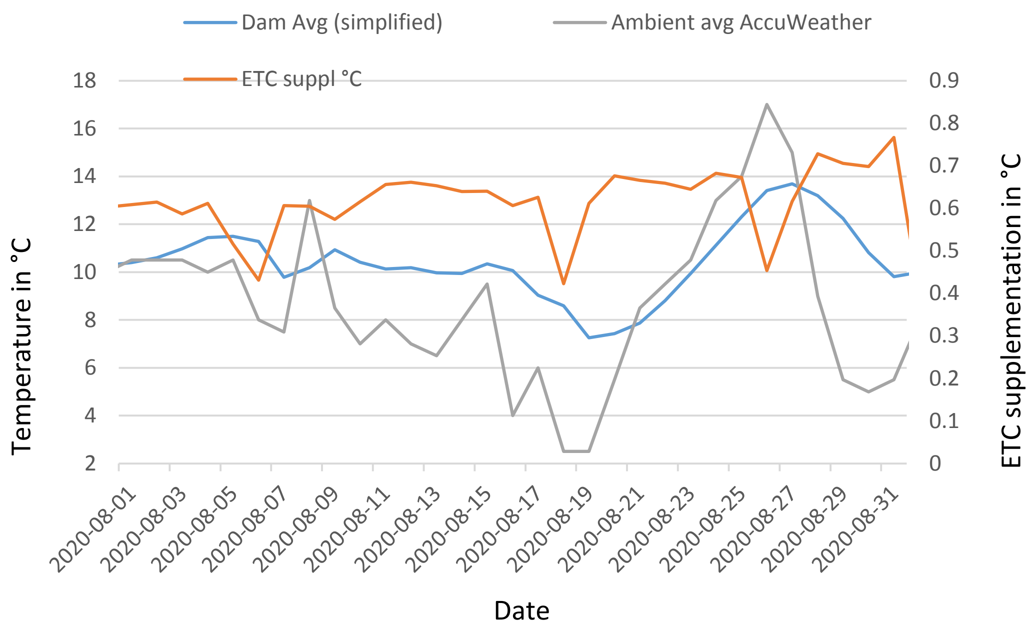

Figure 4.7: Graphic depiction of thermal supplementation and temperature of main reservoir, and measured ambient average for the region, August 2020.

On 16 August, a cold front directly affected the study site, with high insolation from the 19th, enabling ETC supplementation to resume. On 19 August, the minimum dam (average) temperature for the period reached 7.25°C and by 24 August had recovered to 11.125°C. The recovery slope was enhanced due to the additional insolation available during this period, between 25% and 30% higher than harvested supplementation energy at the start of June. The second cold front, affecting the study site from 26 and 27 August (insolation loss and cold temperatures), caused a main reservoir average loss from 13.69°C on 27 August to 9.81°C on 31 August.

Although the overnight temperatures are not extremely low, the main reservoir loss slope is still high. This is better understood when relating the main reservoir temperature to ambient minimum temperature difference: The higher the difference, the steeper the loss slope, which may also be directly related to the initial lumped model equation. The higher the ambient to main reservoir temperature difference, the lower the thermal transfer resistance.

During the study, it was decided to extend the study period to the end of September 2020, partly due to the initial COVID-related installation and implementation delays. Figure 4.8 graphs the September minimum and maximum temperatures, and averages for Bloemfontein. The weather minimum temperature extremes seen in June, July, and August are markedly absent, with the second half of September exhibiting below average temperature lows.

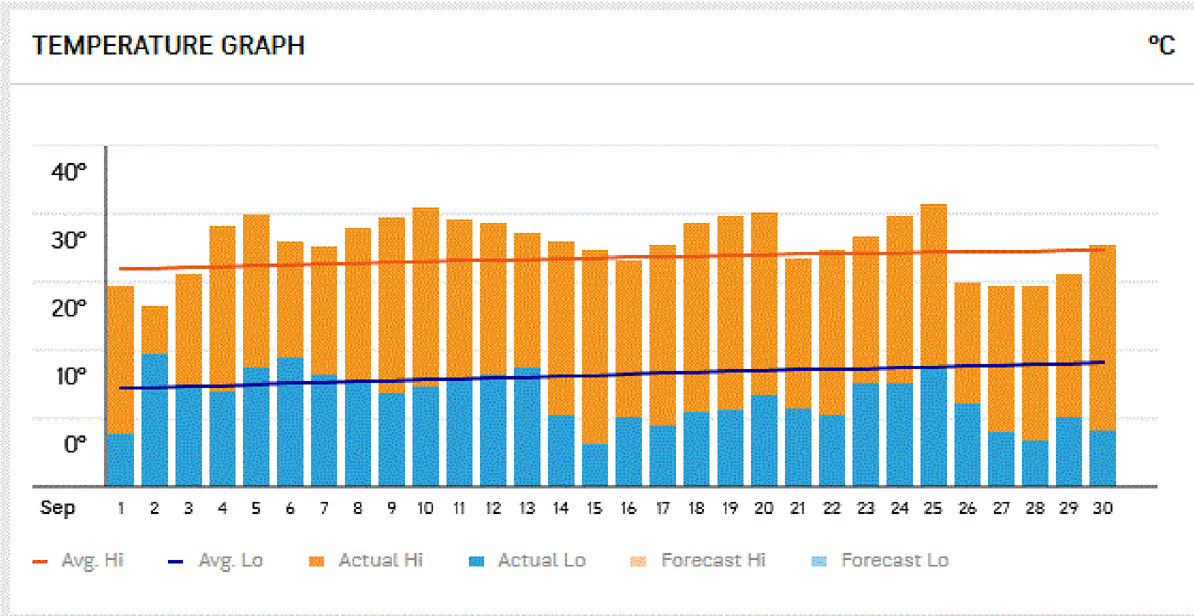

Figure 4.8: September 2020 minimum and maximum temperatures, and averages for Bloemfontein. Reproduced from AccuWeather (2020).

Figure 4.9 visually represents the temperature average as obtained from the monitoring system, from 1-30 September 2020. Note the insolation loss continued from 31 August (Figure 4.7) to 2 September. The period following did not exhibit an extended cold front temperature drop. Instead, minimum temperatures resumed at a 17°C difference between 31 August (-7°C) and 2 September (10°C). This resulted in a steep main reservoir temperature recovery slope from 9.81°C on the 31 August to 15.655°C on 6 September or almost a degree Celsius per day. This was aided by a peak ETC energy harvest contribution of 0.685°C on 5 September.

Note the various ETC insolation harvesting low points for the month (orange trace, Figure 4.9) which are not followed by severely low temperatures. These events are still cold fronts — remnants of Antarctic weather systems crossing the southern African continent — but the effect was greatly attenuated by the much warmer continental weather. Note that each ETC low point is indeed followed by a few days of reduced ambient averages (the grey trace, Figure 4.9), indicating passing cloud cover (insolation loss, orange trace, Figure 4.9) followed by colder weather – typical of such cold fronts. The averages are calculated as the arithmetic mean of the daily maximum and minimum as reported.

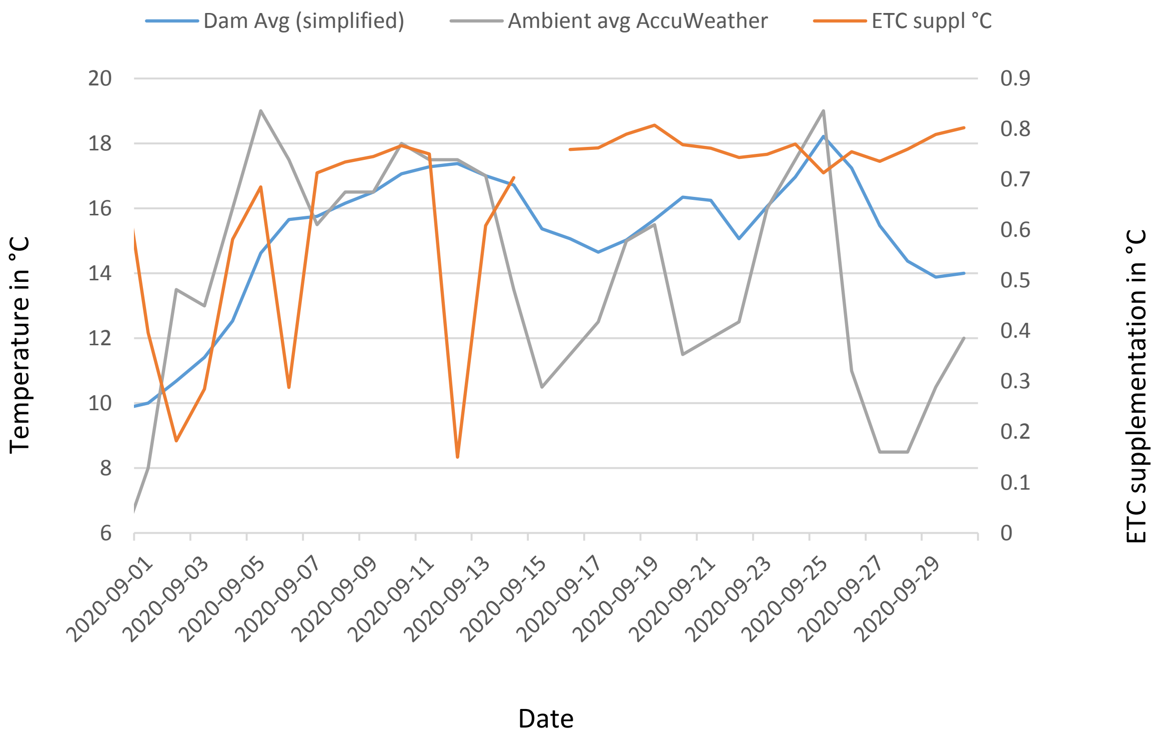

Figure 4.9: Graph of thermal supplementation and temperature of main reservoir, and measured ambient average for the region, September 2020.

The severity of the extreme weather conditions, normally prevalent in June and to some extent July, for the region, is clearly absent in the representation. Note the loss of supplementation data during 14-17 September 2020, referring to Figure 4.9 — the first intimation was a sudden noted apparent increase in the supplementation value, but an absence of the expected rise in main reservoir temperature. The cause was traced to partial and then almost total blockage of the ETC water loop supply from the main reservoir. A smaller specimen of the aquatic species had been introduced to the reservoir and swam into the ETC uptake. The blockage was removed and normal ETC flow restored.

4.4 Review of cloud data, calculation of contributions, insolation, and correlations

To correctly calculate and interpret gathered monitoring system data, the data needs to be contiguous over the interval of interest. The monitoring system logged data to Google Sheets at five-minute intervals, assuming a Wi-Fi connection was made with the on-site Wi-Fi router. If the system failed to connect, it would try again in five minutes, and repeat as necessary. In any case, a local SD-card backup was designed into the system monitoring hardware to ensure a backup to the available Google Sheets spreadsheet document, detailing the system log data, logging such data every minute.

During the study, any extended gaps in the Google Sheets document were filled where possible (an SD card was damaged during a system upgrade attempt, and about ten days of the SD backup were unavailable for such purpose). Where applicable, data were interpolated as necessary. The slow nature of the system thermal change indicates that a longer log interval would also have been acceptable — the approximately 30,000 Google Sheets system log sets (comprising all the sensor data, a time stamp, and all relevant calculations) are cumbersome. The approximately 150,000 SD-card log sets used to fill any gaps in the Google Sheets data make this process impractical for the average application.

It is thus necessary to simplify this approach and evaluate whether such a simplified approach is applicable to the quantification of system results. To continue the discussion around simplification, the methods used to arrive at calculations of the simplified data summary (see Annexure D) are:

- The ETC supplementation daily totals are arrived at by applying the mass-flow computation using the equation and method listed in the previous chapter. The interval calculation was based on the Google Sheets log time stamp and summed daily. The equivalent main reservoir degree Celsius contribution was calculated using the main reservoir mass and the calculated ETC power transfer;
- The flow-loop power transfers of the bio-filter loop and the sump return loop were calculated in the same manner;
- The daily ambient temperature regional maximum and minimum were obtained from AccuWeather and the system sensor measurement maximum and minimum selected from the SHT21 ambient sensor data (at the inflection points). Daily average temperatures are

the mean between minimum and maximum values. Main reservoir minimum and maximum values are at the daily inflection points, and the main reservoir daily average is the mean between the minimum and maximum values;

- The regional insolation data were obtained from a Solys2 data set as measured at the Central University of Technology, Bloemfontein, and averaged per day. The data available was not contiguous over the study period and the data used for correlation purposes comprised full daily data only. The criteria selected for comparative purposes was GHI (Global Horizontal Insolation) — a measure of direct- and reflected/refracted insolation; and
- Correlations, where calculated, were between data (complete for each day) for the selected relevant correlation source data.

The regional temperature data obtained from AccuWeather was averaged daily and correlated to the measured system ambient temperature (SHT21 sensor value) daily average. The degree of correlation (AccuWeather: SHT21) is positive and high at 0.966.

The regional insolation data (GHI as outlined previously) were averaged per day, and the two contiguous data sets available correlated to their respective ETC harvesting totals for the day. The degree of correlation (GHI: ETC) is positive and high at 0.948 and 0.935 respectively. Figure 4.10 visually depicts this relationship, plotting ETC supplementation daily totals vs GHI daily averages (for the two sets of GHI data available).

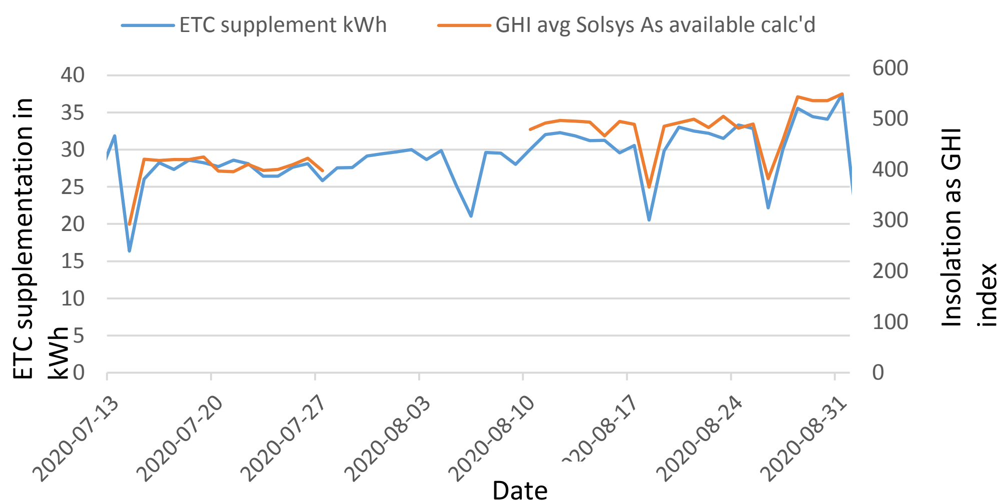

Figure 4.10: Visual representation of the relationship between measured ETC supplementation and available insolation, expressed as GHI index average.

The main reservoir temperature change (expressed as the kWh energy change) was correlated with the average regional daily temperature (Dam kWh: AccuWeather) and found to be moderate and positive at 0.581. This lower correlation is clarified when recalling that the main reservoir temperature is influenced (both directly and by way of the loop return flows) by ambient atmospheric temperature as well as radiant gains and losses. This will be further examined in a later chapter when conclusions are drawn from this data and when re-examining the initial assumptions made to quantify the required system thermal supplementation. Figure 4.11 depicts this relationship visually over the entire study period from June to September.

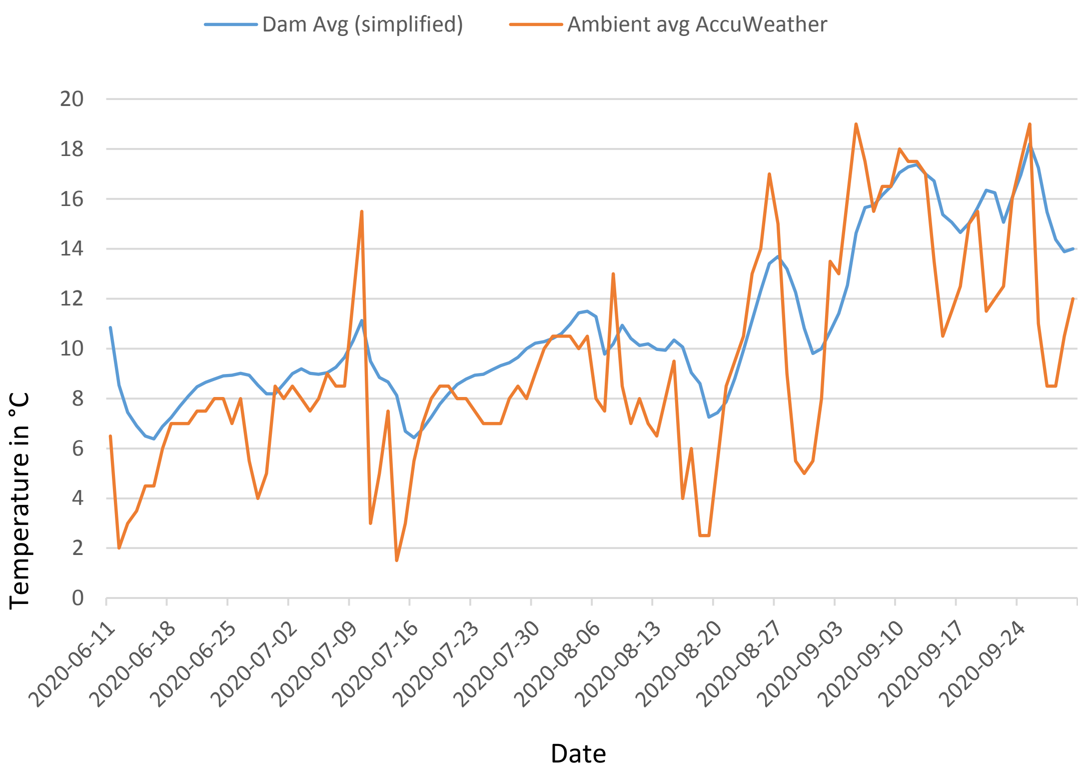

Figure 4.11: Graphic depiction of temperature relationship between the main aquaponic reservoir and the ambient average for the region.

The high degree of positive correlation between the ambient atmospheric sensor (SHT21) and the measured averaged data for the region, according to AccuWeather, indicates that the system ambient sensor measurements are dependable. The unanticipated effect of the ambient sensor placement, mentioned in a previous chapter, may now be further discussed:

It was noted that the measured regional minimum temperatures were significantly lower than those measured by the system ambient atmospheric sensor. Further investigation revealed that the sensor inside the southern ETC panel outlet, located furthest from the main aquaponic reservoir (about 3 m), consistently measured lower overnight minimum temperatures than the ambient sensor, located under the northern ETC panel, about 1.5 m away from the main reservoir.

At this stage, the study was underway and re-siting the atmospheric sensors would invalidate the internal consistency of their measurements. The custom-built Max31850 cold-junction-compensated thermocouple interface with 0.125°C resolution was used as a portable field-test evaluation device to attempt to understand the issue. Readings taken further away from the main reservoir indicated that the ambient temperature dropped markedly. The readings were also colder closer to the ground, as expected. The south-ETC panel outlet sensor was mounted at about 2m vertical height and exposed to overnight low temperatures (the water-loop drains when the pumps are switched off) while the ambient sensors were mounted at 1.8m high and similarly exposed. This apparent discrepancy is most likely explained by the fact that the main reservoir loses a large amount of heat during cold nights, and the closer ambient sensor is experiencing a localised 'heat island' effect: The immediate ambient surround is heated by the energy lost by the main reservoir. Figure 4.12 visually examines the relative measured (SHT21) ambient minimum temperature as it relates to the measured overnight minimum south ETC outlet temperature and minimum for the region.

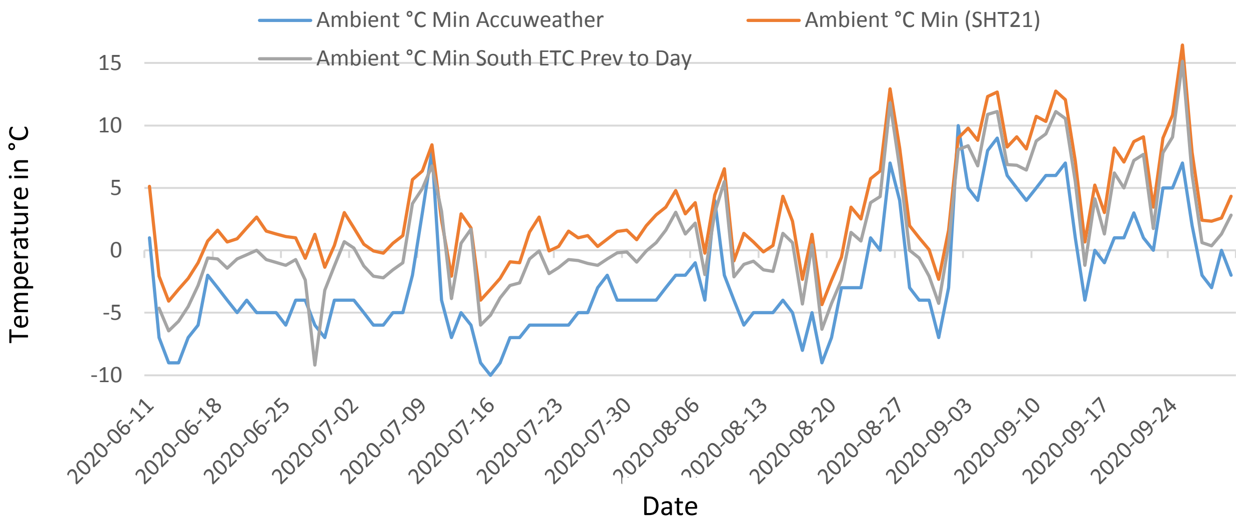

Figure 4.12: Visual comparison of measured system ambient minimum temperature, measured south-ETC outlet minimum temperature and regional overnight minimum.

From visual inspection of Figure 4.12, there is an apparent positive correlation between the South-ETC outlet minimum temperature, and the regional minimum as obtained from AccuWeather. Performing the correlation results in a high positive correlation between the measured south-ETC outlet temperature minimum and the regional minimum of 0.928 which lends some credence to the localised heat-island interpretation. The effect is visually more apparent during the colder month of June, as the measured ambient temperature (orange trace, Figure 4.12) diverges further from the measured south-ETC outlet temperature (grey trace, Figure 4.12) and the regional measured minimum (blue trace, Figure 4.12). The measurement distance from the main reservoir is apparent when considering the relative magnitude of the temperature trace. The closest (SHT21, 1.5 m) sensor measures warmer minimum temperatures than the further sensor (South ETC, 3 m), and both are warmer than the ambient for the region. From visual inspection (and referring to Figure 4.11), it may also be noted that these two measurements tend to converge as they approach the main reservoir average. This further supports the hypothesis of a localised 'heat island' effect.

Note the monthly power transfer contributions of each flow-loop system component. Over the study period, the harvested ETC supplementation energy totalled over 3 MWh, or a total of over 63°C in the main reservoir. This supplementation behaviour was as expected, and subject to available insolation for the period. Table 4.1 lists the system energy transfer totals as contributed by the subsystems, by month.

The sump return power transfer contribution bears further examination. Recall that the sump return flow temperature is directly influenced by the grow bed return inflow into the sump itself, as examined in a previous chapter. During June, the total contribution was over 80 kWh positive. Consider that this is a potential source of supplemental energy at no additional cost – the enclosed structure of the grow bed (covered by a plastic shade-cloth arched tunnel) and its longitudinal aspect with regard to the sun's arc (for more insolation exposure) cause it to be a nett positive contributor to the main aquaponic reservoir energy. The structure and orientation of such grow beds may thus form part of a potential temperature loss-mitigation strategy.

When examining the detail of the power transfer logs (referring to Annexure D, the summarised study results), it may be noted that the sump return power transfer is sometimes negative, and typically supplies energy during the first day or two of a cold front. The implication is that the grow bed enclosure acts as a thermal battery to the main aquaponic reservoir. The nett effect for June was over 20% of the ETC supplementation energy and is thus significant. For July, this effect was significantly larger at almost 40%.

Table 4.1: Monthly summary of loop power transfer totals to main reservoir, 2020.

ETC supplement kWh	ETC supplement °C	Sump kWh	BF kWh
Jun	**Jun**	**Jun**	**Jun**
430.7132	8.823	80.577	-58.686
Jul	**Jul**	**Jul**	**Jul**
811.952	16.633	322.309	-146.032
Aug	**Aug**	**Aug**	**Aug**
939.759	19.254	87.557	-121.361
Sep	**Sep**	**Sep**	**Sep**
930.469	19.061	6.335	45.445
Total	**Total**	**Total**	**Total**
3112.894	63.773	496.780	-280.634

The bio-filter return flow also bears closer scrutiny: The total bio-filter flow-loop power transfer for the study period is -280 kWh. Considering that the power transfer for September was a nett positive 45 kWh, the total for June through August was therefore -325 kWh. This represents almost 10% of the total energy harvested through the ETC implementation for the study period. This percentage is 13.7% for June, 18% for July, and 12.8% for August. The bio-filter flow loop is thus a good candidate for improvement in terms of thermal loss. An obvious solution that presents itself, (more evident in the further study by van Beukering, Hertzog and Swart, 2021b), is to reposition the bio-filter tank and flow loop within the grow bed enclosure.

Lastly, it is desirable to quantify the main reservoir-to-ambient loss separately. This is now possible on completion of the study as the subsystem contributions have been determined. Figure 4.13 illustrates the main reservoir power change 'in system', the total flow loop transfer, and the algebraic difference between the two.

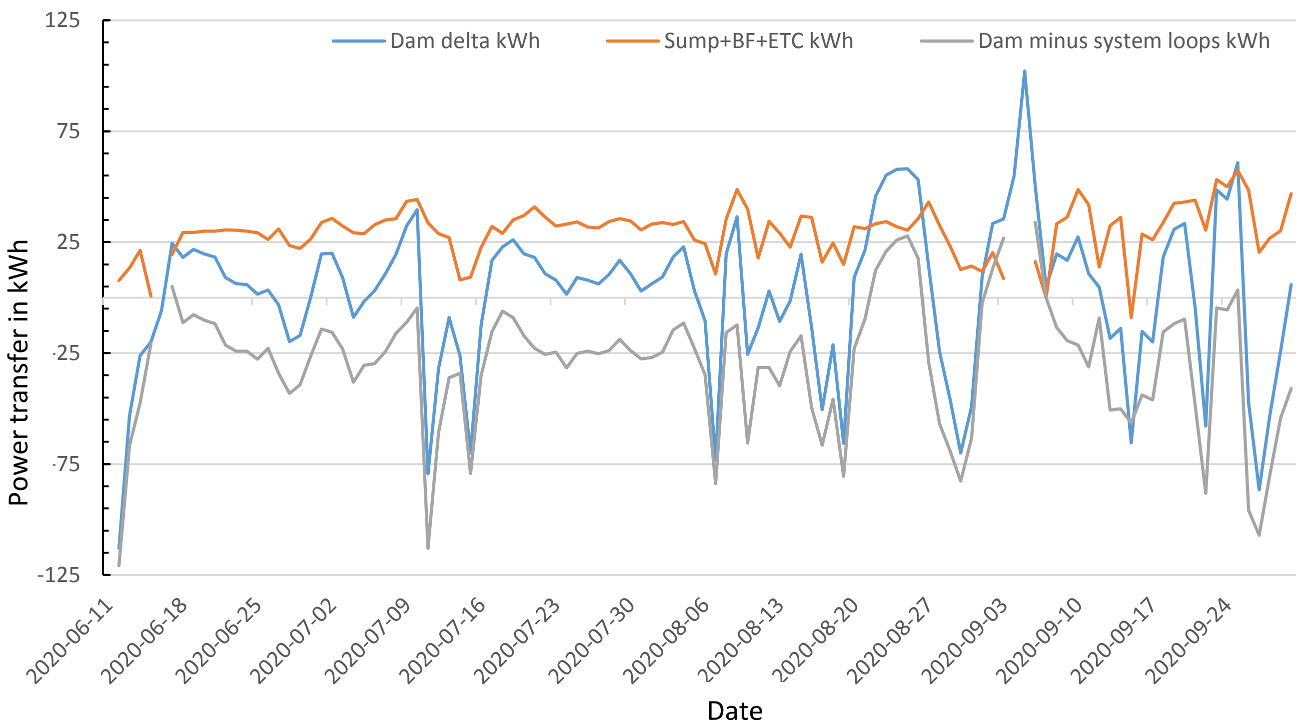

Figure 4.13: Plot of difference between loop-total relative power transfers against main reservoir power change.

The representation in Figure 4.13 is relevant in determining the main reservoir standalone energy change, and serves as a potential guideline to quantifying planned aquaponics installation, especially as pertaining to the retrofit potential of dams around the city of Bloemfontein. It is also useful in determining further potential temperature loss mitigation strategies – the main reservoir is constructed from galvanised sheeting with a PVC liner. This is an inherently thermally inefficient construction, in terms of energy transfer via the dam walls. It may be possible to insulate the dam walls at relatively low additional cost.

The data presented indicates two occasions on which the main aquaponic reservoir average temperature dropped below the identified 7°C minimum. The first instance, around 15 June 2020, coincided with a break in ETC supplementation. On the second occasion, around 15 July 2020, the main reservoir temperature was forced below the required minimum by both the unusual severity of- and closely spaced triple-cold-front weather experienced during this period.

4.5 Comparison of model and experimental data

The adoption of a lumped model representation of the system thermal response seems unsophisticated. The initially available historical records were simple temperature data from the main reservoir, taken for an active aquaponics system. A comparative model seemed desirable: Specifying the study delimitations to exclude a detailed component-level thermal model, and constraining the problem to only the criteria applicable to the sustainability of the system, simplifies the solution. Since the active system was already in place (for historical measurements) and the same active system could be used for supplementation study, it only remained to determine that the basis for measurement and calculation was valid as assumed.

The assumption that the main reservoir be used for the active system equivalence for purposes of calculation was justified in a previous section when discussing the Biot index. The lumped model of system thermal capacity and energy input was utilised to calculate the required energy change (and thus the ETC requirement, as previously outlined). The detailed experimental logs and related energy calculations served to validate the system model as well as the conclusions and recommendations to be discussed in the following chapter.

4.6 Post-experimental thermal model refinement

Visually depicting the main reservoir energy change (the grey trace Figure 4.13), it is now appropriate to revisit the system lumped model thermal interaction description described in Chapter 3. Figure 4.13 visually quantifies the energy change in the main reservoir, and impacts the previous lumped model arrived at (referring to Figure 3.11) in that the system energy change ‘q’ may now be refined, as depicted in Figure 4.14.

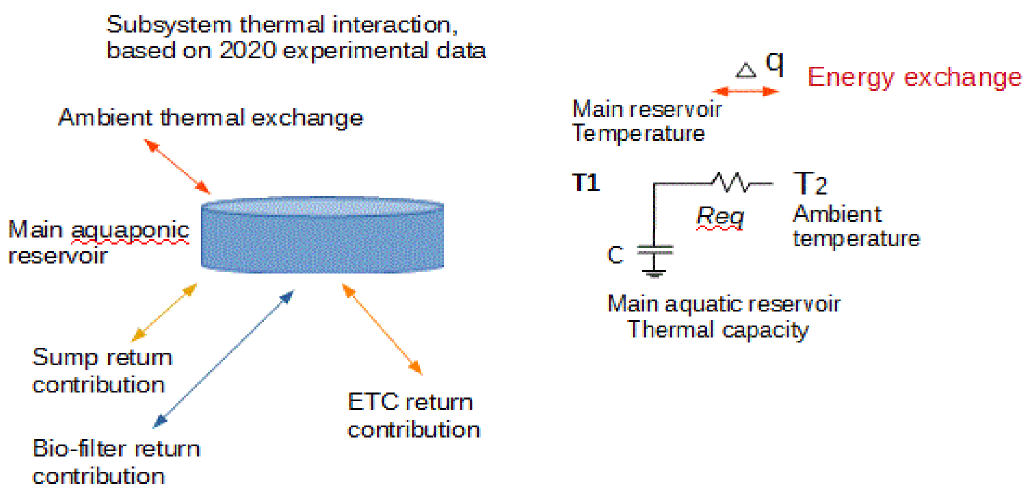

Figure 4.14: Visual representation of subsystem energy contributions, as presented in text.

The lumped model electrical-equivalent thermal exchange based on historical system data gathered in 2019, using the calculated main reservoir thermal capacitance, C, and temperatures differences observed, may be used to calculate the main reservoir-to-ambient equivalent thermal resistance, ‘Req’, for any given interval. For initial calculations, the assumption was made that the main reservoir was equivalent to the functional system. For the system under study, this assumption largely holds true as the system water volume with respect to the subsystems is large. As was experimentally observed, the main reservoir energy change is also large when compared to subsystem contributions. However, this is not necessarily the case for other system topologies, indicating that it is desirable to determine the main reservoir temperature gains and losses more reliably.

From experimental data, it is now possible to refine the main reservoir equivalent thermal resistance calculation (as the example previously determined using equation 9 and relative temperature difference between the main reservoir and the ambient surround). This may be achieved by offsetting the main reservoir temperature used by the sum of the experimentally determined subsystem contributions for any given interval (as in Figure 4.13), i.e. to represent the main reservoir temperature change separately. This is not representative of the system as the main reservoir is inextricably part of the functioning system but becomes relevant if specific temperature loss mitigation strategies pertaining to the main reservoir need to be quantifiably evaluated.

As an example, from visual representation of the temperature and subsystem temperature contributions (see Figure 4.11 and Figure 4.13), it might be considered that the dam could benefit from better insulation, and it is decided that thermal insulation should be applied to the dam walls. This evaluation method could then experimentally quantify the resultant benefit before- and after applying such insulation.

When discussing the determination of a suitable lumped model in a previous chapter (and the various assumptions and relevant criteria used), it was noted that the thermal losses of the main reservoir by implication included radiant, evaporative, and conductive losses. Figure 4.15 indicates these visually.

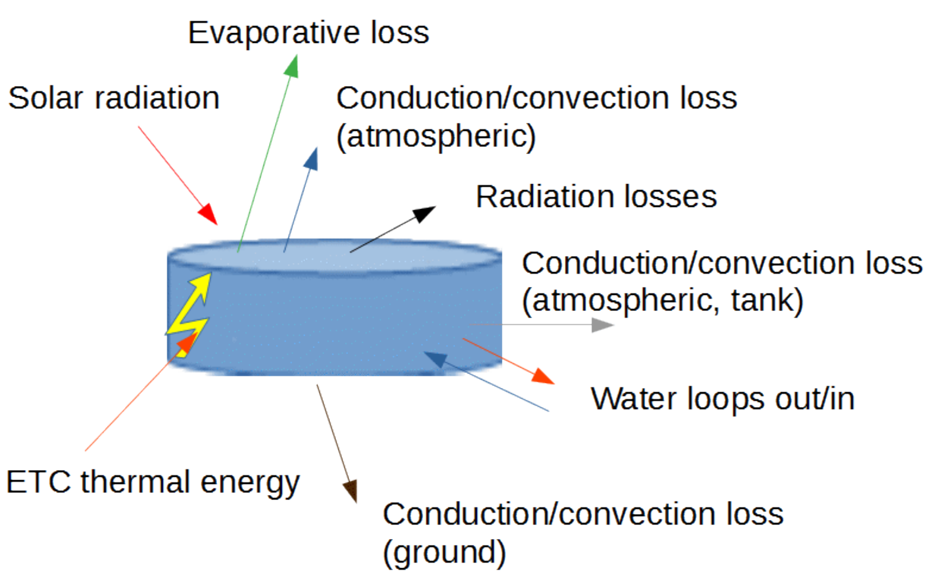

Figure 4.15: Visual representation of main reservoir thermal interaction process.

The accurate dynamic determination of the effects of direct solar radiation at the study site is not readily possible as the main reservoir is shaded under shade-netting mounted at an angle, some distance above the water level, and additionally partially shaded by a tree during the course of the day. Temperature contributions of the various flow-loops have been experimentally quantified (including the ETC contribution) as previously presented. If the method for determining the main reservoir-to-ambient equivalent resistance is applied, the resultant value is therefore influenced by a complex combination of the main reservoir conductive-, convective-, radiant-, and evaporative losses. Since evaporative losses are not constrained to the main reservoir (the particulate filter, sump and grow beds are exposed to atmosphere), it is not feasible to attempt determining main reservoir evaporative loss energy-equivalence.

The previously discussed hypothesis and experimental evidence of the main reservoir acting as a localised ‘heat island’ (refer to Figure 4.11) further renders determination of- and distinguishing between radiant, convective, and conductive losses from the main reservoir impractical (considering such conductive losses partially flow into the subsoil as well as the atmospheric surround). The presented lumped model is thus a realistic practical approach.

Figure 4.16 graphically depicts the benefit of the lumped model, as the system thermal exchange is simplified to consist of the various water-loop power-exchange contributions, and the main reservoir direct losses/gains to the ambient surround.

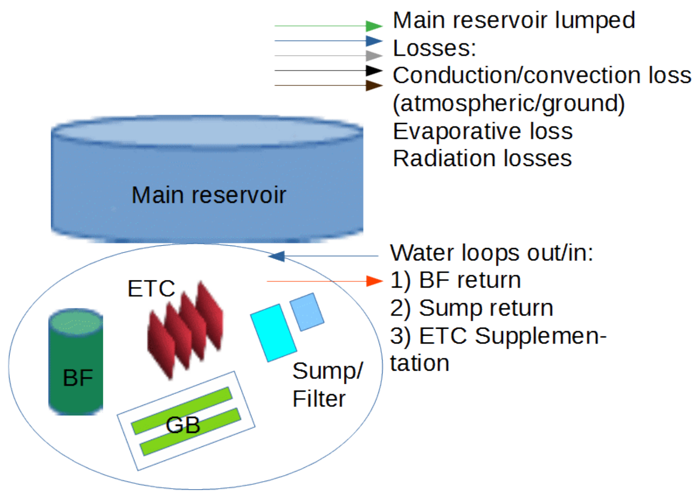

Figure 4.16: System thermal interaction represented as a contribution to the main aquaponic reservoir.

Recall from Chapter 3 (equations 4 and 5) that the active system energy change may be represented as the sum of the power flowing into and out of the main reservoir. Referring to Figure 4.14, the 'q' energy exchange and calculated thermal resistance of the main reservoir-to-ambient is thus the sum of the flow-loop energy exchange and the main reservoir direct losses. To evaluate any envisaged alternative temperature loss mitigation strategy specifically aimed at improving this thermal resistance figure (of the main reservoir only), the loop-transfer contributions should therefore be subtracted from the 'q' value used, to evaluate the impact of any such proposed strategy.

Therefore, hypothetically, it might be suspected that the main reservoir galvanised sheeting construction is excessively contributing to temperature loss. It is decided to evaluate the benefit of covering the main reservoir side walls with an additional insulating material. Using before and after measurements of the loop contributions and main reservoir energy change, under similar temperature/weather conditions, such a temperature loss mitigation strategy might be numerically evaluated, even though the temperature change in the main reservoir is dynamic and interdependent with the flow-loop exchange (which may lag ambient temperature changes).

Such evaluation could still be done considering the limitation on determining the evaporative losses: although the flow loop energy contributions incorporate (by implication, as part of the measured energy difference based on thermal difference flow-loop calculation) evaporative loss in each loop, the ratio of such evaporative loss between the main reservoir and subsystems is not known. Incorporating accurate flow loop return volumetric measurement in any future studies may shed additional light on this topic and could further improve the main reservoir energy exchange determination.

It is important to note that the ‘q’ value is an energy transfer, in Joule (i.e. the kWh representation used in results and the text should first be converted to Joule, if such is required). Recall that 1 kWh = 3.6 MJ.

4.6 Chapter summary

In this chapter, sensor accuracy was discussed. Data was presented and discussed as pertaining to the temperature recovery slope and temperature buffer selection, especially relevant during the unusually cold winter of 2020 in the central South African region. Calculation methodology was briefly described, and presented data discussed, including correlations and some implications regarding system improvements and the viability of the adopted method of quantifying the system thermal interaction. In addition, an unanticipated effect pertaining to the choice of ambient temperature sensor placement was discussed.

In the next chapter, the implications of the data results presented will be further examined, considering the temperature recovery slope and buffer temperature selection. The correlations drawn will be discussed in terms of their meaning to confirm the monitoring system measurements, ETC harvesting calculation accuracy, and validity of the initial assumptions regarding quantification of the system thermal supplementation required. The implemented solution will be examined to determine the feasibility of the method and results discussed to examine additional potential mitigation strategies and solutions.

Chapter 5 – Discussion and conclusions

5.1 Introduction

In the previous chapter, sensor accuracy and presented data was discussed as pertaining to the temperature recovery slope and temperature buffer selection. Calculation methodology was briefly described and presented data correlations mentioned. An unanticipated effect pertaining to the placement of ambient temperature sensors was discussed.

In this chapter, an overview of previous chapter content is listed with relevant aspects noted.

5.2 Consideration of previous chapters

Chapter 1: In this chapter, the principal benefits of aquaponics were listed as motivation towards the implementation of aquaponics systems in the Bloemfontein area, motivating resolution of the problem presented by severe winter minimum temperatures curtailing sustainability. The main issues identified were:

- Determining suitable temperature criteria for an aquaponics system to maintain sustainability in the Bloemfontein area;
- Quantifying the potentially large energy requirement to ensure such sustainability is maintained;
- The inherently interrelated nature of an active aquaponics system's subsystems that potentially further complicate such evaluation; and
- The requirement of a suitable monitoring and control system to quantify experimental data and system interaction.

To attempt to resolve these issues, the aims of the study were formulated. They are summarised as follows:

- A requirement of establishing a suitable system model relevant to resolving energy requirement for sustainability;

- The design and deployment of an appropriate monitoring and control system to manage the supplementation energy exchange so implemented;
- The objective of real-time monitoring of such data via cloud-based deployment of results; and
- Comparison of the experimental data with the criteria determined from the system model.

In addition, the study delimitation, notably that a detailed thermal model of individual system components is not required, was established.

Chapter 2: The literature review highlighted the history of aquaponics and its more modern adoption to supplement agricultural food production, and the potential of establishing urban food security and enhance nutrition. The basic sub-components of a typical aquaponics system were identified. Potential supplementation sources were examined and choice of ETC supplementation source for the study motivated, along with the direct-flow energy exchange method. Thermal model options were briefly listed. The monitoring and control system measurement and control criteria were explored, and some cloud storage options evaluated.

Chapter 3: The method adopted was examined in more detail, notably the use of the main reservoir temperature record for the previous season to determine a maximum loss slope and the collation of multi-year, site-specific historical temperature data (Annexure A) to determine typical inter-cold-front spacing. These led to the formulation of the concepts of a positive recovery slope, and the selection of a suitable temperature buffer. In conjunction with the main reservoir mass and specific heat (of water), this enabled the determination of a numerical description of the lumped system thermal interaction, and the specific determination of an energy supplementation requirement.

A description of water flow-loops of the subsystem components (as contributing energy to the main reservoir) was made, further informing the method adopted for quantifying system interaction. The proposed solar ETC installation was detailed, and the monitoring and control system described along with design criteria (Annexure B) and relevant firmware programming (Annexure C). In addition, criteria relevant to the justification of using the main aquaponics reservoir as equivalent to the active system, for calculation purposes, were examined. Some criteria relevant to thermal modelling but not examined in further detail were listed and the justification presented. It was noted that these criteria are by implication encompassed in the lumped model (and similarly present in the evaluated main reservoir temperature record of the active aquaponic system). The cloud storage (Google Sheets) and local monitoring (Android device via Bluetooth) options were also described. There was some delay in implementation due to the Covid-pandemic which was briefly discussed in Annexure E.

Chapter 4: Results of the system sensor accuracy tests were noted, notably as pertaining to the high-flow, low-temperature-difference bio-filter flow-loop component. The 'localised heat-island' hypothesis arising from the observed overnight ambient temperature sensor measurements results as contrasting to the south-ETC panel measurements was examined. The cause was determined as an unanticipated result of the ambient sensor placement choice, and further assessed with correlation evaluations between the relevant sensors and reported regional temperatures.

Experimental results were visually presented by month, contrasted to reported temperature maxima and minima. These were further discussed in terms of the recovery slope and temperature buffer as presented in the method (see also Annexures F and G). Sustainability criteria were highlighted as applicable. The experimental results were simplified to daily results for the study period (Annexure D), which were used for correlation data. Solar insolation data (GHI) was also correlated to experimental solar ETC supplementation results.

Energy change (in terms of kWh) in the main reservoir was also presented graphically, including the combined subsystem energy contribution and the difference between the main reservoir change and subsystems total.

The study data monthly supplementation totals were listed, and the subsystem contributions specified. The implication for further thermal model refinement was discussed (the possible determination of the main-reservoir-only thermal interaction rather than as an integral system component) in terms of potentially benefitting evaluation of proposed improvements.

In addition, the 2020 winter season weather was discussed and highlighted in terms of its unusual severity. This then informed further discussion of a potential additional extreme weather mitigation strategy (such extremes for the Bloemfontein winter climate as informed by Annexure A).

5.3 Addressing research aims

The relevant questions and issues raised by the adopted method implementation may now be further considered:

1. Determining suitable temperature criteria for an aquaponics system to maintain sustainability, in the Bloemfontein area

The literature reviewed in Chapter 2 indicated that a bio-filter temperature minimum of 7°C was desirable. Since the aquatic species in the system under study are tolerant of temperature below this level, the adoption of the 7°C minimum was indicated. The assumption that the main reservoir temperature and bio-filter temperature would differ marginally (due to high flow volume from the main reservoir through the bio-filter) was physically verified (measured) and further substantiated by experimental results during the study. This allowed the adoption of a method using the main reservoir as a reference for measurement and calculation.

2. Quantifying the potentially large energy requirement to ensure such sustainability is maintained

Consultation of literature dealing with basic physics and thermodynamics indicated that the energy requirement for supplementation to the main aquaponics reservoir could be calculated based on the required temperature change (i.e. supplementation) of the main reservoir and its mass. Since the viability of using the main reservoir as base reference had been justified, it remained to determine the temperature requirement based on the active system historical temperature logs for the previous season.

3. The inherently interrelated nature of an active aquaponics system's subsystems that potentially further complicate such evaluation

The available aquaponics system's main reservoir's historical temperature data was obtained from an active system (i.e. already incorporating the subsystem flow-loops as discussed in the previous chapters), and thus could be directly used to determine a suitable temperature supplementation value. However, it seemed evident that the varied construction of the subsystems (the bio-filter open to the elements, the grow beds in an enclosed tunnel, and the particulate filter and sump protected under a tree and shade netting) would rather indicate a dynamically changing subsystem energy contribution. Thus, the aquaponics system was described in terms of water flow-loops and their energy contribution therefore becoming a mass-transfer of the pumped water through the subsystems as returned to the main reservoir. It must be noted that so describing the loop-energy contribution inherently incorporates any loop-specific to-ambient-surround energy interaction (i.e. it informs the nature of the lumped model derivation).

4. The requirement of a suitable monitoring and control system to quantify experimental data and system interaction

Describing the system in terms of energy-contributing subsystems necessitates the implementation of a monitoring system capable of capturing the relevant data for further evaluation. This informs the implementation of the monitoring and control system as designed and deployed.

The aims of the study were therefore formulated and may now be further discussed:

1. A requirement of establishing a suitable system model relevant to resolving energy requirement for sustainability

A lumped model describing the system interaction in terms of electrical equivalence was derived. This reflects both the nature of the historical active system temperature data used as source, and the current active-system interaction to ambient surround (assuming similar weather conditions). Note that the study delimitations specifically preclude the necessity for a detailed component thermal description. Utilising the system's historical temperature records to determine the maximum temperature loss-slope and the collated multi-year climate data for the study site, in conjunction with the minimum temperature requirement, allowed suitable energy supplementation determination. Also recall the relevance of the temperature recovery slope and chosen temperature buffer value as previously noted. A minimum daily supplementation value of 0.5 °C was determined, equating to 24.406 kWh, daily.

2. The design and deployment of an appropriate monitoring and control system to manage the supplementation energy exchange so implemented

The addition of the solar ETC as supplementation source, coupled with the subsystem flow-loop description informs the adoption of the monitoring and control system as implemented. The system measures all relevant flow-loop temperatures, main reservoir temperature, ambient temperature (and relative humidity, although not specifically required) and ETC output temperature. The supplementation is actively switched as applicable, and data is stored on local backup SD-card (as well as sending it to a cloud-based Google Sheet) in real-time. Locally monitoring the system criteria, while not a specific study aim, was considered beneficial to maintaining and troubleshooting the system and is implemented as a Bluetooth connection to an Android-based serial monitor application. System functional integrity and data contiguity is enhanced by a backup battery and small solar PV panel.

3. The objective of real-time monitoring of such data via cloud-based deployment of results

This objective was achieved by the implementation of an active Google Sheets script, accepting data forwarded from the monitoring and control system via the on-site Wi-Fi access point. Consult Annexure C for additional detail. There are two on-site access points — the system tries the main access point first and switches to the second if a connection failure occurs. A mobile (cell-based battery backed-up) access point was also incorporated in the code in case of fixed-point failure. The relevant system temperature and supplementation criteria are thus available as real-time data for potential integration into third-party monitoring software solutions (potentially managing many such systems). This allows for troubleshooting any site-specific issues, and may potentially include additional criteria such as water quality management, micronutrient addition, remote pump control, irrigation and localised weather monitoring for microclimate conditions. The real-time nature of the data encourages adoption of such monitoring systems into the concept of Sustainable Smart Cities.

4. Comparison of the experimental data with the criteria determined from the system model

The system model and determined supplementation requirement may be compared to experimentally obtained data. However, due to the inherently dynamic nature of weather phenomenon, this is best achieved by considering the successful implementation of the temperature recovery slope, as envisaged in the method presented. In Chapter 4, the section pertaining to the recovery slope specifically addresses this comparison, with further relevant information presented by the van Beukering, Hertzog and Swart, 2020b study (see Annexure G). This instance of failure to maintain sustainability criteria (rapid minimum temperature recovery prevented actual losses) due to weather extremes for the 2020 winter season is causally examined, and system recovery detailed.

5.4 Additional considerations

Recall that the implemented solution targets temperature results around the determined minimum system temperature of 7°C, as outlined in the method presented. Examining the presented main reservoir temperature data gathered during the study period (referring to Figure 4.11), and specifically observing the recovery slope of the main reservoir temperature, the following may be seen:

- The recovery slope (referring to the inter-cold-front positive temperature gradient between cold events) is fairly consistent and conforms to the requirement determined in the method adopted;
- Visually comparing the change in dam temperature with the daily average (mean of daily minima and maxima) temperature as reported by AccuWeather indicates a high positive correlation;
- The loss slope during a cold event is generally higher than the adjacent recovery slope (this is ascribed to the temperature differences but is also impacted by the loss of insolation due to cloud cover, and therefore additional loss of ETC supplementation during such cold fronts); and
- The recovery slope dated further from the winter solstice (21/22 June in the southern hemisphere) is markedly steeper than that of the month of June (and is ascribed to both the higher average temperature and the rise in available insolation, further enhanced by increased ETC supplementation);

Although the inter-cold-event spacing varies and is sometimes less than the identified 10-14 days mentioned in a previous chapter when introducing the methodology (referencing Annexure A), the recovery slope is sufficiently high to establish an effective temperature buffer between cold events. The exceptions are around 14-15 June 2020 (ETC supplementation failure due to installation-related issues) and 15-18 July 2020 with the appearance of three consecutive cold fronts, as further examined by van Beukering, Hertzog and Swart (2021b) and noted by AfriWX (2020b). This worst-case scenario serves as a salient example of the efficacy of the supplementation determination method described and implemented.

In Chapter 4, some correlations drawn from the simplified data set (see Annexure D) were presented. The implication of these may now be further discussed:

- The reported regional temperature data obtained from AccuWeather has a high positive correlation with the system ambient temperature and humidity sensor (type SHT21) of 0.966. This clearly indicates that the system ambient temperature measurement is internally consistent;
- The measured night-time minimum temperature in the south-ETC panel (recall from the installation description that the water drains from the ETC pipes when supplementation is not active at night) has a high positive correlation (0.928) with the AccuWeather regional reported minimum temperatures. This indicates that the south-ETC minimum temperature measurement is also internally consistent;
- The minimum temperature difference measured between the SHT21 (ambient), and south-ETC DS18B20 (indirectly measured and physically distanced ambient) sensors, coupled with the placement distance from the main reservoir, lends credence to the 'localised heat-island' hypothesis previously presented;
- The available insolation data (GHI was used) for the study period is neither contiguous nor complete. Corresponding correlation between GHI and ETC supplementation for the two available contiguous intervals were positive, high at 0.948 and 0.935 respectively. This indicates with a high degree of confidence that the ETC supplementation, as experimentally determined by the temperature difference and the flow-loop energy transfer calculation, may be directly related to available insolation data for any given locale; and
- The correlation between the main reservoir temperature change and the AccuWeather reported regional daily temperature average was moderate and positive at 0.581. This is ascribed to the complexity of the main reservoir thermal interaction (see Figures 4.15 and 4.16) and the indirect lagging nature of the sump-return flow, complemented by the grow bed enclosure (as both thermal storage and insolation effects). The enclosed grow bed acts as a thermal battery during cold events, as seen from the further study by van Beukering,

Hertzog, and Swart (2021a). The initial assumption that the main reservoir be considered as the system equivalent for calculation purposes thus still holds.

The above points confirm the initial assumptions pertaining to the supplementation determination methodology: that the main aquaponic reservoir may be used as a system calculation reference, both because of its physically large mass with respect to the other system components, and since the main reservoir temperature change is largely dependent on the ambient surround temperature.

5.5 Discussion of potential temperature loss mitigation strategies

The detailed evaluation of the aquaponics subsystem energy contribution highlights the need for individually measuring and evaluating the subsystem flow loops. The relevant criteria affecting potential temperature loss mitigation strategies (other than the already adopted and implemented ETC supplementation) are only apparent when examining these obtained results:

- The enclosed grow bed initially acts as a thermal battery (via the combined sump-return flow to the main reservoir) during cold events, as evident when examining the results presented by van Beukering, Hertzog and Swart (2021a);
- The bio-filter contribution during the critical winter period (when the aquaponics system must maintain sustainability and biological integrity by maintaining a temperature above the 7°C required by the bio-filter micro-organisms) was consistently negative. This contribution (see Table 4.1) was sufficiently large that van Beukering, Hertzog and Swart (2021b) recommended relocating the bio-filter into the enclosed grow bed (thus potentially utilising the ‘thermal battery’ effect mentioned). This is a potential low-cost/high-yield solution;
- Additional mass in such an area of nett positive energy contribution to the main reservoir could yield benefit. Placing thermal mass, such as any water storage tanks used in a similar system, within this enclosed space may allow extending the capacity of the thermal battery effect;
- The system particulate filter was implemented after commencement of the study, and as such its thermal effects are not quantified (although implicitly included in the bio-filter and sump-return flow loops). It is likely that relocating the particulate filter into the enclosed grow bed area may yield additional energy benefits;

- An additional mitigation strategy might include adding grow beds in the enclosed space or adding additional enclosed grow bed areas (i.e. the system could be a multi-loop semi-detached topology, passively harvesting additional energy through the enclosed grow beds).
- Managing temperature mitigation around extreme weather events, such as examined by van Beukering, Hertzog and Swart (2021b), may require active strategies. In addition, such weather extremes are predicted by the standard weather forecast, allowing some time to effect temperature change required in the main reservoir. Implementing an ETC solution yields long-term savings at the cost of flexibility in coping with high daily temperature loss. However, adding an additional electrical element to supplement the ETC solution only during such weather extremes presents a low-cost method of ensuring system sustainability. The additional electrical energy required is low (by comparison) and may only be required for a day or two. The energy cost of raising the 42 kl main reservoir temperature by 0.5°C is ~24.6 kWh as in the example presented in a previous chapter;
- In rural areas, or where electricity supply is not reliable, an alternative extreme weather event solution may be possible: using a ‘blanket’ (such as a PVC sheet stretched across the main reservoir, for instance); and
- When constructing or choosing a main aquaponics reservoir, it may be expedient to keep in mind the square/cube law more commonly associated with cell biology: as a given cube (also relevant to other three-dimensional structures) is enlarged (measurement unit dimensions aside), the ratio of surface area to internal volume shrinks. A 1x1x1 cube has a 1 cube volume and a six-square surface area, or a 1/6 ratio. A 2x2x2 cube has an 8 volume and a 24-square surface area, or 1/3 ratio. A cube of 3x3x3 similarly has a 27 volume to 54 surface units, or 1/2 ratio. This becomes relevant because of the nature of the heat loss to ambient surround, which is directly related to the surface area and the thermal resistance to ambient surround. Limiting the exposed surface area to volume ratio is thus desirable. It is intuitively obvious – a large shallow puddle will cool faster than a deep one – but it is less so when dealing with constructed containers.

Discussion around temperature loss mitigation strategy has been limited to retrofitting an existing aquaponics system, as the purpose and nature of the study specifically relates to the examination of an existing system, as supplemented by an ETC. However, the grow bed results obtained (i.e. the nett positive energy contribution and the ‘thermal battery’ effect) yield an obvious further potential solution: The main aquaponics reservoir may be incorporated as a subsurface installation, inside an enclosed grow bed area, when designing new aquaponics systems. This has the potential benefit of limiting main reservoir-to-ambient energy losses (such as those experienced by a free-standing dam exposed to the elements). It also optimises the system footprint, an important factor in potential urban installations.

5.6 Conclusions

The aims of the research as outlined in Chapter 1, and further examined in Chapter 5, have been met. As such, the viability of the deployed monitoring and control system, as well as the feasibility of the implemented solar ETC supplementation scheme are confirmed. The method for supplementation determination as an interrelated factor of the recovery slope and identified temperature buffer, based on historical temperature measurement data and the main reservoir mass, has proven effective.

As presented, it yields a practical approach to the problem of quantifying the energy supplementation requirement for maintaining sustainability of aquaponics systems in the Bloemfontein area. In addition, this also highlights the importance of the discussion surrounding alternative temperature loss mitigation strategies. A multi-year, site-specific temperature data set directly informs the choice of temperature buffer as presented in the method adopted, and thus the determination of the required temperature recovery slope and energy supplementation required.

The nature of the regional winter climate is cold fronts including overcast conditions, interspersed by clear sunny days with consistently high insolation. This lends itself to the successful implementation of the solar ETC. Collation of a multi-year weather data set is therefore necessary to evaluate the method for use in other aquaponics systems.

To further evaluate the validity of results, some relevant statistical correlations were made, confirming the measured system ambient temperature data integrity compared to results reported for the region. The positive, high correlation of reported available insolation (GHI) to experimentally obtained ETC yield data (and thus supplementation energy) indicate that regional insolation data may be used as a basis for calculation of an ETC requirement. This further supports validation of the adopted method and indicates suitability of applying this criterion to additional sites as they may be implemented.

5.7 Recommendations

The method (of quantifying supplementation requirement and describing and quantifying the aquaponics system in terms of contributing energy loops) presented yields practicable results for any given aquaponics system requiring thermal supplementation as outlined. However, the following is of import:

- The system examined is a single semi-detached loop type. The loop-evaluation of contribution towards main reservoir temperature is a flexible approach. The assumption that the main reservoir may be used for calculation purposes as the system equivalent may break down in multi-loop systems, or systems where the mass of the main reservoir does not sufficiently exceed the loop volumes (mass). Evaluation of different system topologies is therefore recommended, using the same methodology, to further validate the approach;
- The complex and dynamic nature of the subsystem energy contribution (specifically the 'thermal battery' nature of the enclosed grow bed section, see Table 4.1) necessitates the implementation of a monitoring and control system to evaluate system energy interaction data. This would be especially important when the aquaponics system structure is more complex (i.e. more grow beds, separate flow returns, and multiple bio-filters). It is therefore recommended to evaluate other aquaponics systems energy interaction, based on their physical layout differences (such as an enclosed/open grow bed area, for example) to compare different construction of these subsystems. This is an important consideration, as a cost/benefit evaluation could potentially indicate significant passive temperature loss mitigation possibilities, based on such construction; and
- The description of energy transfer in terms of grid-equivalence (i.e. kWh energy procurement) allows ready comparison of subsystem energy costs and indicates a measure of potential system improvements as a financial incentive. It is thus recommended that comparable systems be implemented to evaluate subsystem grid-equivalence and potential cost/benefit passive improvements to system topology and/or structural choices.

Some criteria were identified during the study, which may benefit from additional examination. These do not necessarily relate to an ETC implementation, and include the following:

- An anemometer could be added to the measurement and control system functionality. While not directly relevant to the lumped model method described, having access to wind speed data, as measured at the main reservoir, might help refine research data (such as evaporation rates);
- Accurate differential volumetric loop-flow measurements (rather than just the return flow of a flow loop) would yield water usage data. This may prove useful if further studies of plant growth and water usage are required; and
- An additional temperature/humidity sensor in the enclosed grow bed area could be beneficial: The 'thermal battery' nature of the grow bed area could only be indirectly inferred from the sump-return flow temperature measurement as flowing into the main reservoir, see Annexure F. Quantifying the potential of an enclosed grow bed area in terms of energy contribution has the possible benefit of low-cost/high-yield impact on aquaponics system design. The structure is not expensive (it is constructed from shade net and a steel frame), and the potential benefit is significant (see Table 4.1 sump return column). The total sump-return contribution, relative to the total ETC energy contribution was about 1/6th, which is a significant figure considering that the ETC energy harvesting totalled over 3 MWh for the study period.

The implemented monitoring and control system, logging real-time data to the internet, lends itself to inclusion into the concept of Sustainable Smart Cities. In addition, the presentation of the method using mass-flow energy transfer of the subsystem flow-loops may be readily applied to other system topologies.

References

AccuWeather. (2020) [online] Available at: https://www.accuweather.com/ [Accessed October 2020].

AfriWX. (2020) *Mammoth Cold Front Approaches Southern Africa - Biggest in years* (n.d.). , available at: https://weatherblog.co.za/snow/mammoth-cold-front-approaches-southern-africa-biggest-in-decades/ [Accessed 22 April 2021].

AfriWX. (2020) *3 Cold Fronts to hit South Africa - Lesotho to see heaviest snowfall of all.* (n.d.). , available at: https://weatherblog.co.za/cold-front/3-cold-fronts-to-hit-south-africa-lesotho-to-see-heaviest-snowfall-of-all/ [Accessed 22 April 2021].

Alamri, A., Ansari, W.S., Hassan, M.M., Hossain, M.S., Alelaiwi, A. and Hossain, M.A. (2013) A Survey on Sensor-Cloud: Architecture, Applications, and Approaches, *International Journal of Distributed Sensor Networks*, Vol. 9 No. 2, p. 917923.

Albright-Borden, R., Wang, J. and Thompson, S. (2019) Design of an Urban Garden Aquaponics System, *Interdisciplinary Design Senior Theses*, available at: https://scholarcommons.scu.edu/idp_senior/50. [Accessed 3 March 2020]

Assisi, A., Banzi, R., Buonocore, C., Capasso, F., Muzio, V.D., Michelacci, F., Renzo, D., *et al.* (2006) Fish oil and mental health: the role of n-3 long-chain polyunsaturated fatty acids in cognitive development and neurological disorders. *International Clinical Psychopharmacology*, Vol. 21 No. 6, pp. 319–336.

Beveridge, M.C.M., Thilsted, S.H., Phillips, M.J., Metian, M., Troell, M. and Hall, S.J. (2013) Meeting the food and nutrition needs of the poor: the role of fish and the opportunities and challenges emerging from the rise of aquaculturea. *Journal of Fish Biology*, Vol. 83 No. 4, pp. 1067–1084.

Belomestnykh, O., S.E. (n.d.). A rebuilt, more real time Google documents. *Google Drive Blog*, available at: https://drive.googleblog.com/2010/04/a-rebuilt-more-real-time-google.html [Accessed 30 April 2020].

Cannon, W.R. (2014) Concepts, Challenges, and Successes in Modeling Thermodynamics of Metabolism. *Frontiers in Bioengineering and Biotechnology*, Vol. 2, available at: https://doi.org/10.3389/fbioe.2014.00053. [Accessed 27 October 2020]

Chunjie Li, Chew Tin Lee, Yueshu Gao, Haslenda Hashim, Xiaojun Zhang, Wei-Min Wu and Zhenjia Zhang. (2018) Prospect of aquaponics for the sustainable development of food production in urban. *Chemical Engineering Transactions*, Vol. 63, pp. 475–480.

Clarke, A. and Johnston, N.M. (1999) Scaling of metabolic rate with body mass and temperature in teleost fish. *Journal of Animal Ecology*, Vol. 68 No. 5, pp. 893–905.

Close, C.M., Frederick, D.K. and Newell, J.C. (2002) *Modeling and Analysis of Dynamic Systems*, 3rd ed., Wiley, New York, NY.

Coetzee R.A., Aggrey Mwesigye and Zhongjie Huan. (2017) Optimal slope angle selection of an evacuated tube collector for domestic solar water heating. *Journal of Energy in Southern Africa*, Vol. 28 No. 1, pp. 104–119.

Dongellini, M., Falcioni, S., Martelli, A. and Morini, G.L. (2015) Dynamic Simulation of Outdoor Swimming Pool Solar Heating, *Energy Procedia*, Vol. 81, pp. 1–10.

Dasig, D.Jr. (2019), Implementing Zigbee-based Wireless Sensor Network in the Design of Water Quality Monitoring System. *International Journal of Recent Technology and Engineering*, Vol. 8 No. 3, pp. 6174–6179.

Esfandiari, R.S. and Lu, B. (2014), *Modeling and Analysis of Dynamic Systems*, 2nd ed., CRC Press, Taylo and Francis Group, Boca Raton, London, New York.

EUMETSAT (2020), [online], available at: https://sawx.co.za/satellite/animated-satellite/africa-weather-satellite-photoanimated-airmass/ [Accessed July 2020].

Goddek, S., Delaide, B., Mankasingh, U., Ragnarsdottir, K.V., Jijakli, H. and Thorarinsdottir, R. (2015) Challenges of Sustainable and Commercial Aquaponics. *Sustainability*, Vol. 7 No. 4, pp. 4199–4224.

Hertzog, P.E. and Swart, A.J. (2016) Validating the optimum tilt angle for PV modules in a semi-arid region of South Africa for the winter season. *2016 13th International Conference on Electrical Engineering/Electronics, Computer, Telecommunications and Information Technology (ECTI-CON)*, presented at the 2016 13th International Conference on Electrical Engineering/Electronics, Computer, Telecommunications and Information Technology (ECTI-CON), pp. 1–6.

Hoagland, D.R. (1950) *The Water-Culture Method for Growing Plants without Soil*, Rev. ed. / by D.I. Arnon., College of Agriculture, University of California, Berkeley, Calif.

IPCC, (2019) Summary for Policymakers — Special Report on Climate Change and Land. IPCC, 2019.

Izrailevsky, Y. and Bell, C. (2018) Cloud Reliability. *IEEE Cloud Computing*, Vol. 5 No. 3, pp. 39–44.

Karimanzira, D. and Rauschenbach, T. (2018) Optimal Utilization of Renewable Energy in Aquaponic Systems. *Energy and Power Engineering*, Vol. 10 No. 6, pp. 279–300.

Kjellby, R.A., Cenkeramaddi, L.R., Frøytlog, A., Lozano, B.B., Soumya, J. and Bhange, M. (2019) Long-range Self-powered IoT Devices for Agriculture Aquaponics Based on Multi-hop Topology. *2019 IEEE 5th World Forum on Internet of Things (WF-IoT)*, presented at the 2019 IEEE 5th World Forum on Internet of Things (WF-IoT), pp. 545–549.

Liu, Y., Huang, J. and Zikhali, P. (2014) Use of Human Excreta as Manure in Rural China. *Journal of Integrative Agriculture*, Vol. 13 No. 2, pp. 434–442.

Love, D.C., Fry, J.P., Genello, L., Hill, E.S., Frederick, J.A., Li, X. and Semmens, K. (2014) An International Survey of Aquaponics Practitioners. *PLoS ONE*, Vol. 9 No. 7, available at: https://doi.org/10.1371/journal.pone.0102662. [Accessed 22 January 2020].

Nagayo, A.M., Mendoza, C., Vega, E., Izki, R.K.S.A. and Jamisola, R.S. (2017) An automated solar-powered aquaponics system towards agricultural sustainability in the Sultanate of Oman. *2017 IEEE International Conference on Smart Grid and Smart Cities (ICSGSC)*, presented at the 2017 IEEE International Conference on Smart Grid and Smart Cities (ICSGSC), pp. 42–49.

NASA GISS Data.GISS: Insolation at Specified Location. (n.d.), available at: https://data.giss.nasa.gov/modelE/ar5plots/srlocat.html [Accessed 1 October 2020].

Odema, M., Adly, I., Wahba, A. and Ragai, H. (2018), Smart Aquaponics System for Industrial Internet of Things (IIoT) in Hassanien, A.E., Shaalan, K., Gaber, T. and Tolba, M.F. (Eds.), *Proceedings of the International Conference on Advanced Intelligent Systems and Informatics 2017*, Springer International Publishing, Cham, pp. 844–854.

Phillis, Y.A., Chairetis, N., Grigoroudis, E., Kanellos, F.D. and Kouikoglou, V.S. (2018) Climate security assessment of countries. *Climatic Change*, Vol. 148 No. 1, pp. 25–43.

Proksch, G., Ianchenko, A. and Kotzen, B. (2019) Aquaponics in the Built Environment in Goddek, S., Joyce, A., Kotzen, B. and Burnell, G.M. (Eds.), *Aquaponics Food Production Systems: Combined Aquaculture and Hydroponic Production Technologies for the Future*, Springer International Publishing, Cham, pp. 523–558.

Sabiha, M.A., Saidur, R., Mekhilef, S. and Mahian, O. (2015) Progress and latest developments of evacuated tube solar collectors. *Renewable and Sustainable Energy Reviews*, Vol. 51, pp. 1038–1054.

Sishuba, S. Scaling up aquaponics. (n.d.), available at: https://www.farmersweekly.co.za/agri-business/agribusinesses/scaling-up-aquaponics/ [Accessed 21 November 2019].

Statistics SA Quarterly Labour Force Survey (QLFS) - Q3:2019. Available at http://statssa.gov.za/publications/PO2111/PO2114thQuarter2019.pdf [Accessed 21 June 2020]

Stocker, T.F. (n.d.) *IPCC, 2013: Climate Change 2013: The Physical Science Basis. Contribution of Working Group I to the Fifth Assessment Report of the Intergovernmental Panel on Climate Change*, Cambridge University Press, Cambridge, United Kingdom and New York, NY, USA, p. 1535 pp.

Sugita, H., Nakamura, H. and Shimada, T. (2005) Microbial communities associated with filter materials in recirculating aquaculture systems of freshwater fish *Aquaculture*, Vol. 243 No. 1, pp. 403–409.

Tomlinson, L. (2017) Indoor Aquaponics in Abandoned Buildings: A Potential Solution to Food Deserts. *Sustainable Development Law and Policy*, Vol.16: Iss. 1, Article 5. Available at: http://digitalcommons.wcl.american.edu/sdlp/vol16/iss1/5 [Accessed 23 November 2019]

UNOSSC: Good Practices in South-South and Triangular Cooperation for Sustainable Development - Vol. 2 (2018) - In Seven Languages. (2018), *UNOSSC*, 28 November, available at: https://www.unsouthsouth.org/2018/11/28/good-practices-in-south-south-and-triangular-cooperation-for-sustainable-development-vol-2-2018-in-seven-languages/ [Accessed 21 January 2020].

unreeeal. (2020) *Unreeeal/Esp32-Google-Sheets*, available at: https://github.com/unreeeal/esp32-google-sheets [Accessed 9 November 2020].

van Beukering, C.A., Hertzog, P.E. and Swart, A.J. (2021) Investigating thermal supplementation of an aquaponics system under severe climate conditions. *World Journal of Engineering*, Vol. 18 No 4, pp. 639-644.

van Beukering, C.A., Hertzog, P.E. and Swart, A.J. (2021) A Simplified Design Process for Thermal Supplementation of a Medium Sized Aquaponics System to Ensure Sustainability. *REVISTA GEINTEC-GESTAO INOVACAO E TECNOLOGIAS*, Vol. 11 No. 4, pp. 3455–3467.

Vernandhes, W., Salahuddin, N.S., Kowanda, A. and Sari, S.P. (2017) Smart aquaponic with monitoring and control system based on iot. *2017 Second International Conference on Informatics and Computing (ICIC)*, presented at the 2017 Second International Conference on Informatics and Computing (ICIC), pp. 1–6.

Walraven, B.C. (n.d.)., (2014) Aquaponics: Economics and social potential for sustainable food production. *Senior Honours Projects, 2010*-current. 493. Available at: https://commons.lib.jmu.edu.honors201019/493 [Accessed 27 October 2020]

Annexure A

Compiled (2004 – 2016) July temperature, for Bloemfontein, (collated from the **https://freemeteo.co.za** site, accessed Mar 2020)

To visualise the typical weather patterns that were considered to 'incur higher risk' of the aquaponic system under study failing to maintain the required 7˚C bio-filter minimum temperature, a multi-year daily minimum/maximum temperature set was collated from available online data for Bloemfontein in the month of July. The values considered were colourised as follows:

- Daily minimum less than -2˚C highlighted 'Yellow'
- Daily maximum less than 15˚C highlighted 'Red'
- Daily maximum 15˚C or more highlighted 'Green'

Refer to the text in Chapter 3 for additional criteria regarding interpretation of these conditions. Typical 'danger conditions', potentially leading to excessive main reservoir temperature loss, are characterised by consecutive daily yellow and red block combinations.

Date	Daily minimum temperature	Daily maximum temperature	Maximum steady wind	Maximum wind gust	Total daily precipitation
7/1/2004	0°C	20°C	16 Km/h	N/A	0mm
7/2/2004	2°C	14°C	13 Km/h	N/A	0mm
7/3/2004	-2°C	17°C	15 Km/h	N/A	0mm
7/4/2004	-5°C	15°C	21 Km/h	N/A	0mm
7/5/2004	-3°C	16°C	11 Km/h	N/A	0mm
7/6/2004	-3°C	16°C	8 Km/h	N/A	0mm
7/7/2004	-4°C	17°C	9 Km/h	N/A	0mm
7/8/2004	-4°C	16°C	9 Km/h	N/A	0mm
7/9/2004	-5°C	16°C	11 Km/h	N/A	0mm
7/10/2004	-5°C	16°C	N/A	N/A	0mm
7/11/2004	-4°C	17°C	9 Km/h	31 Km/h	0mm
7/12/2004	-4°C	18°C	15 Km/h	N/A	0mm

Date	Daily minimum temperature	Daily maximum temperature	Maximum steady wind	Maximum wind gust	Total daily precipitation
7/13/2004	-3°C	12°C	37 Km/h	61 Km/h	0mm
7/14/2004	-6°C	12°C	15 Km/h	N/A	0mm
7/15/2004	-2°C	15°C	13 Km/h	N/A	0mm
7/16/2004	-5°C	16°C	9 Km/h	N/A	0mm
7/17/2004	-5°C	17°C	8 Km/h	N/A	0mm
7/18/2004	-5°C	17°C	9 Km/h	N/A	0mm
7/19/2004	-4°C	18°C	13 Km/h	N/A	0mm
7/20/2004	-3°C	18°C	9 Km/h	N/A	0mm
7/21/2004	-4°C	18°C	8 Km/h	N/A	0mm
7/22/2004	-4°C	19°C	9 Km/h	N/A	0mm
7/23/2004	-2°C	22°C	21 Km/h	35 Km/h	0mm
7/24/2004	-2°C	22°C	N/A	39 Km/h	0mm
7/25/2004	-2°C	19°C	39 Km/h	N/A	0mm
7/26/2004	-1°C	11°C	15 Km/h	N/A	0mm
7/27/2004	-6°C	13°C	N/A	N/A	0mm
7/28/2004	-2°C	14°C	37 Km/h	N/A	0mm
7/29/2004	-3°C	16°C	16 Km/h	76 Km/h	0mm
7/30/2004	-4°C	20°C	28 Km/h	48 Km/h	0mm
7/31/2004	-1°C	20°C	N/A	N/A	0mm
7/1/2005	1°C	22°C	11 Km/h	N/A	0mm
7/2/2005	-4°C	18°C	13 Km/h	N/A	0mm
7/3/2005	-4°C	19°C	16 Km/h	N/A	0mm
7/4/2005	0°C	19°C	18 Km/h	N/A	0mm
7/5/2005	2°C	18°C	11 Km/h	N/A	0mm
7/6/2005	0°C	17°C	8 Km/h	N/A	0mm
7/7/2005	-1°C	17°C	9 Km/h	N/A	0mm
7/8/2005	-2°C	19°C	9 Km/h	N/A	0mm
7/9/2005	-3°C	19°C	9 Km/h	N/A	0mm

Date	Daily minimum temperature	Daily maximum temperature	Maximum steady wind	Maximum wind gust	Total daily precipitation
7/10/2005	-3°C	19°C	8 Km/h	N/A	0mm
7/11/2005	-4°C	20°C	13 Km/h	N/A	0mm
7/12/2005	-3°C	21°C	9 Km/h	N/A	0mm
7/13/2005	-4°C	21°C	8 Km/h	N/A	0mm
7/14/2005	-2°C	20°C	16 Km/h	N/A	0mm
7/15/2005	0°C	19°C	21 Km/h	N/A	0mm
7/16/2005	-3°C	19°C	8 Km/h	N/A	0mm
7/17/2005	-5°C	19°C	N/A	N/A	0mm
7/18/2005	-2°C	20°C	9 Km/h	N/A	0mm
7/19/2005	-2°C	22°C	N/A	37 Km/h	0mm
7/20/2005	-1°C	22°C	N/A	N/A	0mm
7/21/2005	-1°C	18°C	11 Km/h	N/A	0mm
7/22/2005	-3°C	19°C	9 Km/h	N/A	0mm
7/23/2005	-4°C	22°C	8 Km/h	N/A	0mm
7/24/2005	-3°C	24°C	13 Km/h	N/A	0mm
7/25/2005	-2°C	25°C	16 Km/h	N/A	0mm
7/26/2005	-1°C	25°C	21 Km/h	48 Km/h	0mm
7/27/2005	-5°C	23°C	N/A	N/A	0mm
7/28/2005	-4°C	20°C	16 Km/h	N/A	0mm
7/29/2005	-2°C	21°C	15 Km/h	N/A	0mm
7/30/2005	-1°C	23°C	16 Km/h	N/A	0mm
7/31/2005	-1°C	23°C	N/A	N/A	0mm
	Note 2006 logs unavailable from this source				
7/1/2007	-5°C	19°C	42 Km/h	61 Km/h	0mm
7/2/2007	-7°C	14°C	13 Km/h	N/A	0mm
7/3/2007	-6°C	15°C	9 Km/h	N/A	0mm
7/4/2007	-6°C	16°C	9 Km/h	N/A	0mm
7/5/2007	-5°C	16°C	16 Km/h	N/A	0mm

Date	Daily minimum temperature	Daily maximum temperature	Maximum steady wind	Maximum wind gust	Total daily precipitation
7/6/2007	-4°C	16°C	16 Km/h	N/A	0mm
7/7/2007	-5°C	19°C	N/A	N/A	0mm
7/8/2007	-5°C	19°C	26 Km/h	N/A	0mm
7/9/2007	-8°C	16°C	8 Km/h	N/A	0mm
7/10/2007	-8°C	18°C	13 Km/h	N/A	0mm
7/11/2007	-6°C	18°C	N/A	N/A	0mm
7/12/2007	-5°C	17°C	24 Km/h	46 Km/h	0mm
7/13/2007	-7°C	21°C	13 Km/h	N/A	0mm
7/14/2007	-6°C	21°C	11 Km/h	N/A	0mm
7/15/2007	-5°C	21°C	9 Km/h	N/A	0mm
7/16/2007	-5°C	22°C	11 Km/h	N/A	0mm
7/17/2007	-4°C	22°C	8 Km/h	N/A	0mm
7/18/2007	-3°C	21°C	13 Km/h	N/A	0mm
7/19/2007	-4°C	20°C	11 Km/h	N/A	0mm
7/20/2007	-4°C	21°C	16 Km/h	N/A	0mm
7/21/2007	-3°C	21°C	15 Km/h	N/A	0mm
7/22/2007	-2°C	22°C	15 Km/h	N/A	0mm
7/23/2007	3°C	23°C	15 Km/h	N/A	0mm
7/24/2007	-2°C	23°C	N/A	N/A	0mm
7/25/2007	-2°C	13°C	9 Km/h	N/A	0mm
7/26/2007	-6°C	14°C	13 Km/h	N/A	0mm
7/27/2007	1°C	13°C	37 Km/h	N/A	N/A
7/28/2007	-4°C	9°C	16 Km/h	N/A	0mm
7/29/2007	-4°C	14°C	N/A	N/A	0mm
7/30/2007	-4°C	16°C	9 Km/h	N/A	0mm
7/31/2007	-7°C	22°C	8 Km/h	N/A	0mm
7/1/2008	-4°C	19°C	13 Km/h	N/A	0mm
7/2/2008	-3°C	21°C	16 Km/h	N/A	0mm

Date	Daily minimum temperature	Daily maximum temperature	Maximum steady wind	Maximum wind gust	Total daily precipitation
7/3/2008	-3°C	21°C	22 Km/h	N/A	0mm
7/4/2008	-2°C	21°C	11 Km/h	N/A	0mm
7/5/2008	-3°C	18°C	N/A	N/A	0mm
7/6/2008	1°C	12°C	9 Km/h	N/A	0mm
7/7/2008	-4°C	17°C	N/A	N/A	0mm
7/8/2008	1°C	22°C	35 Km/h	55 Km/h	0mm
7/9/2008	-2°C	9°C	21 Km/h	N/A	0mm
7/10/2008	-8°C	11°C	11 Km/h	N/A	0mm
7/11/2008	-8°C	13°C	8 Km/h	N/A	0mm
7/12/2008	-7°C	13°C	16 Km/h	N/A	0mm
7/13/2008	-8°C	15°C	13 Km/h	N/A	0mm
7/14/2008	-3°C	20°C	13 Km/h	N/A	0mm
7/15/2008	1°C	22°C	24 Km/h	N/A	0mm
7/16/2008	2°C	22°C	9 Km/h	N/A	0mm
7/17/2008	0°C	22°C	15 Km/h	N/A	0mm
7/18/2008	2°C	22°C	16 Km/h	N/A	0mm
7/19/2008	0°C	20°C	8 Km/h	N/A	0mm
7/20/2008	0°C	20°C	9 Km/h	N/A	0mm
7/21/2008	0°C	21°C	11 Km/h	N/A	0mm
7/22/2008	-1°C	22°C	8 Km/h	N/A	0mm
7/23/2008	-1°C	22°C	9 Km/h	N/A	0mm
7/24/2008	0°C	21°C	16 Km/h	N/A	0mm
7/25/2008	0°C	20°C	N/A	N/A	0mm
7/26/2008	-1°C	20°C	13 Km/h	N/A	0mm
7/27/2008	0°C	22°C	N/A	N/A	0mm
7/28/2008	-2°C	22°C	9 Km/h	N/A	0mm
7/29/2008	-3°C	20°C	11 Km/h	N/A	0mm
7/30/2008	-3°C	23°C	15 Km/h	N/A	0mm

Date	Daily minimum temperature	Daily maximum temperature	Maximum steady wind	Maximum wind gust	Total daily precipitation
7/31/2008	0°C	24°C	21 Km/h	41 Km/h	0mm
7/1/2009	-4°C	16°C	9 Km/h	N/A	0mm
7/2/2009	-5°C	16°C	15 Km/h	N/A	0mm
7/3/2009	-4°C	16°C	9 Km/h	N/A	0mm
7/4/2009	-5°C	17°C	31 Km/h	N/A	0mm
7/5/2009	-1°C	17°C	15 Km/h	N/A	0mm
7/6/2009	-5°C	16°C	11 Km/h	N/A	0mm
7/7/2009	-4°C	18°C	11 Km/h	N/A	0mm
7/8/2009	-5°C	18°C	15 Km/h	N/A	0mm
7/9/2009	-3°C	18°C	9 Km/h	N/A	0mm
7/10/2009	-3°C	18°C	15 Km/h	N/A	0mm
7/11/2009	-4°C	20°C	24 Km/h	N/A	0mm
7/12/2009	-1°C	20°C	22 Km/h	N/A	0.2mm
7/13/2009	-6°C	16°C	N/A	N/A	0mm
7/14/2009	-2°C	16°C	13 Km/h	N/A	0mm
7/15/2009	-5°C	10°C	13 Km/h	N/A	0mm
7/16/2009	-7°C	15°C	8 Km/h	N/A	0mm
7/17/2009	-7°C	18°C	9 Km/h	N/A	0mm
7/18/2009	-6°C	18°C	11 Km/h	N/A	0mm
7/19/2009	-5°C	19°C	8 Km/h	N/A	0mm
7/20/2009	-5°C	19°C	13 Km/h	N/A	0mm
7/21/2009	-4°C	18°C	13 Km/h	N/A	0mm
7/22/2009	-4°C	18°C	16 Km/h	N/A	0mm
7/23/2009	-2°C	17°C	37 Km/h	N/A	0mm
7/24/2009	-4°C	11°C	22 Km/h	N/A	0mm
7/25/2009	-7°C	14°C	9 Km/h	N/A	0mm
7/26/2009	-7°C	18°C	8 Km/h	N/A	0mm
7/27/2009	-6°C	18°C	9 Km/h	N/A	0mm

Date	Daily minimum temperature	Daily maximum temperature	Maximum steady wind	Maximum wind gust	Total daily precipitation
7/28/2009	-5°C	18°C	15 Km/h	N/A	0mm
7/29/2009	-4°C	19°C	11 Km/h	N/A	0mm
7/30/2009	-1°C	19°C	11 Km/h	N/A	0mm
7/31/2009	2°C	19°C	15 Km/h	N/A	4.8mm
7/1/2010	0°C	20°C	21 Km/h	N/A	0mm
7/2/2010	-1°C	20°C	13 Km/h	N/A	0mm
7/3/2010	7°C	19°C	13 Km/h	N/A	0mm
7/4/2010	4°C	20°C	9 Km/h	N/A	0mm
7/5/2010	3°C	20°C	16 Km/h	N/A	0mm
7/6/2010	-1°C	21°C	16 Km/h	N/A	0mm
7/7/2010	6°C	22°C	16 Km/h	N/A	0mm
7/8/2010	4°C	22°C	24 Km/h	N/A	0mm
7/9/2010	2°C	19°C	15 Km/h	N/A	0mm
7/10/2010	5°C	21°C	24 Km/h	N/A	0mm
7/11/2010	1°C	21°C	26 Km/h	N/A	0mm
7/12/2010	-3°C	14°C	26 Km/h	42 Km/h	0mm
7/13/2010	-6°C	14°C	26 Km/h	N/A	0mm
7/14/2010	-1°C	16°C	31 Km/h	46 Km/h	0mm
7/15/2010	0°C	16°C	24 Km/h	N/A	0mm
7/16/2010	-3°C	12°C	22 Km/h	N/A	0mm
7/17/2010	-6°C	20°C	9 Km/h	N/A	0mm
7/18/2010	-4°C	21°C	21 Km/h	N/A	0mm
7/19/2010	-4°C	22°C	9 Km/h	N/A	0mm
7/20/2010	-3°C	22°C	11 Km/h	N/A	0mm
7/21/2010	-4°C	22°C	N/A	N/A	0mm
7/22/2010	0°C	21°C	N/A	35 Km/h	0mm
7/23/2010	-1°C	21°C	15 Km/h	N/A	0mm
7/24/2010	2°C	22°C	21 Km/h	N/A	0mm
7/25/2010	1°C	22°C	9 Km/h	N/A	0mm

Date	Daily minimum temperature	Daily maximum temperature	Maximum steady wind	Maximum wind gust	Total daily precipitation
7/26/2010	-1°C	23°C	15 Km/h	31 Km/h	0mm
7/27/2010	0°C	23°C	15 Km/h	N/A	0mm
7/28/2010	0°C	24°C	13 Km/h	N/A	0mm
7/29/2010	0°C	24°C	15 Km/h	N/A	0mm
7/30/2010	5°C	24°C	16 Km/h	N/A	0mm
7/31/2010	1°C	20°C	15 Km/h	N/A	0mm
7/1/2011	-6°C	13°C	11 Km/h	N/A	0mm
7/2/2011	-8°C	15°C	24 Km/h	N/A	0mm
7/3/2011	-7°C	15°C	8 Km/h	N/A	0mm
7/4/2011	-6°C	16°C	34 Km/h	52 Km/h	0mm
7/5/2011	1°C	16°C	35 Km/h	48 Km/h	0.2mm
7/6/2011	-2°C	14°C	24 Km/h	N/A	0mm
7/7/2011	-4°C	17°C	8 Km/h	N/A	0mm
7/8/2011	-4°C	17°C	11 Km/h	N/A	0mm
7/9/2011	-3°C	17°C	16 Km/h	N/A	0mm
7/10/2011	-3°C	17°C	11 Km/h	N/A	0mm
7/11/2011	-4°C	17°C	13 Km/h	N/A	0mm
7/12/2011	-4°C	17°C	9 Km/h	N/A	0mm
7/13/2011	-4°C	17°C	9 Km/h	N/A	0mm
7/14/2011	-4°C	17°C	11 Km/h	N/A	0mm
7/15/2011	-4°C	17°C	11 Km/h	N/A	0mm
7/16/2011	-5°C	18°C	8 Km/h	N/A	0mm
7/17/2011	-6°C	18°C	11 Km/h	N/A	0mm
7/18/2011	-6°C	17°C	15 Km/h	N/A	0mm
7/19/2011	-5°C	19°C	N/A	N/A	0mm
7/20/2011	-5°C	19°C	24 Km/h	42 Km/h	0mm
7/21/2011	-5°C	20°C	15 Km/h	29 Km/h	0mm
7/22/2011	-3°C	22°C	9 Km/h	N/A	0mm
7/23/2011	-3°C	22°C	16 Km/h	N/A	0mm

Date	Daily minimum temperature	Daily maximum temperature	Maximum steady wind	Maximum wind gust	Total daily precipitation
7/24/2011	-2°C	22°C	28 Km/h	N/A	0mm
7/25/2011	5°C	22°C	41 Km/h	59 Km/h	N/A
7/26/2011	2°C	15°C	15 Km/h	N/A	0.2mm
7/27/2011	-4°C	16°C	N/A	N/A	0mm
7/28/2011	1°C	17°C	31 Km/h	44 Km/h	0mm
7/29/2011	0°C	17°C	24 Km/h	N/A	N/A
7/30/2011	-5°C	16°C	9 Km/h	N/A	0mm
7/31/2011	-5°C	19°C	9 Km/h	N/A	0mm
7/1/2012	-4°C	23°C	22 Km/h	N/A	0mm
7/2/2012	-1°C	23°C	24 Km/h	N/A	0mm
7/3/2012	0°C	23°C	26 Km/h	N/A	0mm
7/4/2012	-2°C	23°C	31 Km/h	N/A	0mm
7/5/2012	-1°C	21°C	22 Km/h	N/A	0mm
7/6/2012	2°C	21°C	26 Km/h	N/A	0mm
7/7/2012	2°C	20°C	29 Km/h	N/A	3.8mm
7/8/2012	1°C	14°C	15 Km/h	N/A	4mm
7/9/2012	-4°C	16°C	11 Km/h	29 Km/h	0mm
7/10/2012	-4°C	18°C	15 Km/h	N/A	0mm
7/11/2012	-3°C	18°C	11 Km/h	N/A	0.2mm
7/12/2012	-4°C	18°C	16 Km/h	N/A	0mm
7/13/2012	-3°C	18°C	26 Km/h	37 Km/h	0.7mm
7/14/2012	1°C	18°C	28 Km/h	41 Km/h	6.3mm
7/15/2012	1°C	10°C	22 Km/h	44 Km/h	0.2mm
7/16/2012	0°C	13°C	N/A	N/A	0mm
7/17/2012	-3°C	18°C	24 Km/h	N/A	0mm
7/18/2012	-3°C	19°C	11 Km/h	N/A	0mm
7/19/2012	-3°C	19°C	13 Km/h	N/A	0mm
7/20/2012	-3°C	20°C	24 Km/h	N/A	0mm
7/21/2012	-3°C	21°C	26 Km/h	N/A	0mm

Date	Daily minimum temperature	Daily maximum temperature	Maximum steady wind	Maximum wind gust	Total daily precipitation
7/22/2012	-3°C	21°C	N/A	N/A	0mm
7/23/2012	-6°C	16°C	9 Km/h	N/A	0mm
7/24/2012	-5°C	17°C	13 Km/h	N/A	0mm
7/25/2012	-5°C	20°C	9 Km/h	N/A	0mm
7/26/2012	-5°C	21°C	15 Km/h	N/A	0mm
7/27/2012	-4°C	21°C	26 Km/h	N/A	0.7mm
7/28/2012	-1°C	18°C	21 Km/h	N/A	0mm
7/29/2012	-6°C	17°C	15 Km/h	N/A	0mm
7/30/2012	-7°C	19°C	11 Km/h	N/A	0mm
7/31/2012	-4°C	21°C	28 Km/h	N/A	0mm
7/1/2013	1°C	24°C	39 Km/h	N/A	0mm
7/2/2013	2°C	24°C	22 Km/h	N/A	0mm
7/3/2013	0°C	23°C	9 Km/h	N/A	0mm
7/4/2013	1°C	22°C	41 Km/h	N/A	0mm
7/5/2013	8°C	21°C	39 Km/h	57 Km/h	2.2mm
7/6/2013	4°C	17°C	22 Km/h	N/A	0mm
7/7/2013	3°C	21°C	13 Km/h	N/A	0mm
7/8/2013	2°C	23°C	15 Km/h	N/A	0mm
7/9/2013	1°C	23°C	11 Km/h	N/A	0mm
7/10/2013	4°C	23°C	29 Km/h	N/A	0mm
7/11/2013	4°C	20°C	N/A	N/A	0mm
7/12/2013	0°C	19°C	13 Km/h	N/A	0mm
7/13/2013	-1°C	19°C	13 Km/h	N/A	0mm
7/14/2013	-2°C	21°C	9 Km/h	N/A	0mm
7/15/2013	0°C	21°C	31 Km/h	44 Km/h	0mm
7/16/2013	1°C	22°C	26 Km/h	N/A	0mm
7/17/2013	-1°C	23°C	22 Km/h	N/A	0mm
7/18/2013	5°C	23°C	41 Km/h	55 Km/h	0mm
7/19/2013	4°C	20°C	31 Km/h	N/A	0mm

Date	Daily minimum temperature	Daily maximum temperature	Maximum steady wind	Maximum wind gust	Total daily precipitation
7/20/2013	-3°C	17°C	22 Km/h	29 Km/h	0mm
7/21/2013	-3°C	19°C	9 Km/h	N/A	0mm
7/22/2013	-3°C	19°C	22 Km/h	42 Km/h	0mm
7/23/2013	2°C	21°C	29 Km/h	48 Km/h	0mm
7/24/2013	-3°C	21°C	N/A	N/A	0mm
7/25/2013	0°C	21°C	16 Km/h	N/A	0mm
7/26/2013	-3°C	23°C	22 Km/h	N/A	0mm
7/27/2013	-1°C	23°C	29 Km/h	46 Km/h	0mm
7/28/2013	-2°C	23°C	26 Km/h	N/A	0mm
7/29/2013	-6°C	17°C	21 Km/h	N/A	0mm
7/30/2013	-5°C	21°C	11 Km/h	N/A	0mm
7/31/2013	-2°C	21°C	11 Km/h	N/A	0mm
7/1/2014	0°C	23°C	16 Km/h	N/A	0mm
7/2/2014	1°C	22°C	13 Km/h	N/A	0mm
7/3/2014	-2°C	21°C	15 Km/h	N/A	0mm
7/4/2014	-1°C	21°C	N/A	N/A	0mm
7/5/2014	-2°C	21°C	28 Km/h	N/A	0mm
7/6/2014	-6°C	15°C	13 Km/h	N/A	0mm
7/7/2014	-3°C	10°C	13 Km/h	N/A	0mm
7/8/2014	-4°C	11°C	21 Km/h	N/A	0mm
7/9/2014	-8°C	12°C	11 Km/h	N/A	0mm
7/10/2014	-9°C	15°C	15 Km/h	N/A	0mm
7/11/2014	-8°C	15°C	N/A	N/A	0mm
7/12/2014	-3°C	15°C	15 Km/h	N/A	0mm
7/13/2014	-8°C	8°C	5 Km/h	N/A	0mm
7/14/2014	-7°C	19°C	15 Km/h	N/A	0mm
7/15/2014	-7°C	20°C	24 Km/h	37 Km/h	0mm
7/16/2014	-5°C	21°C	N/A	N/A	0mm
7/17/2014	-2°C	21°C	34 Km/h	48 Km/h	0mm

Date	Daily minimum temperature	Daily maximum temperature	Maximum steady wind	Maximum wind gust	Total daily precipitation
7/18/2014	-2°C	21°C	24 Km/h	N/A	0mm
7/19/2014	-7°C	15°C	15 Km/h	N/A	0mm
7/20/2014	-6°C	20°C	11 Km/h	N/A	0mm
7/21/2014	-6°C	20°C	11 Km/h	N/A	0mm
7/22/2014	-4°C	21°C	N/A	N/A	0mm
7/23/2014	-2°C	22°C	21 Km/h	N/A	0mm
7/24/2014	-3°C	25°C	21 Km/h	N/A	0mm
7/25/2014	0°C	25°C	42 Km/h	61 Km/h	0mm
7/26/2014	-2°C	10°C	N/A	N/A	0mm
7/27/2014	-6°C	14°C	35 Km/h	N/A	0mm
7/28/2014	-3°C	21°C	15 Km/h	N/A	0mm
7/29/2014	1°C	19°C	26 Km/h	N/A	0mm
7/30/2014	-1°C	20°C	15 Km/h	N/A	0mm
7/31/2014	0°C	21°C	N/A	N/A	0mm
7/1/2015	-3°C	19°C	9 Km/h	N/A	0mm
7/2/2015	-1°C	22°C	11 Km/h	N/A	0mm
7/3/2015	-1°C	22°C	16 Km/h	N/A	0mm
7/4/2015	0°C	21°C	15 Km/h	N/A	0mm
7/5/2015	1°C	22°C	11 Km/h	N/A	0mm
7/6/2015	1°C	23°C	9 Km/h	N/A	0mm
7/7/2015	4°C	23°C	29 Km/h	N/A	0mm
7/8/2015	2°C	20°C	21 Km/h	N/A	0mm
7/9/2015	1°C	22°C	15 Km/h	N/A	0mm
7/10/2015	1°C	22°C	N/A	N/A	0mm
7/11/2015	3°C	22°C	32 Km/h	N/A	0mm
7/12/2015	8°C	21°C	39 Km/h	55 Km/h	0mm
7/13/2015	3°C	21°C	15 Km/h	N/A	0mm
7/14/2015	0°C	18°C	24 Km/h	N/A	N/A
7/15/2015	6°C	20°C	28 Km/h	N/A	0mm

Date	Daily minimum temperature	Daily maximum temperature	Maximum steady wind	Maximum wind gust	Total daily precipitation
7/16/2015	4°C	22°C	48 Km/h	66 Km/h	0mm
7/17/2015	0°C	10°C	26 Km/h	N/A	0mm
7/18/2015	-4°C	18°C	15 Km/h	N/A	0mm
7/19/2015	-2°C	21°C	15 Km/h	N/A	0mm
7/20/2015	-2°C	23°C	24 Km/h	N/A	0mm
7/21/2015	3°C	23°C	21 Km/h	N/A	0mm
7/22/2015	10°C	22°C	39 Km/h	50 Km/h	0mm
7/23/2015	5°C	20°C	26 Km/h	N/A	11.9mm
7/24/2015	1°C	15°C	N/A	N/A	0mm
7/25/2015	0°C	14°C	32 Km/h	50 Km/h	0mm
7/26/2015	0°C	15°C	24 Km/h	N/A	0mm
7/27/2015	-2°C	15°C	4 Km/h	N/A	0mm
7/28/2015	-2°C	19°C	21 Km/h	N/A	0mm
7/29/2015	0°C	22°C	42 Km/h	68 Km/h	0mm
7/30/2015	-4°C	13°C	16 Km/h	N/A	0mm
7/31/2015	-3°C	14°C	24 Km/h	N/A	0mm
7/1/2016	3°C	21°C	26 Km/h	N/A	0mm
7/2/2016	0°C	21°C	29 Km/h	N/A	0mm
7/3/2016	-3°C	15°C	28 Km/h	N/A	0mm
7/4/2016	-1°C	18°C	24 Km/h	N/A	0mm
7/5/2016	5°C	18°C	26 Km/h	N/A	0mm
7/6/2016	2°C	18°C	16 Km/h	21 Km/h	0mm
7/7/2016	-4°C	16°C	15 Km/h	N/A	0mm
7/8/2016	-4°C	18°C	11 Km/h	N/A	0mm
7/9/2016	-2°C	20°C	11 Km/h	N/A	0mm
7/10/2016	-1°C	20°C	13 Km/h	N/A	0mm
7/11/2016	-1°C	20°C	11 Km/h	N/A	0mm
7/12/2016	-2°C	20°C	21 Km/h	N/A	0mm
7/13/2016	-1°C	20°C	26 Km/h	N/A	1mm

Date	Daily minimum temperature	Daily maximum temperature	Maximum steady wind	Maximum wind gust	Total daily precipitation
7/14/2016	-1°C	19°C	15 Km/h	N/A	0mm
7/15/2016	-1°C	19°C	16 Km/h	N/A	0mm
7/16/2016	-1°C	20°C	15 Km/h	N/A	0mm
7/17/2016	2°C	20°C	24 Km/h	N/A	0mm
7/18/2016	0°C	21°C	15 Km/h	N/A	0mm
7/19/2016	0°C	21°C	13 Km/h	N/A	0mm
7/20/2016	0°C	22°C	24 Km/h	N/A	0mm
7/21/2016	2°C	22°C	22 Km/h	N/A	0mm
7/22/2016	-1°C	22°C	29 Km/h	N/A	0mm
7/23/2016	-3°C	19°C	21 Km/h	N/A	0mm
7/24/2016	-3°C	14°C	11 Km/h	N/A	0mm
7/25/2016	6°C	14°C	39 Km/h	50 Km/h	30.9mm
7/26/2016	2°C	12°C	24 Km/h	N/A	0mm
7/27/2016	-2°C	12°C	29 Km/h	N/A	0mm
7/28/2016	2°C	12°C	24 Km/h	37 Km/h	0mm
7/29/2016	1°C	14°C	13 Km/h	N/A	0mm
7/30/2016	0°C	16°C	11 Km/h	N/A	0mm
7/31/2016	1°C	19°C	45 Km/h	55 Km/h	N/A

Annexure B

B.1 System computational core selection

Pursuant to the requirement of the electronic control system not only monitoring and controlling the aquaponic system components, but also logging these data to a data client in the cloud and considering that a Wi-Fi access point is present at the site under study, it was decided to use an ESP32 development module as the computational core for the electronic control system. The module features twin cores, megabit flash storage space, kilobyte variable storage capacity, multiple serial ports, timers, ADC, and communication ports (I2C, TWI, SPI among others), on-board 3.3 V regulation from VCC supply, some 5 V tolerant inputs (e.g., the I2C bus) and various other features. Importantly, it features a micro-USB interface for direct coupling to a PC for development, is supported in the Arduino IDE development platform, and features on-board Bluetooth as well as Wi-Fi functionality. It implements the IP stack protocol, and interestingly supports hardware encryption under various encryption schemes. It is also available at very low cost, considering the large feature set. Figure B.1 illustrates the ESP32 development module and the pin functionality.

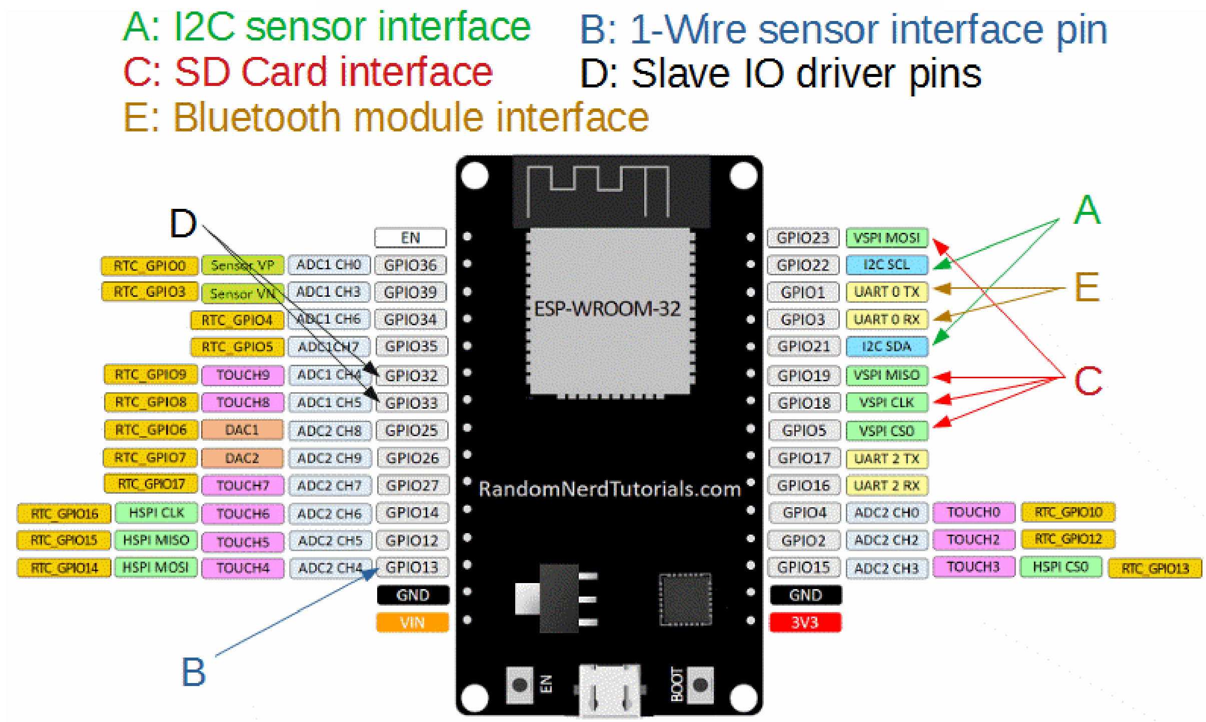

Figure B1: ESP32 development board, from www.randomnerdtutorials.com

The alphabetically listed items in Figure B.1 indicate the physical interfacing connections to the external hardware devices. The following lists some noteworthy points:

1) The SHT21 temperature/humidity sensor utilises a modified I2C bus (‘A’ in Figure B.1) protocol, but is bus-compatible with I2C hardware.
2) The 1-Wire sensor bus is connected to pin13 (‘B’ in Figure B.1) on the ESP32 module, but the normal pull-up to Vcc (the sensor is supplied from the ESP32 module 3.3 V output) is instead taken to the 5 V external point-of-load regulator. This markedly improves temperature reading reliability.
3) The micro-SD Card (‘C’ in Figure B.1) connects using a micro-SD to SD adapter as a carrier, with the adapter soldered to the CPU.
4) The slave relay IO PCB is driven from two GPIO pins (‘D’ in Figure B.1) – the slave IO is active low, i.e. the ESP32 initial tri-state inputs do not affect it and the ESP32 GPIO pins are tolerant of the 5 V pull-up generated from the slave PCB side.
5) The serial interface (‘E’ in Figure B.1) Bluetooth module used is a ‘pass-through’ type, i.e. it echoes the serial input to the Bluetooth transmission stream.

6) Not specifically indicated is the ESP32 micro-USB programming port (which can also power the ESP32). It is generally not advisable to simultaneously connect a USB cable and a DC supply, but due to the implemented point-of-load 5V regulator supplying the ESP32, there is no voltage contention. This is important as it therefore allows in-system live programming and monitoring, via a PC serial terminal.

B.2 System support hardware selection justification

The system needed to be powered, indicating a DC supply from mains voltage supply. A suitable PSU was built, delivering over 16.5 V DC at 3.5 VA. In addition, considering the South African national electricity supplier (ESCOM) record of planned power cuts (load shedding) and the prospect of unforeseen mains power outages, it was decided that a backup battery needed to be included. To meet a 24 h outage supply backup, the required capacity and voltage selected was a 12 V 7 Ah lead-acid type (commonly available as it is also used in household alarm systems). A photovoltaic panel (12 V 10 W type, nominally 19 V no-load and ≈1 A under optimal conditions, and ≈4 W expected during temperature-critical measurement period) was added. To maintain battery charge, a custom-built linear regulator was included, maintaining 13.6 V DC on the battery terminals (from the DC supply input as well as the solar PV module input).

Since a 220 V AC capable switching capacity (to control circulation pumps) was indicated, an existing PCB featuring digital IOs, optically isolated inputs, and four relay outputs were utilised. This board was used as a slave-device to the ESP32 development module, reading digital inputs and switching corresponding relay outputs.

As a loss of mains supply voltage also means that the site Wi-Fi connection would be lost, it was necessary to implement local storage of all log data. To realise this, a micro-SD card interface was used.

During firmware development, it transpired that the inclusion of the Bluetooth code library for the Arduino IDE, required to implement Bluetooth communication protocol on the ESP32 development board, caused code bloating to the extent that the object code no longer fitted the ESP32 flash storage section. To maintain the envisaged Bluetooth communication capability (although not required by the interpretation and realisation of the study goals), it was decided to use an HC06 serial-pass-through Bluetooth module. This enables the system to be locally monitored by any

Bluetooth-capable Android device, using any Bluetooth terminal emulator available from the Google Play Store. This very convenient feature was often used during development, and subsequently during site monitoring of the system. Figure B.2 depicts a screenshot of the system reporting logs to a Bluetooth terminal emulator running on an Android device.

Note the previously mentioned capability to monitor the system — the Bluetooth device in the aquaponics system was named ‘Test1’ and the log shows the Android device connecting to the main aquaponics Bluetooth broadcast at 09h04:46. The current system 1-Wire bus temperature measurements are listed by enumerator (starting from 0), description, and value. Note the log at 09h06:32.159 which illustrates a physical aquaponics control system reset, locating the 10 x 1-Wire devices on the 1-Wire sensor net, and listing their read values (in ‘enumerator, value’ order). The log at 09h06:38 indicates a resumption of normal timed operation.

Figure B2: Screenshot of system status updates to a generic Android Bluetooth terminal emulator application, from the Google Play Store.

Implementing the various components as a system, several functionally significant switches were also added, notably mains voltage disconnect, battery disconnect, and digital power disconnect. These are useful when performing testing or fault finding.

To monitor the results locally, the Bluetooth scheme outlined above was implemented. However, a LoRa machine-to-machine monitoring station was also tested (the further development of which was halted, as the Bluetooth range and flexibility of connection proved more useful). Figure B3 illustrates the 3D printed enclosure with supporting electronics. In the picture, a Nextion intelligent display is featured. Slave monitoring station development was not continued due to the Bluetooth solution determination. Figure B4 illustrates received test values using an alphanumeric LCD.

Figure B3: A 3D-printed enclosure showing perfboard with Arduino Nano, RFM95 LoRa transceiver.

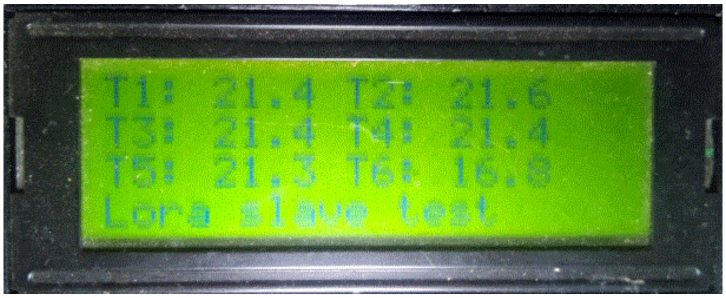

Figure B4: Results from LoRa base station test, 4x20 LCD.

B.3 Schematics and layouts

Figure B.5 and Figure B.6 detail the electrical panel wiring as well as a photo of the panel. The electrical panel is mounted below the north-ETC, on its frame.

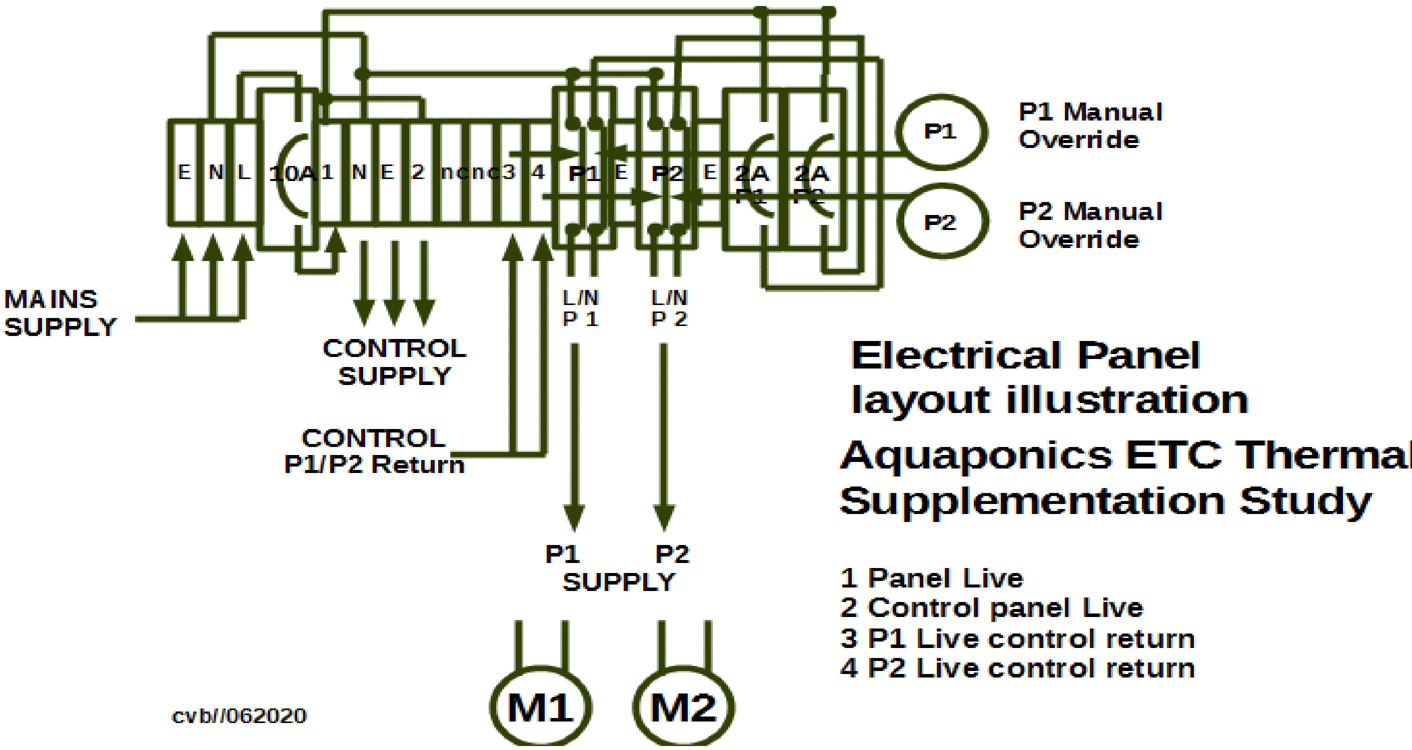

Figure B5: Illustration of electrical panel functional layout

The ‘Wilo Star RS25/4’ type circulation pump, used to pump water through the ETC loop, has inbuilt thermal protection, so installing thermal protection was not additionally required in the panel circuit. During commissioning and testing, P1 (refer to Figure B.5) was removed and the flow to the two ETC panels combined into P2.

Figure B6: Electrical panel physical layout

Annexure C

C.1 Program listing: Site-specific aquaponic log system

Note that the Google security root certificate is periodically re-issued. The certificate used in this example expires on 21 May 2022.

```
// ESP32 based aquaponic log system

// CvB 2020

// Note: Libraries available from within Arduino library manager, and GitHub
#include <TimeLib.h>
#include <OneWire.h>
#include <DallasTemperature.h>
#include <WiFi.h>
#include <HTTPClient.h>
#include "FS.h"
#include "SPI.h"
#include "SD.h"
#include <Wire.h>
#include <HTU21D.h>
#include "RTClib.h" // include for ease of use timestrings
RTC_Millis rtc;

HTU21D RHSensor (HTU21D_RES_RH11_TEMP11); // SHT21 equivalent sensor, setup resolution for measurement

#define SD_CS 5 //SD chip select for SD

//time server related setups
const char* ntpServer = "pool.ntp.org";
const long gmtOffset_sec = 7200;
const int daylightOffset_sec = 0;
// Note: google sheet dateTimeFormat = "dd/MM/yyyy HH:mm"
// Keep SD logs format compatible with any changes to google sheet format

// removed actual access point login
const char* ssid = "accesspoint1";
const char* password = "accesspointpassword";
const char* ssid1 = "accesspoint2";
const char* password1 = "accesspoint2password";
const char* ssid2 = "accesspoint3";
const char* password2 = "accesspoint3password";
// end removed actual access point login
```

```
int SlaveIO3 = 33, SlaveIO4= 32; //32=4=pump2 33=3=pump1 – See system layout for slave relay IO driver PCB

// Sensor net ID: AS INSTALLED 04/06/2020 - 1Wire sensor addresses on 1Wire bus
// Sump enum0 #1 28b079c40400002E
// Pump feed from dam enum1 #2 283891c50400000e
// RETURN FLOW TO DAM, PANELS ENUM2 #3 285C70C404000089
// 1.5kl tank enum3 #4...BC7FC404000CF
// dam temp enum4 #5 285AD96B040000C8
// North panel enumerated 5, number 6 28e59a0004000048 pump2
// Ambient hat ENUM 6 #7 28F5D900040000B4
// BIOFILTER RETURN ENUM7 #8 28E3266B04000090
// South Panel enum8 #9 , 280B1F6B0400006F pump1
// Grow bed return enum9 #10 28DBE3C40400001F

//script ID from deployed script
String GOOGLE_SCRIPT_ID = "AKfycbwAzcfAkzzlETOwYVxZRiTxDBUXcAHbw0qr5G2K7cDA4c2-M0g"; // System log set - as deployed
29/05/2020
//end script ID from deployed script

// Root certificate expires 21 May 2022
const char * root_ca=\
"-----BEGIN CERTIFICATE-----\n" \
"MIIDujCCAqKgAwIBAgILBAAAAAABD4Ym5g0wDQYJKoZIhvcNAQEFBQAwTDEgMB4G\n" \
"A1UECxMXR2xvYmFsU2lnbiBSb290IENBIC0gUjIxEzARBgNVBAoTCkdsb2JhbFNp\n" \
"Z24xEzARBgNVBAMTCkdsb2JhbFNpZ24wHhcNMDYxMjE1MDgwMDAwWhcNMjExMjE1\n" \
"MDgwMDAwWjBMMSAwHgYDVQQLExdHbG9iYWxTaWduIFJvb3QgQ0EgLSBSMjETMBEG\n" \
"A1UEChMKR2xvYmFsU2lnbjETMBEGA1UEAxMKR2xvYmFsU2lnbjCCASIwDQYJKoZI\n" \
"hvcNAQEBBQADggEPADCCAQoCggEBAKbPJA6+Lm8omUVCxKs+IVSbC9N/hHD6ErPL\n" \
"v4dfxn+G07IwXNb9rfF73OX4YJYJkhD10FPe+3t+c4isUoh7SqbKSaZeqKeMWhG8\n" \
"eoLrvozps6yWJQeXSpkqBy+0Hne/ig+1AnwblrjFuTosvNYSuetZfeLQBoZfXklq\n" \
"tTleiDTsvHgMCJiEbKjNS7SgfQx5TfC4LcshytVsW33hoCmEofnTlEnLJGKRILzd\n" \
"C9XZzPnqJworc5HGnRusyMvo4KD0L5CLTfuwNhv2GXqF4G3yYROIXJ/gkwpRl4pa\n" \
"zq+r1feqCapgvdzZX99yqWATXgAByUr6P6TqBwMhAo6CygPCm48CAwEAAaOBnDCB\n" \
"mTAOBgNVHQ8BAf8EBAMCAQYwDwYDVR0TAQH/BAUwAwEB/zAdBgNVHQ4EFgQUm+IH\n" \
"V2ccHsBqBt5ZtJot39wZhi4wNgYDVR0fBC8wLTAroCmgJ4YlaHR0cDovL2NybC5n\n" \
"bG9iYWxzaWduLm5ldC9yb290LXIyLmNybDAfBgNVHSMEGDAWgBSb4gdXZxwewGoG\n" \
"3lm0mi3f3BmGLjANBgkqhkiG9w0BAQUFAAOCAQEAmYFThxxol4aR7OBKuEQLq4Gs\n" \
"J0/WwbgcQ3izDJr86iw8bmEbTUsp9Z8FHSbBuOmDAGJFtqkIk7mpM0sYmsL4h4hO\n" \
"291xNBrBVNpGP+DTKqttVCL1OmLNIG+6KYnX3ZHu01yiPqFbQfXf5WRDLenVOavS\n" \
"ot+3i9DAgBkcRcAtjOj4LaR0VknFBbVPFd5uRHg5h6h+u/N5GJG79G+dwfCMNYxd\n" \
"AfvDbbnvRG15RjF+Cv6pgsH/76tuIMRQyV+dTZsXjAzlAcmgQWpzU/qlULRuJQ/7\n" \
"TBj0/VLZjmmx6BEP3ojY+x1J96relc8geMJgEtslQIxq/H5COEBkEveegeGTLg==\n" \
"-----END CERTIFICATE-----\n";
// end Root certificate expires 21 May 2022

WiFiClientSecure client;
```

```
#define ONE_WIRE_BUS 13
// Setup a oneWire instance
OneWire oneWire(ONE_WIRE_BUS);

// Pass oneWire reference to Dallas Temperature.
DallasTemperature sensors(&oneWire);

// Number of temperature devices found //Sleep not implemented
RTC_DATA_ATTR int numberOfDevices; //store in RTC so not affected by deep sleep
// Use this array to store found device addresses
RTC_DATA_ATTR DeviceAddress tempDeviceAddress[12]; // reserve 12 sensor instances in RTC memory. Actual deployed amount is ten
RTC_DATA_ATTR char FirstBoot=1;
RTC_DATA_ATTR unsigned long myToSleepTime=0; //end Sleep not implemented


//GLOBALS
float SHTTemp, SHTHumidity;
float SenseTemps[12];
int WiFistatusreturn;
char SDfailflag=0;
String statusstring="";
String mystringtophone="";
String mystringtoSD="";

struct tm timeinfo;

int GoogleLogDowncounter, GoogleLogDowncounterDefault=4; // Only send every n+1 to log to sheets
int WiFiConnectfailDowncounter, WiFiConnectfailDowncounterDefault=10; // if xx reconnect attempts are missed, then restart the ESP
int PumpStatus, SensorsFailed;
int STATICSensorCount=10; // hard definition for 1-Wire sensor net. If it doesn't detect this amount on initial hard reset, this prevents
// the system from running, as sensors are used in enumerated mode and incorrect enumeration results in the wrong sensor used for
//switching and logging purposes
//END GLOBAL

int Pump1Differential=1; // three °C leads to large lags. Gain requirement in degrees C
int Pump2Differential=1; // three °C leads to large lags. Gain requirement in degrees C
int DamOptimal=21;// dam optimal temp

void PumpSwitchFunction() {

if (SenseTemps[4]<DamOptimal)
{
// between 09h00 and 17h00 if differential gain then switch pump
// between 08h00 and 18h00 if differential gain then switch pump 15/07
// between 07h00 and 19h00 if differential gain then switch pump 28/08
// three months no glitches, -127C or 85C readings. Maybe a million log points. Can probably fairly safely remove ETC switch control time
```

```
if
((/*((timeinfo.tm_hour)>6)&&((timeinfo.tm_hour)<19)*/1)&&((SenseTemps[5]>(SenseTemps[4]+Pump2Differential))||(SenseTemps[9]>(SenseTemps[4]+Pump1Differential)))) //north panel > feed+differential then pump switches: also referenced to dam temp
{
digitalWrite(SlaveIO4, LOW); //slave PCB active low OP
digitalWrite(SlaveIO3, LOW); //slave PCB active low OP
PumpStatus=1;
} else
{
digitalWrite(SlaveIO4, HIGH); //slave PCB active low OP
digitalWrite(SlaveIO3, HIGH); //slave PCB active low OP
PumpStatus=0;
};
SenseTemps[10]=PumpStatus;
} else
{
digitalWrite(SlaveIO4, HIGH); //slave PCB active low OP
digitalWrite(SlaveIO3, HIGH); //slave PCB active low OP
PumpStatus=0;
};
}

void printLocalTime() //checks and makes timestring
{
//gets time from time server, on failure uses last synchronized time from the internal RTC
if(!getLocalTime(&timeinfo)){
Serial.println("Failed to obtain NTP time");
Serial.println("Using RTC time..");
} else {
Serial.println("Using NTPtime..");
rtc.adjust(now());
}
//e.g. Monday, April 20 2020 10:32:04
//"%A, %B %d %Y %H:%M:%S"
Serial.println(&timeinfo, "%d/%m/%Y %H:%M");
//mystringtoSD=(&timeinfo, "%d/%m/%Y %H:%M"); - Start SD string ‘massage’
if (timeinfo.tm_mday<10) mystringtoSD+="0";
mystringtoSD+=String(timeinfo.tm_mday); mystringtoSD+="/";
if ((timeinfo.tm_mon + 1)<10) mystringtoSD+="0";
mystringtoSD+=String (timeinfo.tm_mon + 1); mystringtoSD+="/";
mystringtoSD+=String (timeinfo.tm_year + 1900); mystringtoSD+=" ";
if ((timeinfo.tm_hour)<10) mystringtoSD+="0";
mystringtoSD+=String (timeinfo.tm_hour); mystringtoSD+=":";
if ((timeinfo.tm_min)<10) mystringtoSD+="0";
mystringtoSD+=String (timeinfo.tm_min); //mystringtoSD+=":";
//mystringtoSD+=String (second()); mystringtoSD+="/";
//"dd/MM/yyyy HH:mm"; - End manual SD string ‘massage’
```

```
mystringtoSD+=",";
}

//SD file functions - from examples
void writeFile(fs::FS &fs, const char * path, const char * message){
Serial.printf("Writing file: %s\n", path);

File file = fs.open(path, FILE_WRITE);
if(!file){
Serial.println("Failed to open file for write..");
return;
}
if(file.print(message)){
Serial.println("File written");
} else {
Serial.println("Write failed");
}
file.close();
}

void appendFile(fs::FS &fs, const char * path, const char * message){
Serial.printf("Appending to file: %s\n", path);

File file = fs.open(path, FILE_APPEND);
if(!file){
Serial.println("Failed to open file for append..");
return;
}
if(file.print(message)){
Serial.println("Message appended");
} else {
Serial.println("Append failed");
}
file.close();
}
//end SD file functions - from examples

// checks and retries defined WiFi connections
void reconnectWiFi(){
char i;
char incrementer=0;
WiFistatusreturn=1;

//WiFi.mode(WIFI_STA);
while (WiFistatusreturn) {
WiFi.mode(WIFI_STA);
for (i=0; i<3; i++) {
```

```
if (i==0) WiFi.begin(ssid, password);
if (i==1) WiFi.begin(ssid1, password1);
if (i==2) WiFi.begin(ssid2, password2);
if (i==0) Serial.println (ssid);
if (i==1) Serial.println (ssid1);
if (i==2) Serial.println (ssid2);
//Serial.println("Started");
Serial.print("Connecting WiFi..");
while (WiFi.status() != WL_CONNECTED) {
delay(1000);
Serial.print(".");
incrementer++;
if (incrementer==30) {
incrementer=0;
break;
}
}
if (WiFi.status() == WL_CONNECTED) {
if (i==0) Serial.println (ssid);
if (i==1) Serial.println (ssid1);
if (i==2) Serial.println (ssid2);
Serial.println("WiFi connected");
WiFistatusreturn=0;
WiFiConnectfailDowncounter=WiFiConnectfailDowncounterDefault; //reset the CPU restart counter
} else {
if (i==0) Serial.println (ssid);
if (i==1) Serial.println (ssid1);
if (i==2) Serial.println (ssid2);
Serial.println("WiFi NOT connected");
}
if (!WiFistatusreturn) {
break;
} else if (i==2)
{
WiFiConnectfailDowncounter--; // decrement CPU restart counter
Serial.println ("WiFi connection could not be made on ANY STATION!");
Serial.print (WiFiConnectfailDowncounter, DEC);
Serial.println (" connect attempts remaining before reset..");
Serial2.println ("WiFi connection could not be made on ANY STATION!");
Serial2.print (WiFiConnectfailDowncounter, DEC);
Serial2.println (" connect attempts remaining before reset..");
// forwarded to Bluetooth and serial monitor
}
}
break;
}
}
```

```
//SHT21 readings
void getSHTreadings() { // remember SHT11 and SHT21 Temperature conversion done on any RH conversion, can just read the registers.
RHSensor.softReset();
delay(50);
RHSensor.setResolution(HTU21D_RES_RH11_TEMP11);//HTU21D_RES_RH12_TEMP14);
SHTHumidity = RHSensor.readCompensatedHumidity();
SHTTemp = RHSensor.readTemperature();
}
//end SHT21 readings

/*void ResetSensorBus() damaged pins when soldering on site, NOT IMPLEMENTED
// removed hardware implementation to provide a control over the 1Wire Vcc supply voltage
//to implement a hard-reset in case of sensor failure
{*/
/*digitalWrite (12, LOW);
delay (500);
digitalWrite (12, HIGH);
delay (2000);
sensors.begin();*/
/*digitalWrite (25, LOW);
digitalWrite(26,LOW);
delay (1);
}*/ // 1-Wire sensor bus hardware power implementation. NOT IMPLEMENTED

void setup(){
setCpuFrequencyMhz(80); //default is 240MHz
WiFiConnectfailDowncounter=WiFiConnectfailDowncounterDefault;
// NB! check if WiFi operates OK??!!!
// start serial port
Serial.begin(115200);
Serial2.begin(9600);
// Enable 1wire sensor net slave power/bus board //NOT IMPLEMENTED
/*pinMode(12, OUTPUT);
digitalWrite (12, HIGH);
delay (2000);
SensorsFailed=0;
// NOT IMPLEMENTED
// End enable 1wire sensor net slave power/bus board */ //NOT IMPLEMENTED
sensors.begin();
delay(500); // added 13062020 - very important
/***********************************************/
// slave PCB driver
pinMode(SlaveIO3, OUTPUT);
pinMode(SlaveIO4, OUTPUT);
digitalWrite (SlaveIO3, HIGH);
digitalWrite(SlaveIO4, HIGH);
```

```
GoogleLogDowncounter=GoogleLogDowncounterDefault;
/*********************************************/
if (FirstBoot)
{
setCpuFrequencyMhz(80); //default is 240MHz
// NB! check if WiFi operates OK??!!!
//myToSleepTime=10000000; //get this from BT or Nextion. Firstboot sets defaults. Sleep mode not implemented as RTC accuracy was an issue
numberOfDevices = sensors.getDeviceCount();
// locate devices on the bus at first startup
Serial.print("Locating devices...");
Serial.print("Found ");
Serial.print(numberOfDevices, DEC);
Serial.println(" devices.");
Serial2.print("Locating devices...");
Serial2.print("Found ");
Serial2.print(numberOfDevices, DEC);
Serial2.println(" devices.");
// Loop through each device, print out address to serial monitor. Allows immediate verification on Bluetooth monitor of system sensor
//net integrity
for(int i=0;i<numberOfDevices; i++){
// Search the wire for address
if(sensors.getAddress(tempDeviceAddress[i], i)){
Serial.print("Found device ");
Serial.print(i, DEC);
Serial.print(" with address: ");
printAddress(tempDeviceAddress[i]);
Serial.println();
printAddress(tempDeviceAddress[i]);
}
}
if (numberOfDevices!=STATICSensorCount) //Hard coded sensor count, so that a missing sensor on reset won't confuse enumeration
{
Serial.print ("Did NOT find the expected ");
Serial.print (STATICSensorCount, DEC);
Serial.println (" devices..");
Serial.println ("Resetting..");
Serial2.print ("Did NOT find the expected ");
Serial2.print (STATICSensorCount, DEC);
Serial2.println (" devices..");
Serial2.println ("Resetting..");
delay(5000); // sensible delay so user gets to read the notifications
ESP.restart(); // go to start.
} //END
}
FirstBoot=0;
//esp_sleep_enable_timer_wakeup(myToSleepTime); //SLEEP NOT IMPLEMENTED. RTC timer accuracy in sleep mode is horrible
getSHTreadings();
```

```
Serial.print("Initializing SD card...");
if (!SD.begin(SD_CS)) {
Serial.println("ERROR - SD card initialization failed!");
statusstring =+ "SD Failed!";
SDfailflag=1;
//break; // init failed
} else {
File file = SD.open("/syslogs.txt");
if(!file) {
Serial.println("File doens't exist");
Serial.println("Creating file...");
writeFile(SD, "/syslogs.txt", "Timestamp, T Ambient, %RH, T1, T2, T3, T4, T5, T6, T7, T8, T9, T10, Pump \r\n");
SDfailflag=0;
}
file.close();
}

reconnectWiFi();
//moved (re-)connection to function call
//init and get the time
configTime(gmtOffset_sec, daylightOffset_sec, ntpServer);
printLocalTime(); //start SD string for this iteration
//Serial2.begin(9600);
if (!RHSensor.begin()){
Serial.println("Did not find %RH sensor!");
} else {
Serial.println("%RH sensor present");
getSHTreadings();
}
//esp_sleep_enable_timer_wakeup(10000000); //NOT IMPLEMENTED

sensors.requestTemperatures(); // Send the command to get temperatures
delay(500);
// Loop through each device, print out temperature data
for(int i=0;i<numberOfDevices; i++){
float tempC = sensors.getTempC(tempDeviceAddress[i]);
SenseTemps[i]=tempC;
Serial.print(i,DEC);
Serial2.print(i,DEC);
mystringtophone+=String ("S");
mystringtophone+= String (i+1,DEC);
mystringtophone+= String (" ");
Serial.print(',');
Serial.print(tempC);
Serial2.print(',');
Serial2.print(tempC);
mystringtophone+=String (tempC);
```

```
mystringtophone+= String ("C");
if (i<(numberOfDevices-1))
{
Serial.print(',');
Serial2.print(',');
mystringtophone+=(", ");
} else
{
Serial.println(';');
Serial2.println(';');
}
}
}

String getstatusstring() { //can append this to google sheets as a status indicator extra column
String localstring="";
if (SDfailflag) localstring+= "SD Card failed!";
return localstring; // .. so general error and status string can be implemented here
}

void loop(){
if (!WiFiConnectfailDowncounter)
{
Serial.println ("WiFi fail CPU RESTART..");
Serial2.println ("WiFi fail CPU RESTART..");
delay(5000);
ESP.restart(); // if xx WiFi reconnects have been missed, reset the whole thing.
}
String mystringtoBT="";
mystringtoSD="";
printLocalTime();
float tempC;
sensors.requestTemperatures(); // Send the command to get temperatures
delay(500); // delay in case sensors lost 5V and run from pullup parasite power
// Loop through each device, check 85C data bus fail //NOT IMPLEMENTED. Hardware 1Wire Vcc control
/*for(int i=0;i<numberOfDevices; i++){
float temperaturecheck = sensors.getTempC(tempDeviceAddress[i]);
if ((temperaturecheck==85)||(temperaturecheck==-127)) SensorsFailed=1;
}
if (SensorsFailed)
{
ResetSensorBus();
sensors.requestTemperatures(); // Send the command to get temperatures
}*/ //end NOT IMPLEMENTED
// refresh SHT, in case RF has caused issues
getSHTreadings();
// end refresh SHT, in case RF has caused issues
```

```
mystringtoSD+=String(SHTTemp, 2);
mystringtoSD+=",";
mystringtoSD+=String(SHTHumidity, 2);
mystringtoSD+=",";
Serial.print("Humidity:");
Serial.print(SHTHumidity, 2);
Serial.print("\tTemperature: ");
Serial.println(SHTTemp, 2);
//********************* BT
Serial2.print("%RH:");
Serial2.print(SHTHumidity, 2);
Serial2.print(" Temp:");
Serial2.println(SHTTemp, 2);
//Bluetooth readings sent

for(int i=0;i<numberOfDevices; i++){
// Search the wire for address
//note max sensors always less than 13, see defined array type
tempC = sensors.getTempC(tempDeviceAddress[i]);
SenseTemps[i]=tempC; //store in array as they arrive
Serial.print(i,DEC);
Serial.print(',');
//mystringtoSD+=","; development debug here
Serial2.print(i,DEC);
// Switch statements (Case) had issues,  rather use 'if..then'
Serial2.print(',');
if (!i) Serial2.print("Sump");
if (i==1) Serial2.print("Pump Feed");
if (i==2) Serial2.print("ETC Dam Return");
if (i==3) Serial2.print("Dam Top");
if (i==4) Serial2.print("Dam");
if (i==5) Serial2.print("N Hot");
if (i==6) Serial2.print("Ambient");
if (i==7) Serial2.print("Biofilter Return");
if (i==8) Serial2.print("Bed Return");
if (i==9) Serial2.print("S Hot");
Serial2.print(',');
//Serial.print(AddressArray[i],HEX); development debug
Serial.print(tempC);
mystringtoSD+=String(tempC); //build log string
Serial2.print(tempC);
if (i<(numberOfDevices-1))
{
Serial.print(',');
Serial2.print(',');
mystringtoSD+=",";
} else
```

```
{
//Serial.println(';');
//Serial2.println(';');
Serial.println(',');
Serial2.println(',');
//mystringtoSD+= "\r\n";
}
}
PumpSwitchFunction(); //switch the pumps
mystringtoSD+=",";
if (PumpStatus)
{
Serial.println ("Pump ON;");
Serial2.println ("Pump ON;");
mystringtoSD+="1";
} else
{
Serial.println ("Pump Off;");
Serial2.println ("Pump Off;");
mystringtoSD+="0";
}
//***************************************************************
// if (WiFistatusreturn==-1) >> add status string WIFI FAIL to SD logs
if (WiFistatusreturn==-1) {
mystringtoSD+=",WiFi reconnect failed! \r\n";
// .. and set (WiFistatusreturn=0)
WiFistatusreturn=0;
} else {
mystringtoSD+= "\r\n";
}
//********************REMOVE when development debug done
Serial.print ("SD String: ");
Serial.println (mystringtoSD);
//********************end REMOVE when development debug done
if (SD.begin(SD_CS)) {
appendFile(SD, "/syslogs.txt", mystringtoSD.c_str()); // string.c_str() forces to char<<
} else {
SDfailflag=1;
statusstring+="SD Failed!";
}
//***************************************************************
//PumpSwitchFunction(); 10062020 moved prior to SD write to get pump status
if (GoogleLogDowncounter) GoogleLogDowncounter--; else
{
sendData("info1=" +String(SHTTemp)+"&info2="+String(SHTHumidity)+"&info3="+String(SenseTemps[0])+"&info4="+String(SenseTemps[1])
+"&info5="+String(SenseTemps[2])+"&info6="+String(SenseTemps[3])+"&info7="+String(SenseTemps[4])+"&info8="+String(SenseTemps[5])
+"&info9="+String(SenseTemps[6])+"&info10="+String(SenseTemps[7])+"&info11="+String(SenseTemps[8])+"&info12="+String(SenseTemps[9])
```

```
+"&info13="+String(SenseTemps[10]));//ERROR temps[8]>[6] 30/05/2020 > 04062020 sensetemps[10] is pump status
if (WiFistatusreturn==-1) {
reconnectWiFi(); // retry and also check any of the alternative access points if log fails
sendData("info1=" +String(SHTTemp)+"&info2="+String(SHTHumidity)+"&info3="+String(SenseTemps[0])+"&info4="+String(SenseTemps[1])
+"&info5="+String(SenseTemps[2])+"&info6="+String(SenseTemps[3])+"&info7="+String(SenseTemps[4])+"&info8="+String(SenseTemps[5])
+"&info9="+String(SenseTemps[6])+"&info10="+String(SenseTemps[7])+"&info11="+String(SenseTemps[8])+"&info12="+String(SenseTemps[9])
+"&info13="+String(SenseTemps[10]));
}
if (WiFistatusreturn == 302)
{
statusstring=""; // success clears
WiFiConnectfailDowncounter=WiFiConnectfailDowncounterDefault; //reset the CPU restart counter // added 24/06/2020
}
//delay(sendInterval);
if (WiFistatusreturn==-1) {
Serial.println ("Wifi reconnect failed!");
//add diverse alarms and klaxons here
Serial2.println ("Wifi reconnect failed!");
};
GoogleLogDowncounter=GoogleLogDowncounterDefault;
};
delay(60000); // Sleep and/or interrupt driven code not implemented. Simple Do/Wait/Repeat
//esp_deep_sleep_start(); - NOT IMPLEMENTED - ESP32 deep sleep RTC accuracy issues
}

// function to print a 1-wire device address
void printAddress(DeviceAddress deviceAddress) {
for (uint8_t i = 0; i < 8; i++){
if (deviceAddress[i] < 16) Serial.print("0");
Serial.print(deviceAddress[i], HEX);
}
}

void sendData(String params) {
HTTPClient http;
String url="https://script.google.com/macros/s/"+GOOGLE_SCRIPT_ID+"/exec?"+params;
//Serial.print(url);
Serial.println("Making a request");
http.begin(url, root_ca); //Specify the URL and certificate
int httpCode = http.GET();
WiFistatusreturn = httpCode;
http.end();
Serial.println(String(WiFistatusreturn)+" >> Request done ");
// ADD request fail WiFi reconnect!!
}
```

C.2 Creating a Google Sheet for use with the system

The example for the creation of a suitable sheet in Google Sheets for data logging was obtained from GitHub (unreeeal, 2020). The matching script ID may be obtained when publishing the script, for use in the Arduino source code.

```
var timeZone = "GMT+2:00"; //get yours at https://www.timeanddate.com/time/zones/
var dateTimeFormat = "dd/MM/yyyy HH:mm";
var enableSendingEmails = true;
var emailAddress = ""; // comma separate for several emails
function doGet(e) {
   var result = 'Ok'; // default result
  if (e.parameter == 'undefined') {
    result = 'No Parameters';
  } else {
    var alarm= e.parameter.alarm;
    if (typeof alarm != 'undefined') {
      sendEmail("alarm text:" + stripQuotes(alarm));
      return ContentService.createTextOutput(result);
    }
    var sheet = getSpreadSheet();
    var lastRow = sheet.getLastRow();
    var newRow = 1;
    if (lastRow > 0) {
      var lastVal = sheet.getRange(lastRow, 1).getValue();
     //if there was no info for (sentEmailIfUnitIsOutForMinutes) checkIfDead() function will append row with 'dead' text
     // so checking do we need to override it
      if (lastVal == 'dead')
        newRow = lastRow; //to overwrite "dead" value
      else
        newRow = lastRow + 1;
    }
    var rowData = [];
    var namesOfParams=[];
    for (var param in parseQuery(e.queryString))
     namesOfParams.push(param);
//    namesOfParams=namesOfParams.reverse();
   //creatating headers if first row
    if (newRow == 1) {
      rowData[0] = "Date";
      var i = 1;
      for (var i=0; i<namesOfParams.length;i++  ) {
        rowData[i+1] = namesOfParams[i];
      }
      var newRange = sheet.getRange(newRow, 1, 1, rowData.length);
```

```
            newRange.setValues([rowData]);
            rowData = [];
            newRow++;
        }
        //************************************************************************************************
        rowData[0] = Utilities.formatDate(new Date(), timeZone, dateTimeFormat);
        //rowData[0] = "dfhghere";
        //************************************************************************************************
        for (var i=0; i<namesOfParams.length;i++  ) {
            var value = stripQuotes(e.parameter[namesOfParams[i]]);
            rowData[i+1] = value;
        }
        var newRange = sheet.getRange(newRow, 1, 1, rowData.length);
        newRange.setValues([rowData]);
    }
    // Return result of operation
    return ContentService.createTextOutput(result);
}
/**
 * Remove leading and trailing single or double quotes
 */
function stripQuotes(value) {
    return value.replace(/^['"]|['"]$/g, "");
}
function parseQuery(queryString) {
    var query = {};
    var pairs = (queryString[0] === '?' ? queryString.substr(1) : queryString).split('&');
    for (var i = 0; i < pairs.length; i++) {
        var pair = pairs[i].split('=');
        query[decodeURIComponent(pair[0])] = decodeURIComponent(pair[1] || '');
    }
    return query;
}
function getSpreadSheet() {
    return SpreadsheetApp.getActiveSheet();

}
```

Annexure D

Results summary: Daily

Date	°C Min Accuw	°C Min SHT21	°C Min South ETC	Dam Avg (simplified)	ETC supplement kWh	ETC suppl °C	Sump+ kWh	BF+ kWh	Dam delta kWh	Avg AccuWeather	Avg SHT21	GHI avg Solsys
			Prev to Day				Prev to Day	Prev to Day				As available calc'd
2020-06-11	1	5.13		10.845	22.22720364	0.45535107				6.5	8.81	
2020-06-12	-7	-2.06	-4.62	8.53	23.97243449	0.49110423	-17.975599	1.73987	-113.0029	2	4.21	
2020-06-13	-9	-4.08	-6.44	7.44	24.87075808	0.50950747	-12.596422	1.155211	-53.20653	3	4.995	
2020-06-14	-9	-3.12	-5.69	6.905	25.04291747	0.51303437	-4.638148	0.924796	-26.11513	3.5	6.355	
2020-06-15	-7	-2.24	-4.5	6.495			1.22024481	-0.53607	-20.01347	4.5	6.315	
2020-06-16	-6	-1	-2.81	6.375					-5.8576	4.5	6.935	
2020-06-17	-2	0.75	-0.62	6.875	11.16172847	0.22866147	10.9897246	-2.73363	24.406667	6	7.545	
2020-06-18	-3	1.62	-0.69	7.245	23.10591104	0.47335245	8.19250948	-1.99536	18.060933	7	8.895	
2020-06-19	-4	0.66	-1.44	7.69	26.10986711	0.53489212	7.38378838	-4.11612	21.721933	7	9.295	
2020-06-20	-5	0.93	-0.69	8.095	24.7324701	0.50667448	10.5613675	-5.37479	19.7694	7	9.825	
2020-06-21	-4	1.8	-0.345	8.47	25.094943	0.51410017	9.73312676	-4.83323	18.305	7.5	10.305	
2020-06-22	-5	2.67	0	8.655	25.8515671	0.52960053	8.90488604	-4.29168	9.0304667	7.5	11.44	
2020-06-23	-5	1.54	-0.75	8.785	25.45366933	0.52144911	9.37658032	-4.39983	6.3457333	8	10.83	
2020-06-24	-5	1.32	-0.97	8.905	25.34629815	0.51924948	8.99442557	-4.40375	5.8576	8	10.46	
2020-06-25	-6	1.1	-1.19	8.935	25.0214737	0.51259506	8.61227083	-4.40767	1.4644	7	10.085	
2020-06-26	-4	1.01	-0.75	9.005	23.73959896	0.48633431	8.37660277	-5.92026	3.4169333	8	9.82	
2020-06-27	-4	-0.65	-2.37	8.94	24.69945156	0.50599805	9.4220664	-3.18976	-3.172867	5.5	6.76	
2020-06-28	-6	1.27	-9.19	8.535	22.83956961	0.46789613	5.23089975	-4.60517	-19.7694	4	7.23	
2020-06-29	-7	-1.36	-3.19	8.185	25.58632222	0.52416667	2.46663517	-5.91086	-17.08467	5	7.28	
2020-06-30	-4	0.39	-1.25	8.185	25.85704988	0.52971285	6.32220763	-5.78859	0	8.5	9.205	
2020-07-01	-4	3.03	0.69	8.59	25.09165333	0.51403278	11.9700035	-3.17879	19.7694	8	10.83	
2020-07-02	-4	1.79	0.19	9	25.21932095	0.5166482	13.8660765	-3.43585	20.013467	8.5	10.565	
2020-07-03	-5	0.48	-1.25	9.185	26.10840504	0.53486216	10.4127318	-4.3293	9.0304667	8	10.04	
2020-07-04	-6	-0.04	-2.06	9.005	25.64407421	0.52534979	7.49298932	-3.84025	-8.7864	7.5	9.735	
2020-07-05	-6	-0.22	-2.19	8.97	26.20916641	0.53692638	6.41994502	-3.83869	-1.708467	8	9.78	
2020-07-06	-5	0.57	-1.56	9.035	27.51668839	0.56371255	9.04741806	-3.6694	3.1728667	9	10.955	
2020-07-07	-5	1.18	-1	9.255	26.107674	0.53484719	12.4828698	-3.58476	10.738933	8.5	10.735	
2020-07-08	-2	5.65	3.75	9.655	22.99659653	0.47111301	15.5794666	-2.96405	19.525333	8.5	12.185	
2020-07-09	3	6.36	4.94	10.315	24.42604343	0.50039696	20.1639381	-1.2618	32.2168	12	13.24	
2020-07-10	8	8.45	6.75	11.125	21.90079527	0.4486642	24.0076752	-1.71009	39.5388	15.5	14.81	

Date	°C Min Accuw	°C Min SHT21	°C Min South ETC	Dam Avg (simplified)	ETC supplement kWh	ETC suppl °C	Sump+ kWh	BF+ kWh	Dam delta kWh	Avg AccuWeather	Avg SHT21	GHI avg Solsys
			Prev to Day				Prev to Day	Prev to Day				As available calc'd
2020-07-11	-4	2.42	3.12	9.5	14.93028913	0.30586498	18.9444171	-0.16615	-79.32167	3	6.145	
2020-07-12	-7	-2.06	-3.87	8.845	26.62354299	0.54541538	4.82259946	-2.68661	-31.97273	5	6.93	
2020-07-13	-5	2.93	0.56	8.66	31.86642409	0.65282213	1.28207485	-6.14284	-9.030467	7.5	10.65	
2020-07-14	-6	1.79	1.69	8.125	16.37721952	0.33550709	-4.1163116	-4.29638	-26.11513	1.5	4.865	292.16
2020-07-15	-9	-4	-6	6.69	26.04181968	0.53349808	-11.668076	-5.22431	-70.04713	3	4.38	420.02
2020-07-16	-10	-3.12	-5.19	6.435	28.23511577	0.5784304	1.32661778	-6.96418	-12.4474	5.5	7.23	417.69
2020-07-17	-9	-2.24	-3.81	6.78	27.32422219	0.55976964	12.1164902	-7.3341	16.8406	7	9.08	419.35
2020-07-18	-7	-0.92	-2.81	7.25	28.57047935	0.58530072	6.65242944	-6.24159	22.942267	8	10.475	419.31
2020-07-19	-7	-1	-2.62	7.785	28.21671799	0.5780535	13.5630909	-6.71496	26.115133	8.5	10.3	424.6
2020-07-20	-6	1.45	-0.69	8.19	27.7196123	0.56786969	14.7561157	-5.43592	19.7694	8.5	11.525	397.13
2020-07-21	-6	2.67	-0.06	8.56	28.579861	0.58549292	17.3638652	-5.08951	18.060933	8	12.005	395.49
2020-07-22	-6	-0.04	-1.87	8.78	28.1140681	0.57595059	14.4839155	-6.24472	10.738933	8	10.395	410.12
2020-07-23	-6	0.3	-1.37	8.94	26.42543175	0.54135684	12.2518739	-6.36071	7.8101333	7.5	10.21	398.27
2020-07-24	-6	1.54	-0.75	8.97	26.42683291	0.54138554	12.367559	-5.7259	1.4644	7	10.39	399.96
2020-07-25	-5	1.01	-0.81	9.155	27.6548995	0.56654397	12.1372633	-5.62401	9.0304667	7	9.82	409.42
2020-07-26	-5	1.18	-1.06	9.315	28.09938642	0.57564982	10.3876608	-6.59426	7.8101333	7	9.86	422
2020-07-27	-3	0.3	-1.19	9.44	25.82884772	0.52913509	11.0559839	-5.461	6.1016667	8	9.555	397.56
2020-07-28	-2	0.905	-0.69	9.655	27.53221175	0.56403056	12.1191763	-5.32306	10.494867	8.5	9.9025	
2020-07-29	-4	1.51	-0.19	10	27.60301177	0.56548098	13.1823688	-5.18513	16.8406	8	10.815	
2020-07-30	-4	1.62	-0.13	10.22	29.13758488	0.59691856	10.6638007	-5.27134	10.738933	9	11.395	
2020-07-31	-4	0.84	-0.94	10.28	29.42487975	0.60280415	7.17390771	-6.13187	2.9288	10	11.91	
2020-08-01	-4	1.97	-0.06	10.405	29.70699942	0.60858371	8.44357834	-4.99076	6.1016667	10.5	12.745	
2020-08-02	-4	2.85	0.62	10.595	29.98911908	0.61436327	8.9385529	-5.08089	9.2745333	10.5	13.67	
2020-08-03	-3	3.47	1.62	10.97	28.65759469	0.58708539	9.43352747	-5.17102	18.305	10.5	13.495	
2020-08-04	-2	4.79	3.06	11.44	29.86581737	0.61183729	8.76986041	-4.31519	22.942267	10	13.985	
2020-08-05	-2	2.93	1.31	11.5	25.17706291	0.5157825	5.24200266	-4.44842	2.9288	10.5	13.095	
2020-08-06	-1	3.82	2.19	11.285	21.05711898	0.43138048	7.3100078	-4.01111	-10.49487	8	11.18	
2020-08-07	-4	-0.22	-1.94	9.785	29.6082484	0.60656067	-13.144046	-5.80113	-73.22	7.5	8.81	
2020-08-08	4	4.42	3	10.19	29.5218641	0.60479099	8.50303259	-2.53457	19.7694	13	12.71	
2020-08-09	-2	6.53	5.5	10.935	28.02469873	0.57411975	21.4207225	-0.71162	36.365933	8.5	12.495	
2020-08-10	-4	-0.83	-2.12	10.41	30.02323417	0.61506216	13.5691796	-3.74934	-25.627	7	8.33	478.83
2020-08-11	-6	1.35	-1.12	10.13	32.01470292	0.6558598	-9.1663415	-5.05816	-13.66773	8	11.825	491.03
2020-08-12	-5	0.66	-0.88	10.19	32.27336845	0.66115887	4.82259946	-2.68661	2.9288	7	10.93	496.15
2020-08-13	-5	-0.13	-1.56	9.97	31.86642409	0.65282213	2.0479483	-4.88261	-10.73893	6.5	9.12	495.09
2020-08-14	-5	0.39	-1.69	9.94	31.19728085	0.63911392	-4.1163116	-4.29638	-1.4644	8	10.91	493.31
2020-08-15	-4	4.34	1.37	10.34	31.24004656	0.63999003	9.69928081	-4.14591	19.525333	9.5	13.36	465.89

Date	°C Min Accuw	°C Min SHT21	°C Min South ETC	Dam Avg (simplified)	ETC supplement kWh	ETC suppl °C	Sump+ kWh	BF+ kWh	Dam delta kWh	Avg AccuWeather	Avg SHT21	GHI avg Solsys
			Prev to Day				Prev to Day	Prev to Day				As available calc'd
2020-08-16	-5	2.33	0.62	10.065	29.58333219	0.60605024	6.93823965	-0.36522	-13.42367	4	7.895	494.25
2020-08-17	-8	-2.32	-4.31	9.03	30.56030326	0.62606467	-10.192823	-4.34027	-50.5218	6	8.595	488.8
2020-08-18	-5	1.27	0.44	8.595	20.51036141	0.42269549	5.98768792	-1.92326	-21.2338	2.5	5.96	365.33
2020-08-19	-9	-4.35	-6.31	7.25	29.84400808	0.6113905	-10.616524	-4.34497	-65.65393	2.5	4.25	485.02
2020-08-20	-7	-2.41	-4.25	7.435	33.02907876	0.67664051	3.0944864	-4.15374	9.0304667	5.5	8.375	491.9
2020-08-21	-3	-0.57	-2.37	7.875	32.51043763	0.66601552	4.0375168	-5.47354	21.477867	8.5	9.425	498.9
2020-08-22	-3	3.47	1.44	8.81	32.18552208	0.65935923	6.87377118	-5.73687	45.640467	9.5	12.925	482.33
2020-08-23	-3	2.5	0.75	9.94	31.48591893	0.64502702	6.36017239	-3.59416	55.159067	10.5	13.53	504.42
2020-08-24	1	5.74	3.81	11.125	33.29633399	0.68211556	3.90786355	-5.26507	57.8438	13	15.62	481.5
2020-08-25	0	6.36	4.31	12.315	32.8251851	0.6724635	3.4239919	-5.88578	58.087867	14	17.19	489.62
2020-08-26	7	12.94	11.81	13.405	22.15653665	0.45390337	16.5451157	-3.11609	53.206533	17	19.66	381.77
2020-08-27	4	8.2	6.62	13.69	30.05746016	0.61576332	12.9252113	0.053293	13.9118	15	17.08	458.23
2020-08-28	-3	1.97	0	13.19	35.53172567	0.72791025	-1.6783291	-1.36682	-24.40667	9	12.09	542.8
2020-08-29	-4	1.01	-0.62	12.25	34.43309773	0.70540353	-9.1470009	-2.10509	-45.88453	5.5	8.59	535.42
2020-08-30	-4	0.05	-2.06	10.815	34.09355047	0.6984475	-16.427282	-4.97195	-70.04713	5	7.06	535.42
2020-08-31	-7	-2.34	-4.25	9.81	37.43303309	0.76686083	-16.247844	-6.88738	-49.0574	5.5	7.75	548.61
2020-09-01	-3	1.62	0.5	10	19.3632413	0.39667935	-2.167215	-5.38576	9.2745333	8	10.08	
2020-09-02	10	8.99	8.06	10.685	8.903552773	0.18240002	15.8907607	-4.44686	33.437133	13.5	12.32	
2020-09-03	5	9.77	8.38	11.41	13.92748806	0.28532139	11.3088435	-16.6103	35.389667	13	14.775	
2020-09-04	4	8.82	6.75	12.535	28.38071413	0.58141315	7.88127006	NULL	54.915	16	18.55	
2020-09-05	8	12.31	10.88	14.625	33.45521286	0.68537038	14.1604987	NULL	102.01987	19	21.125	
2020-09-06	9	12.68	11.12	15.655	14.06553237	0.28814939	-0.0891814	2.326096	50.277733	17.5	19.925	
2020-09-07	6	8.28	6.87	15.75	34.82298455	0.71339083	-8.5073305	NULL	4.6372667	15.5	16.89	
2020-09-08	5	9.08	6.81	16.155	35.86897777	0.73481927	-3.6442592	0.968684	19.7694	16.5	18.73	
2020-09-09	4	8.11	6.44	16.5	36.38192261	0.74532756	-2.3051058	2.208538	16.8406	16.5	18.68	
2020-09-10	5	10.74	8.75	17.06	37.44144002	0.76703305	7.50126425	3.77442	27.335467	18	20.6	
2020-09-11	6	10.31	9.31	17.28	36.62718578	0.75035207	1.31157514	3.95311	10.738933	17.5	20.3	
2020-09-12	6	12.76	11.12	17.375	7.351315889	0.15060057	-2.8828149	9.318492	4.6372667	17.5	21.31	
2020-09-13	7	12.06	10.56	17	29.70267411	0.6084951	-3.0855518	5.816808	-18.305	17	19.955	
2020-09-14	1	7.15	5.5	16.715	34.3623089	0.70395334	-3.3057997	5.086376	-13.9118	13.5	16.505	
2020-09-15	-4	0.66	-1.19	15.375			-14.928748	5.959446	-65.40987	10.5	13.04	
2020-09-16	0	5.22	4.12	15.065	37.06848892	0.7593927	-7.4865798	-0.89188	-15.13213	11.5	14.84	
2020-09-17	-1	3.03	1.31	14.655	37.22078846	0.76251274	-10.424909	-0.76962	-20.01347	12.5	14.705	
2020-09-18	1	8.2	6.19	15.03	38.55420136	0.78982931	-5.3569714	0.601901	18.305	15	18.985	
2020-09-19	1	7.06	5	15.66	39.41914089	0.80754864	-0.8420298	3.890412	30.7524	15.5	18.89	
2020-09-20	3	8.72	7.19	16.345	37.51612772	0.76856312	1.76679414	3.794797	33.437133	11.5	19.845	

Date	°C Min Accuw	°C Min SHT21	°C Min South ETC	Dam Avg (simplified)	ETC supplement kWh	ETC suppl °C	Sump+ kWh	BF+ kWh	Dam delta kWh	Avg AccuWeather	Avg SHT21	GHI avg Solsys
			Prev to Day				Prev to Day	Prev to Day				As available calc'd
2020-09-21	1	9.08	7.69	16.25	37.18703888	0.76182134	0.80979557	5.935935	-4.637267	12	17.205	
2020-09-22	0	3.47	1.75	15.065	36.29431991	0.74353291	-8.6645619	2.755578	-57.8438	12.5	14.8	
2020-09-23	5	8.99	7.81	16.06	36.59270516	0.74964569	13.6121586	2.971886	48.569267	16	18.335	
2020-09-24	5	10.82	9.06	16.97	37.58192112	0.76991098	9.3561653	3.083175	44.420133	17.5	20.77	
2020-09-25	7	16.43	15.13	18.215	34.82140063	0.71335838	16.9272704	5.550342	60.7726	19	23.795	
2020-09-26	2	7.85	6.06	17.245	36.8560006	0.75503962	6.06075218	5.559746	-47.34893	11	14.555	
2020-09-27	-2	2.42	0.62	15.47	35.92392744	0.73594498	-15.46706	0.009405	-86.64367	8.5	11.88	
2020-09-28	-3	2.33	0.37	14.375	37.10772128	0.76019642	-9.8393206	-0.50315	-53.4506	8.5	11.71	
2020-09-29	0	2.59	1.31	13.88	38.50924254	0.78890827	-8.4618444	-0.0047	-24.1626	10.5	12.53	
2020-09-30	-2	4.34	2.81	14	39.16169376	0.80227452	7.20757457	0.492179	5.8576	12	15.45	

Annexure E

The impact of the Covid-19 pandemic on system implementation, installation, and data gathering

During early 2020, the world became aware of a viral infection that quickly spread around the globe, which became colloquially known as Covid-19. The full impact of infection, infection rates, potential mitigation and correct approach to treatment was, during June 2020, still hotly debated. However, the direct impact on this research project may be summarised considering the timeline of the progression of social and medical guidelines, rules and decisions implemented in South Africa:

- During February and March, information regarding Covid-19 is slowly disseminated, but the seriousness is understated and underestimated;
- South Africa officially began a countrywide lockdown 27 Mar 2020. No member of the public is allowed outside their residence, including shopping, social and sports events, schools and churches, restaurants, and pubs. Businesses close. No commercial activity, apart from essential services. Shelter in place standing orders are issued;
- During the following two weeks, rules are defined, with lockdown divided into stage 5 (strict) to stage 1 (resumption of normal activity). Businesses essential to societal function are identified and allowed to operate under strict guidelines. Social distancing and face masks are mandatory;
- No online purchases or courier deliveries (unless accompanied by a certificate of exemption for the business supplying the goods). Obtaining electronic components and supplies not possible;
- Lockdown level 4 was implemented 1 May 2020. Once-off movement across provincial borders is allowed, as well as persons returning to their primary residence. Roadblocks and police presence restrict travel. Shopping hours for food and groceries are restricted, as well as maximum people allowed inside any given establishment. Some businesses allowed to reopen. Obtaining electrical and electronic parts still problematic; and
- Lockdown level 3 was implemented 1 June 2020. Most businesses reopen (although many have closed permanently due to the economic impact).

The above merits some comment in terms of the impact on the study:

- ETC installation was expected to have concluded Feb 2020. It was delayed until 29 May 2020, with automated functionality established on 10 June.
- Control system implementation was delayed by approximately three months, curtailing live comprehensive site logs leading up to the winter solstice.
- Various ETC installation- and commissioning issues were still being resolved up to 10 June, when serviceable log-sets commenced; and
- Some sensor- and sensor-net issues, as well as firmware changes required, were still being implemented during and after this period.

Annexure F: Publication to World Journal of Engineering

Investigating thermal supplementation of an aquaponics system under severe climate conditions

Chris Van Beukering, Pierre Hertzog and Arthur James Swart
Faculty of Engineering, Built Environment and Information Technology, Central University of Technology, Bloemfontein, South Africa

Abstract

Purpose – Climate change strains scarce water resources and food production infrastructure, necessitating establishment of sound scientific basis for operation of sustainable alternative food production methodologies - such as aquaponics, which promises high yield versus small footprint. In a climate (such as in Bloemfontein, South Africa) including temperatures below freezing, real-time aquaponics monitoring and control is necessary to mitigate thermal losses and to ensure sustainability of fish stock and bio-filter micro-organisms. The system thermal energy also needs sustainable supplementation during wintertime. This study/paper aims to address the problem of monitoring and controlling thermal energy in a medium sized aquaponics system, to ensure biological sustainability, especially during extreme cold weather events.

Design/methodology/approach – Required supplementation was determined and the aquaponics system described and quantified in terms of mass-flow power transfer by measuring loop differential temperature and flow rate. Cold front temperature data evaluation determined implementation suitability and -sustainability. Subsystem temperature contributions to the main reservoir, and their cumulative influence on the biological component, were considered.

Findings – Results indicate thermal supplementation enabled 1.3 °C temperature loss mitigation for a 42-kl water reservoir over a period of three days, offsetting severe system temperature decrease during a cold front event, and preventing organism mortality

Originality/value – Quantification of flow loop power transfer, and successful supplementation monitoring and control, demonstrates the approach and implementation merit in the Bloemfontein area. Wi-Fi-enabled online real-time data potentially facilitates incorporation into the concept of "Sustainable Smart Cities".

Keywords Solar energy, WiFi, Cloud data, Bluetooth, LoRa

Paper type Research paper

1. Introduction

Population growth and dwindling food security, in context of climate change predictions by the United Nations (IPCC, 2019) indicate that aquaponics systems will very likely become widely adopted, due to their much larger yield-per-hectare and –per litre of water, according to Goddek *et al.* (2015). This is especially relevant now in arid southern African areas such as Namibia and the Kalahari, as these are areas with water scarcity and unreliable precipitation. Long-term predictions indicate increasingly arid conditions in southern Africa, including Bloemfontein (Phillis *et al.*, 2018).

Hydroponics is the science of cultivating plants without soil, irrigating roots directly with fertilised water as (Goddek *et al.*, 2015) indicates. Aquaponics expands the concept by adding fish to the system. The animal life produces ammonia compounds, broken down to Nitrites and Nitrates by microbiota in the bio-filter, which feeds the plants (which in turn produce oxygen and cleans the water). The sustainable closed cycle nature of the method, coupled with the compact implementation potential, yields the feasibility of incorporating it into suburban areas, as (Proksch *et al.*, 2019) examines. Increased population and demands on land-use further drive the need for embracing this technology.

Urban adoption of aquaponics promotes local food security, with potential for job creation and economic empowerment, as (Walraven, 2014) has investigated. In addition, the fresh plant produce has direct health benefits, with the added plus of production of fish proteins (also a source of amino acids considered important to adolescent development, especially critical in impoverished rural areas, as the study by Assisi *et al.* (2006) examines. This is especially important in these impoverished rural areas, as also noted by Beveridge *et al.* (2013). The sustainability of such systems depends on maintaining a suitable temperature range for the biological components,

The current issue and full text archive of this journal is available on Emerald Insight at: **https://www.emerald.com/insight/1708-5284.htm**

World Journal of Engineering
© Emerald Publishing Limited [ISSN 1708-5284]
[DOI 10.1108/WJE-10-2020-0532]

Of special note is the financial contribution of the Central University of Technology, towards both the physical installation of the system and student fees. The support of the Centre for Sustainable Smart Cities, at the Central University of Technology, is also acknowledged.

Received 29 October 2020
Revised 25 November 2020
10 December 2020
11 December 2020
Accepted 12 December 2020

especially in areas that experience extreme temperatures in wintertime.

The critical limits of the minimum temperature for aquaponics systems are species dependent. However, the bio-filter component may typically experience organism mortality below 7°C (Sugita *et al.*, 2005). In Africa, extreme cold winter temperatures, coupled with exposure to Antarctic weather systems, is mainly limited to South Africa and the kingdom of Lesotho. Lesotho (approximately 200 km East of Bloemfontein) is a mountainous country, where the winter temperature extremes further contrast due to elevation differences (warmer valleys and exposed, cold mountain tops and plateaux).

The main aim of the research is to actively monitor and control the main aquaponics reservoir and bio-filter water temperature, by thermal supplementation, to prevent organism mortality, thereby ensuring its sustainability. Realising this goal, in Bloemfontein, South Africa (which experiences severe climate conditions during wintertime) necessitates the use of thermal energy supplementation. A comprehensive study, by Karamanzira and Rauschenbach (2018) details potential aquaponics system energy supplementation sources and cost effectiveness. In addition, they also highlight the use of solar and wind energy due to its non-polluting nature and low maintenance.

The feasibility of such supplementation will firstly be examined (refer to Section 2). Second, the aquaponics system under study will be described in terms of water flow loops and mass-flow power transfer, as further described in Section 2. Third, the solar thermal supplementation loop will be presented, refer to Section 3. Results, discussion and conclusions then end the paper, see Sections 4 and 5.

2. Literature review

The IPCC report (IPCC, 2019) highlights the urgency of timeously adopting aquaponics systems. Generic aquaponics system functional components are the main reservoir, the bio-filter(s), the sump, grow beds and the circulation system (pumps, valves, filters and so on). Such a system may be passively maintained or include a monitoring- and/or control system for these various components. Implementing such a monitoring and control system, as informed by Vernandhes *et al.* (2017) enables a detailed examination of the thermal contribution of each subsystem within an aquaponics system.

Quantifying the various thermal contributions using thermal modelling is epistemologically computationally complex, especially so for active systems with a biological component (Cannon, 2014). Alternatively viewing the nature of the problem from a subsystem viewpoint allows the use of a simplified model realisation, which is based on energy transfer of the mass-flow components, represented as water flow loops. This aquaponic subsystem energy interaction may be described examining the individual energy transfer loops, as illustrated in Figure 1. Note that the main reservoir 'direct' losses (such as evaporative and conductive losses that do not form part of the identified flow loop descriptions) are not described specifically but become apparent when examining the loop contributions and temperature data.

Figure 1 Proposed thermal supplementation and water flow loops, illustrating temperature measurement points

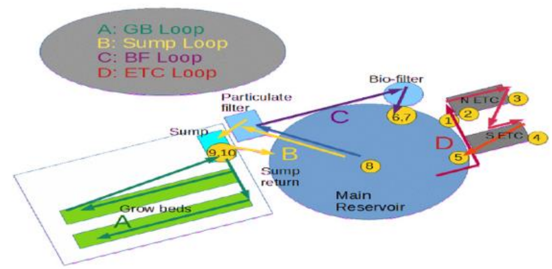

Temperature at various points (the numbered points in Figure 1) could be measured, thus determining the relevant flow loop energy transfer, calculated using the following equation:

$$Q = V * cp * (T1 - T2) \tag{1}$$

With Q ≈ flow-loop power transfer, V ≈ experimentally determined volumetric loop water flow rate, cp ≈ water specific heat and T1/T2 ≈ entry- and exit loop temperature. The system global energy transfer is informed by the individual energy transfer loops, as shown in Figure 1. Observe the North- and South ETC panels (on right) that could possibly provide the required thermal supplementation.

Of note is the ETC flow-loop (the red loop 'D' in Figure 1), the bio-filter flow loop (purple loop 'C', which has low temperature loss but high comparative flow) and the sump return flow loop (yellow loop 'B' - like the bio-filter loop, a continuous source of power exchange into the main reservoir). The intermixed nature of the Sump Loop and the GB Loop further implies that the grow beds indirectly impact the main reservoir in as much as the grow bed flow loop directly contributes to the sump temperature. This kind of interaction is typical of the semi-detached nature of the grow bed/main reservoir implementation. The grow bed thermal interaction data will thus not specifically be presented, as the implied contribution to the sump return flow already incorporates this indirect thermal contribution to the main aquaponics reservoir.

The basic electronic system requirements are temperature measurements at relevant points, logging this data to cloud storage (specifically Google Sheets) through wireless communication, and an independent power source. The study by Alamri *et al.* (2013) further informs the adoption of an implementation incorporating an IoT (the Internet of Things) -type implementation approach.

3. ETC estimation for the study context

Adoption in the central region of South Africa dictates the requirement of thermal supplementation, and, in line with sustainability goals, the possible inclusion of an ETC system as the source of the thermal energy. As outlined by Sugita *et al.* (2005), the bio-filter micro biota would be adversely affected by the minimum temperature extremes, as found in Bloemfontein, located in the central region of South Africa. A study by Coetzee *et al.* (2017) provides quantification of the expected yield of an ETC system, including the desired mounting angle for optimal output during wintertime, when temperature extremes occur. Energy loss is determined using equation (2), with the ETC required determined by the average day-on-day loss, around the 7°C critical minimum, in a 42-kl reservoir, using specific historic temperatures obtained from 2019 site-specific temperature logs:

$$Powerloss = \frac{cp * T * m}{t} \text{ Wh} \tag{2}$$

where cp ≈ water specific heat, T ≈ temperature difference, m ≈ reservoir mass and t ≈ time. Figure 2 illustrates the maximum aquaponic reservoir temperature loss slope that was extracted from data logged at the research site for 2019 (9.38°C to 7.44°C over 2 days). Note that these dates are close to the Southern hemisphere winter solstice (21/22 June), the time of critical interest, as potential solar ETC supplementation will thus be at a minimum also.

This maximum daily loss (0.97°C per day) informs the chosen temperature 'buffer' value and in conjunction with the thermally supplemented daily average-positive temperature recovery slope (daily gain) determines the required temperature buffer recovery time. These concepts are further explored later in this section and are of relevance in system thermal recovery after an extreme weather event such as a cold front.

The required daily supplementation minimum (at Bloemfontein −29³ latitude, assuming optimal solstice insolation conditions), was determined to be ≈0.5°C. This estimation is arrived at by examining the average daily temperature loss slope ≈0.25°C as taken around the critical 7°C bio-filter minimum temperature value and establishing a daily ≈0.25°C net positive recovery slope. A 'buffer' estimation of ≈3°C was arrived at by using the aforementioned figure of maximum decrease in the reservoir temperature of ~1°C per day (01 to 03 July), and assuming consecutive daily conditions similar to these might prevail for two to three days. This approach would allow for about a one-week requirement for the system temperature buffer to recover following any adverse extreme weather sequence, i.e. at least one week of average weather following any extreme weather event (such as the cold front data presented later).

Figure 2 Historical data from 2019 used to determine ETC requirement

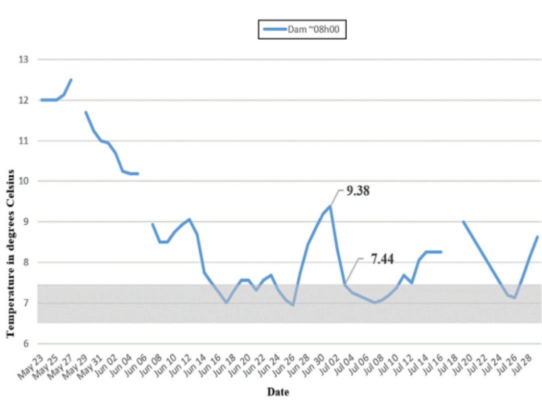

Using equation (2) and substituting the identified 0.5°C requirement and 42-kl capacity, a power transfer may be calculated, which directly represents the required ETC thermal supplementation, in terms of kWh. A simplified kWh subsystem power transfer approach, such as presented with the loop flow descriptions, thus has the benefit of directly comparing ETC supplementation and kW ratings. Calculation of the solstice ETC minimum supplementation requirement, using the values noted, yields (from equation (2)) a power loss of 24.406. kWh.

The South African study by Coetzee *et al.* (2017) indicated that a 33-tube × 1.6 m collector averages about 13.2 kWh per day during the winter solstice, i.e. each tube thus potentially produces 400 Wh per day. At their study latitude, −25.75³ (NASA GISS, 2020) indicates an average insolation of 241.45 W.m^2 for June, while the corresponding average insolation for Bloemfontein is 219.76 W.m^2. This represents a ~9% relative decrease in terms of available insolation at the Bloemfontein study site which enables a baseline comparison for calculating the minimum required ETC output, ETC_{min}. Assuming a 24.4 kWh total requirement with 400 Wh per day per tube and a factor of 91% (accounting for the 9% relative decrease) yields the following:

$$ETC_{min} = \frac{24400}{400*0.91} = 67 \text{ ETC tubes minimum} \tag{3}$$

These 1.6-m tubes are commercially available in sets of 20. This then equates to 4 × 20 tubes to cover the requirement of 67, thereby yielding a potential thermal supplementation of ≈32 kWh (or 0.65°C) daily in the 42-kl reservoir. This value compares favorably with the previously identified 0.5°C minimum requirement and allows for a margin.

The site under investigation has an existing Wi-Fi node available, required to log real-time data to an online client. A suitable example of incorporation of such implementation is found in (Vernandhes *et al.*, 2017). The requirement for real time online data is further informed by Alamri *et al.* (2013). The implemented monitoring and control system are realised using an ESP32 development module, with ancillary support devices (DC supply, backup battery, charge controller, backup 10 W PV panel and relay driver PCB). A circulation pump controls the ETC loop flow and is switched based on potential energy transfer gain. Temperature measurements were made using a 1-wire bus with multiple DS18B20 digital temperature sensors, and an SHT21 digital temperature/humidity sensor.

In addition to the identified required basic functionality, a Bluetooth device broadcasting data measurement was implemented, allowing system monitoring from any smart phone with an installed Bluetooth serial terminal. Similarly, a monitoring station, communicating via a LoRa transceiver to the control system, was also implemented. The implementation of such a monitoring and control system, with real time online data, promotes the potential adoption of an electronically managed aquaponics system into the concept of "Sustainable Smart Cities".

4. Results

Data was gathered and logged to Google Sheets every 5 min, with data integrity being insured by embedding an SD memory card into the control system, logging data every minute. A combined three-month data set (10 June 2020 to 30 September 2020) is comprehensive and informs the thermal contribution of each subsystem within the aquaponics system. The specific conditions of notable interest occur during the passing of a cold front. In the central region of South Africa, a cold front typically comprises weather systems that transport cold Antarctic air to the African continent and may include rain or snow. Figure 3, (EUMETSAT, 2020), graphically depicts a cold front passing over South Africa on 11 June 2020.

Conditions during such cold fronts cause a more dynamic power exchange interaction between the aquaponics subsystems, highlighting the relevance of implementing a real-time monitoring and control system for evaluation of temperature criteria. Figure 4 illustrates the ambient - as measured by the system SHT21 sensor, and main reservoir temperature for this cold front. The DOT on the right indicates the main reservoir temperature has reached the identified minimum acceptable value of 7°C on 13 June 2020.

Figure 4 illustrates the main reservoir relative temperature change (Dam relative change), and the subsystem cumulative daily thermal contribution to the main reservoir, expressed in degrees Celsius. This period of interest coincides with Figure 5.

Figure 3 Graphic representation of passing cold front, colourised air-mass representation, reproduced from SAWX website

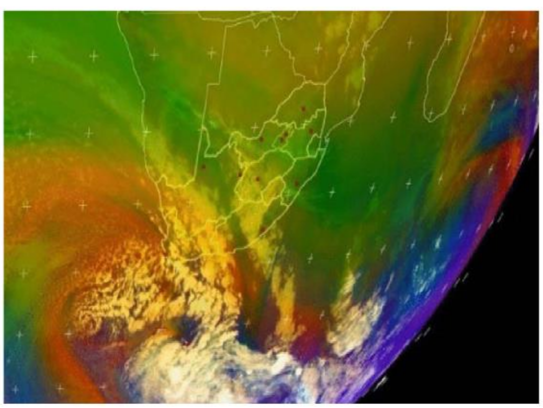

Figure 4 Main reservoir temperature vs measured ambient temperature, period 10–13 June 2020

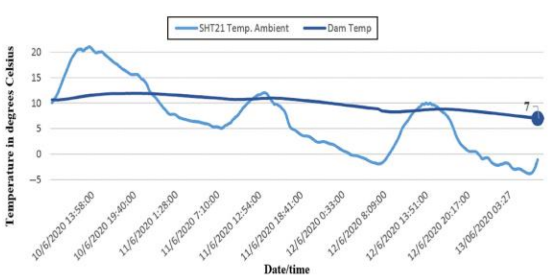

Figure 5 Relative main reservoir change- and dynamic subsystem cumulative thermal contribution

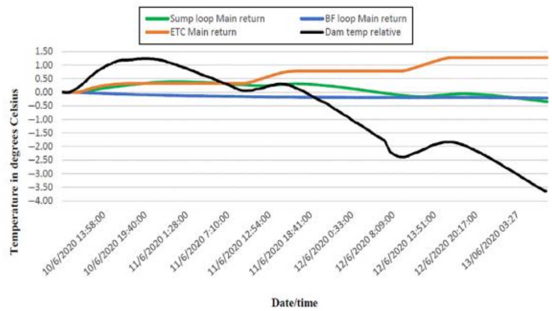

Of note is the relative thermal contributions of each energy transfer loop. The main reservoir temperature falls by ~3.7°C, over the three-day period coinciding with the passing of the cold front. This ~1.25°C per day contrasts well with the 2019 historical site log data maximum temperature loss slope of 0.97°C per day. The result is informed by the severe weather conditions of the passing cold front, and the below average cold winter experienced in Bloemfontein. The temperature loss, however, has been mitigated by the ETC thermal supplementation over the three-day period, contributing to around ~1.3°C (ETC Main return). This means that the un-supplemented temperature loss would have been ~5.0°C, or approximately 1.6°C per day. The resultant potential extended period exceeding the minimum 7°C bio-filter requirement could result in organism mortality, possibly leading to toxic build-up in the system and resulting in an extended bio-filter rehabilitation and regrowth period. Such toxicity in the system would most likely also lead to fish mortality in the main aquaponic reservoir.

The value of thermal supplementation of the system is thus highlighted. The main reservoirs' bio-filter return (BF loop Main return) contribution was consistently negative, while the sump return (Sump loop Main return) contribution varied both towards a positive and negative contribution. This is mainly due to the aforementioned semi-detached nature of the grow beds. The mixed flow exchange (see Figure 1, at numbered markers 9/10) largely determines the sump water reservoir temperature.

Table 1 lists the corresponding values for the measured criteria. Note that the subsystems' temperature contribution to the main reservoir may also be expressed as a kWh power transfer. The ambient listed values are the official minimum/maximum for the area.

Of note is the minimum temperatures reported for the area, as per (AccuWeather, 2020), as the cold front passes: −7°C, −9°C, −9°C. This reflects the severe climate conditions for this central region of South Africa. In addition, the main reservoir average temperature had decreased to 7.44°C as the cold front passed (12–13 June) – and thus the minimum allowable temperature of 7°C was maintained using thermal supplementation by the ETC system.

Table 1 Précis of aquaponics system and subsystem conditions 10–13 June 2020

Date	10–11 June	11–12 June	12–13 June
AccuWeather ambient max. temperature, in °C	12	11	15
AccuWeather ambient min. temperature, in °C	−7	−9	−9
Main reservoir max. temperature, in °C	10.94	8.81	7.94
Main reservoir avg. temperature, in °C	10.845	8.53	7.44
Main reservoir min. temperature, in °C	10.75	8.25	6.94
ETC thermal supplementation, in kWh	22.23	23.97	24.87
Sump-return thermal contribution, in kWh	14.14	−17.98	−5.97
Bio-filter return thermal contribution, in kWh	−7.56	−1.72	−0.627

5. Conclusions

The main aim of the research was to actively monitor and control the main aquaponics reservoir and bio-filter water temperature, by thermal supplementation, to prevent organism mortality, thereby ensuring its sustainability. During the three-day period presented here, coinciding with a passing cold front that brought severe weather conditions, the ETC supplementation method resulted in a 1.3°C mitigation of temperature loss in the main aquaponics reservoir of 42-kl. The average temperature of the reservoir was maintained above 7°C, as a direct consequence, which represents a desirable outcome in terms of preventing bio-filter organism mortality.

The presented data relates to the aquaponics system thermal interaction, in terms of mass-flow power transfer as previously described. The loop energy-transfers were stated as contributing to the main reservoir temperature, with the ETC loop, bio-filter loop and sump return loop noted along with the semi-detached grow bed loop impact.

6. Future recommendations

It is recommended that this electronic monitoring and control system be continually used in this study region, in conjunction with an ETC implementation system as outlined above, to ensure the sustainability of the existing aquaponics system. In the African context, such implementation would be particularly applicable to Lesotho, which experiences the same severe climatic conditions. It is also recommended to install such a system in other locations of the world where similar severe climate conditions occur during wintertime. The process outlined in this article for determining the ETC size requirement may be followed as a guideline. The thermal supplementation via ETC is both a 'green-' and sustainable solution that makes the system ideally suited for a 'Sustainable Smart City'. The adopted method for determining the ETC supplementation requirement may also be used by other researchers in this field, for different main reservoir sizes.

References

AccuWeather (2020), [online], available at: www.accuweather.com/, (accessed October 2020).

Alamri, A., Ansari, W.S., Hassan, M.M., Hossain, M.S., Alelaiwi, A. and Hossain, M.A. (2013), "A survey on Sensor-Cloud: architecture, applications, and approaches", *International Journal of Distributed Sensor Networks*, Vol. 9 No. 2, pp. 917-923, doi: 10.1155/2013/917923.

Assisi, A., Banzi, R., Buonocore, C., Capasso, F., Di Muzio, V., Michelacci, F., Renzo, D., Tafuri, G., Trotta, F., Vitocolonna, M. and Garattini, S. (2006), "Fish oil and mental health: the role of n-3 Long-Chain polyunsaturated fatty acids in cognitive development and neurological disorders", *International Clinical Psychopharmacology*, Vol. 21 No. 6, pp. 319-336, doi: 10.1097/01.yic.0000224790.98534.11.

Beveridge, M.C.M., Thilsted, S.H., Phillips, M.J., Metian, M., Troell, M. and Hall, S.J. (2013), "Meeting the food and nutrition needs of the poor: the role of fish and the opportunities and challenges emerging from the rise of aquaculturea", *Journal of Fish Biology*, Vol. 83 No. 4, pp. 1067-1084, doi: 10.1111/jfb.12187.

Cannon, W.R. (2014), "Concepts, challenges and successes in modeling thermodynamics of metabolism", *Frontiers in Bioengineering and Biotechnology*, Vol. 2, doi: 10.3389/fbioe.2014.00053.

Coetzee, A.F., Mwesigye, A. and Huan, Z. (2017), "Optimal slope angle selection of an evacuated tube collector for domestic solar water heating", *Journal of Energy in Southern Africa*, Vol. 28 No. 1, pp. 104-119, doi: 10.17159/2413-3051/2017/v28i1a1621.

EUMETSAT (2020), [online], available at: https://sawx.co.za/satellite/animated-satellite/africa-weather-satellite-photo-animated-airmass/ (accessed July 2020).

Goddek, S., Delaide, B., Mankasingh, U., Ragnarsdottir, K.V., Jijakli, H. and Thorarinsdottir, R. (2015), "Challenges of sustainable and commercial aquaponics", *Sustainability*, Vol. 7 No. 4, pp. 4199-4224, doi: 10.3390/su7044199.

IPCC (2019), "IPCC, 2019 Summary for policymakers – special report on climate change and land", IPCC, available at: www.ipcc.ch.srccl/chapter/summary-for-policymakers/, (accessed 20 October 2020).

Karamanzira, D. and Rauschenbach, T. (2018), "Optimal utilization of renewable energy in aquaponic systems", *Energy and Power Engineering*, Vol. 10 No. 6, pp. 279-300, doi: 10.4236/epe.2018.106018.

NASA GISS (2020), [online], available at: https://data.giss.nasa.gov/modelE/ar5plots/srlocat.html (accessed October 2020).

Phillis, Y.A., Chairetis, N., Grigoroudis, E., Kanellos, F.D. and Kouikoglou, V.S. (2018), "Climate security assessment of countries", *Climatic Change*, Vol. 148 Nos 1/2, pp. 25-43, doi: 10.1007/s10584-018-2196-0.

Proksch, G., Ianchenko, A. and Kotzen, B. (2019), In *Aquaponics Food Production Systems: Combined Aquaculture* *and Hydroponic Production Technologies for the Future*, in Goddek, S., Joyce, A., Kotzen, B. and Burnell, G.M. (Eds), Springer International Publishing, Cham, pp. 523-558, doi: 10.1007/978-3-030-15943-6_21.

Sugita, H., Nakamura, H. and Shimada, T. (2005), "Microbial communities associated with filter materials in recirculating aquaculture systems of freshwater fish", *Aquaculture*, Vol. 243 Nos 1/4, pp. 403-409, doi: 10.1016/j.aquaculture.2004.09.028.

Vernandhes, W., Salahuddin, N.S., Kowanda, A. and Sari, S.P. (2017), "Smart aquaponic with monitoring and control system based on IoT", *Proceedings of the 2017 Second International Conference on Informatics and Computing (ICIC), Jayapura, Papua, Indonesia*, pp. 1-6. 10.1109/IAC.2017.8280590.

Walraven, B.C. (2014), "Aquaponics: economics and social potential for sustainable food production", *Senior Honors Projects, 2010-current*, p. 493, available at: https://commons.lib.jmu.edu/honors201019/493.

Corresponding author

Chris Van Beukering can be contacted at: chris.vanbeukering@gmail.com

Annexure G: Publication to journal Revista GEINTECH

www.revistageintec.net
ISSN: 2237-0722
revista GEINTEC
Gestão, Inovação e Tecnologias

A Simplified Design Process for Thermal Supplementation of a Medium Sized Aquaponics System to Ensure Sustainability

C.A. Van Beukering[1]; P.E. Hertzog[2]; A.J. Swart[3]

[1]Centre for Sustainable Smart Cities, Department of Electrical, Electronics and Computer Engineering, Central University of Technology, Free State.

[1]chris.vanbeukering@gmail.com

[2]Centre for Sustainable Smart Cities, Department of Electrical, Electronics and Computer Engineering, Central University of Technology, Free State.

[3]Centre for Sustainable Smart Cities, Department of Electrical, Electronics and Computer Engineering, Central University of Technology, Free State.

Abstract

Growing climate change awareness incentivizes establishment and implementation of efficient alternative food production methodologies such as aquaponics, with potentially high yield versus reduced footprint, urban implementation and local food security and employment. Viably maintaining such systems during freezing winter climate necessitates thermal supplementation to maintain biological viability of the fish stock and bio-filter micro-organisms. The purpose of this study is to present a simplified baseline approach for determining thermal supplementation for establishing sustainability of a medium sized aquaponics system. An existing aquaponics system is examined and described through historical temperature data, system thermal interaction via mass-flow loop energy transfer and a physical layout. Applicable historical measurements for initial supplementation determination are be listed. The chosen solar supplementation source is discussed in terms of cost and energy input. Further examination of study data informs system energy interaction and system micro-biota viability. The presented method results in an inter-cold-front positive system temperature recovery slope of 0.278°C per day and an extrapolated temperature buffer recovery in 15 days, validating the viability of the method as presented. The value of adopting this method lies in promoting aquaponics system adoption by simplifying system-viability supplementation estimation where direct grid energy unit-cost comparison allows for informed decisions. Adopting the method for the Bloemfontein area, or locations with similar climate, is thus recommended.

Key-words: Sustainability, Solar.

ISSN: 2237-0722
Vol. 11 No. 4 (2021)
Received: 14.06.2021 – Accepted: 16.07.2021

1. Introduction

Diminishing food security and increased population would suggest a general adoption of aquaponics systems, due to their increased yield and water efficiency as [1] clarifies. Climate change predictions [2] indicate special relevance of such systems to arid southern-African regions, including Bloemfontein in South Africa, as [3] shows.

Aquaponics expands established hydroponics to include fish in the cycle. Ammonia compounds produced by aquatic fauna is broken down to Nitrites and Nitrates by bio-filter micro-organisms, the nitrogen-rich water feeds the plants, returning clean water to the aquatic component. Compact implementation and sustainable closed-cycle aspect promotes urban adoption [4] which directly impacts local food security, job creation and economic empowerment as [5] examines. Additional benefits include a reduced carbon footprint, lower fertilizer input, minimized water wastage and ready scalability [1]. The fresh produce promotes health and the fish protein serves as a source of amino acids beneficial to adolescent cognitive development [6], especially significant in poor rural communities [7]. Promoting urban and rural aquaponics adoption, and especially in terms of a skill-transfer integration into African traditional agricultural method, is therefore of rising importance to timeously disseminate this knowledge and equip a new generation to become more sustainable in terms of food generation.

Sustainably maintaining aquaponics systems in areas which experience freezing winter temperatures, presents challenges. The biological viability of the aquatic fauna, as pertaining to temperature, is species dependent. In addition, the micro-organisms in the bio-filter may die below 7˚C [8]. Aquaponics' circular nature means that a break in the chain (such as micro-organism die-off) causes system toxicity build-up. It is thus necessary to thermally supplement such aquaponics systems in areas of extreme cold, where freezing temperatures can occur. It is also desirable to quantify the sub-system thermal interaction, directly indicating areas for further potential thermal loss mitigation and cost savings. The purpose of this study is to present a simplified baseline approach for determining thermal supplementation for establishing sustainability of a medium sized aquaponics system.

Firstly, potential thermal supplementation methods will be examined. Secondly, a simplified historical-data approach to initial determination of required system energy input will be presented, coupled with the description of the system energy exchange interaction in terms of its mass-flow power transfer. Thirdly, supplementation will be examined as relating to the system biological viability and sustainability by way of data interpretation. Fourthly, benefits of a monitoring system in refining

ISSN: 2237-0722
Vol. 11 No. 4 (2021)
Received: 14.06.2021 – Accepted: 16.07.2021

understanding of the system thermal interaction is investigated, and applicability to thermal interaction of different system topologies considered. Anticipated results, discussion and conclusions then follow.

2. Literature Review

Aquaponics system implementation is varied, yet scalable with system size varying from hobby implementation to large-scale commercial enterprises. Of interest in the South African (and specifically Bloemfontein in the Free State Province) context, and mindful of the issues surrounding economic empowerment and establishment of local food security, is the supplementation requirement for medium-sized aquaponics systems. A local retrofitting opportunity exists for existing dams that maybe considered 'medium' size reservoirs of between 10 kl to 100 kl. This criteria also informs the focus of single-loop, rather than multiple decoupled loop system topologies, as [1] informs.

Aquaponics systems may typically require both electrical (e.g. continuous water pumping) and thermal (typically water heating in winter time) energy input. Rising electrical heating costs and the unreliable nature of the electrical grid supply in South Africa makes it desirable to investigate other supplementation methods. A comprehensive study by [9] investigates alternatives, including photovoltaic and solar thermal modules, wind turbines, hydropower, biomass converters, heat pumps, gas boilers and interfacing to the electrical grid. Cost-effectiveness and least-cost methods, as well as suitability of harvesting methods are listed and renewables highlighted.

Functionally, an aquaponics system may be represented by the main reservoir (a dam for aquatic species), the bio-filter (micro-biota habitat) and the grow-bed(s) (plant produce cultivation). Circulating pumps, filters and water aeration maintain a viable environment. Thermal modelling of complex dynamic systems also containing an active biological component is potentially computationally complex, as [10] opines. Consideration of [11] suggests some applicable approaches to quantifying thermal supplementation, and draws attention to the requirement for a uniform temperature distribution in the main reservoir. Of further note is the impact of optimizing main reservoir temperature in order to maximize fish growth, as [12] have detailed for a range of temperatures. Maximized fish growth throughout the year is considered desirable, and impacts the choice of supplementation strategy, if so implemented. An electronic monitoring system is a requirement to enable evaluation of the results, where relevant system temperature data may be logged to Google Sheets. Local monitoring of the data may be achieved via Bluetooth to a generic Android device serial terminal application.

3. Quantifying Sub-system Thermal Contributions

Describing an aquaponics system in terms of the sub-system thermal contribution is advantageous, and has the benefit of potentially identifying areas for optimizing thermal loss mitigation. The various components are typically physically separate and exposed to varying energy exchange to the ambient surround, requiring mention of some relevant criteria to the simplified supplementation design process: Water exchange flow rate between the main reservoir and bio-filter component is typically high, up to one third of the main reservoir volume per hour is desirable. Furthermore, the bio-filter volume required for sufficient ammonia compound breakdown is small in comparison with the main reservoir [1]. Presuming nominal close proximity of these components, therefore, implies a small temperature difference. The assumption that the main reservoir temperature may be utilized as a system temperature base calculation reference is thus justified. As Figure 1 illustrates, there are many points of temperature monitoring interest in a basic aquaponic system. The figure describes the supplemented layout as presented by [13] and lists temperature measurement points for water entry- and exit used to describe the mass-flow energy transfer of each water flow loop.

Figure 1 - Example Aquaponics System Flow Loops, Illustrating Potential Temperature Measurement Points, Reproduced from [13].

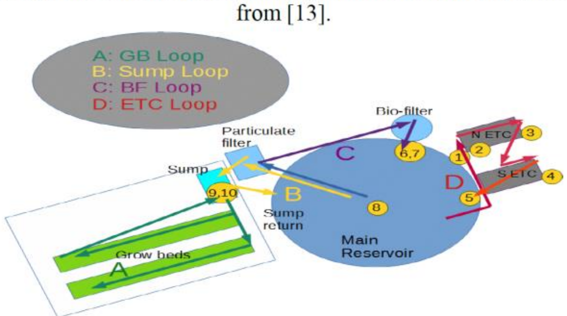

Simply summarised, the main aquatic reservoir temperature is the sum of its' ambient exchange (i.e. convective, evaporative and radiant losses and gains), and the contributions of each returning water flow loop in terms of power transferred (i.e. energy change). This may be expressed as follows:

$$P_{main} = P_{atm} + P_{bioftr} + P_{sumpret} + P_{suppl} \qquad (1)$$

Where:

- *Pmain* = total power change of the main aquaponic reservoir;
- *Patm* = the main reservoir thermal exchange to ambient surround;
- *Pbioftr* = the bio-filter mass-flow loop power contribution;

ISSN: 2237-0722
Vol. 11 No. 4 (2021)
Received: 14.06.2021 – Accepted: 16.07.2021

- *Psumpret* = the sump return mass-flow loop power contribution; and
- *Psuppl* = the supplementation return mass-flow loop power contribution (note that this term may not necessarily be a 'flow' return, but is still a kWh contribution from any other source).

These are stated in terms of kWh energy gains or losses: as grid-supplied power is sold in kWh units, this is a readily interpreted reference. Recall that in terms of S.I. unit equivalence, 1 kWh equates to 3.6 MJ. As the main aquaponic reservoir is used as the basis for calculation reference, it is also desirable to state the total power contributions in terms of its temperature change, and vice versa:

$$Power\ loss = \frac{cp*T*m}{t}\ \text{Wh} \qquad (2)$$

Where:

- cp = the specific heat of water and is assumed to be 4.184 J.K^{-1}.g^{-1};
- T = represents a measured temperature difference in degrees Celsius or Kelvin;
- m = the main reservoir water mass in kg; and
- t = time.

The preceding section suggests that a simplified approach to initial sizing of the required supplementation would be as follows:

- Step 1: Determine the volume of water in the main reservoir (this may generally be readily obtained for manmade structures, typically applying basic mathematical equations). The water mass may be assumed to be 1 litre = 1 kilogram, and fulfils the term '*m*' in equation (2);
- Step 2: For existing aquaponics systems, gather some historical site reservoir temperature data, specific to the site reservoir and active system as incorporating the grow beds and bio-filter, as outlined below. This satisfies the term '*T*' in equation (2). Note that this value comprises by implication the sum of '*Patm', 'Pbioftr' and 'Psumpret'* in equation (1). For retrofit purposes, gather the same data for the intended main reservoir, representing only '*Patm'* in equation (1). This preparatory data may be gathered manually with a thermometer(s);
- Step 3: Apply a suitable required daily temperature gain in terms of the reservoir water mass, using equation (2), to determine the minimum required power input in kWh. Note that 'daily' by implication satisfies the term '*t'* in equation (2). This required temperature gain is further detailed in the next section discussing 'positive recovery slope' and 'temperature buffer'. If the application is a retrofit aquaponics implementation (implementing a new aquaponics system to an existing dam structure), the terms '*Pbioftr*' and '*Psumpret*' from equation (1)

ISSN: 2237-0722
Vol. 11 No. 4 (2021)
Received: 14.06.2021 – Accepted: 16.07.2021

will not be known. These may, by estimation, be compensated for if data from a similar grow-bed in the area is available. Data for the study site in the Bloemfontein area, listed in a later section, shows the dynamic thermal contribution for its' specific construction, size, orientation, flow rate and system configuration; and

- Step 4: Implement a monitoring system to enable evaluation and verification of the results.

The site temperature data so gathered should include the maximum day-to-day temperature drop, which should coincide with minimum insolation (i.e. the winter solstice, which is 21/22 June in the southern hemisphere), where possible. Measurements should be taken daily, at a set time coinciding with the commencement of insolation at the site (i.e. temperature rise- or harvestable sunshine early in the morning). Of direct consideration is the average day-to-day temperature drop as determined by this datum set, around the previously identified 'critical' bio-filter temperature-limit of 7˚C. A multi-year collation of site-specific temperature maxima and -minima is also desirable at this stage, as differentiation between averaged daily expected winter minimum temperatures, and extreme cold events is of import. Such extreme events might be better accommodated by additional electrical supplementation, or other mitigation strategies. Determination of a suitable method for supplementation may now be made, with criteria such as cost, implementation constraints, predicted system life, predicted yield income, maintenance, etc.

It should be noted that choosing an ETC supplementation approach may mean long term savings gained at the cost of flexibility in coping with extreme temperatures. This does not preclude additional electrical supplementation, with no implied running costs otherwise. The recent study by [13] into thermal supplementation of an existing aquaponics system in the Bloemfontein area in South Africa serves as example of such historical temperature data, gathered for a 42 kl main reservoir active aquaponic system. Their maximum site-specific historical day-on-day loss was 0.97˚C, while their average historical loss slope around the bio-filter temperature-limit of 7˚C was ≈ 0.25˚C per day. These inform further discussion around a supplementation determination:

It is desirable to exceed the average daily loss slope as determined by the gathered historical data, as the system needs a positive temperature recovery slope to regain temperature, not just maintain it. This average daily loss slope is the average day-on-day main reservoir temperature loss around the 7˚C critical main reservoir temperature, as experienced during cold weather. The magnitude of the recovery slope is informed by the maximum day-on-day temperature loss observed, and considering long term collated temperature data for the site area, of which [14] is a common source. Examining such site-specific long-term data, [13] noted that a temperature buffer of 3˚C would be suitable for their study. This buffer represents the amount of degrees Celsius by which the main reservoir temperature

ISSN: 2237-0722
Vol. 11 No. 4 (2021)
Received: 14.06.2021 – Accepted: 16.07.2021

would drop during a passing cold front, and thus the required temperature rise (buffer) above the 7°C minimum main reservoir temperature. To summarise: the magnitude of the temperature buffer relates to the positive recovery slope in that the daily temperature rise required should re-establish the identified temperature buffer within the identified inter-cold front time period.

Having thus determined the required daily system thermal supplementation requirement, realizing supplementation presents the choice of implementation methodology. In their site-specific study, [13] determined that supplementation was possibly needful over about a two-and-a-half month period; thus their potential total energy required approximates ~1830.45 kWh. In South Africa, electrical grid energy is supplied at different rates. The 1830 kWh may imply roughly a R2 (or 0.13 $ at an exchange rate of R15/1 $) cost per kWh unit or in excess of R3600 (240 $) supplementation cost for the winter period only. Consider that the temperature may be required to be optimal for species growth maximization throughout the year, thus extending the required supplementation period and costs. The implemented supplementation choice for the [13] study thus becomes clear – ETC systems are installed for long-life low-maintenance, with once-off installation cost and low running costs (a small sub-kW pump, for example), while grid-supplied energy costs are high and continue rising. The intended lifetime of the aquaponics implementation should be considered, as the initial installation costs will be amortized through the planned lifetime.

It must also be noted that if implementing ETC supplementation, then the site-specific insolation for the period of temperature buffer establishment becomes relevant. Such may be evident when local historic weather data are collated for any planned aquaponics system implementation, when evaluating for similar climate locations.

In the system implemented by [13] the ETC flow was directly returned to the main aquaponic reservoir. With some prior preparation, such a supplementation system may be set up in a matter of days, including a suitable control system. In Figure 1, this is indicated by the red 'ETC Loop' section (two sets of 40 ETC tubes, a pump and electronic monitoring and control).

4. Benefit of Implementing a Monitoring System

Having discussed the simplified design process above, it is now necessary to address the benefit of implementing electronic monitoring of the system. Strictly speaking, any supplementation towards system viability, regardless of choice of source energy, only needs to cater for the identified 'buffer' temperature value and 'positive recovery slope' as previously discussed. If grid electric energy is used, it need only be used until the main reservoir temperature reaches the minimum predetermined value of

ISSN: 2237-0722
Vol. 11 No. 4 (2021)
Received: 14.06.2021 – Accepted: 16.07.2021

7˚C plus the chosen buffer temperature, and then to maintain it sporadically. If ETC- or PV-derived energy is used, there is no additional direct cost involved in raising the temperature even further. In order to interpret the system energy interaction a continuous monitoring scheme needs to be implemented. Such data would typically be derived from monitoring the various loop-flow energy contributions, with functional flow loops as illustrated in Figure 1. Determining water flow return energy transfer necessitates differential temperature- and flow rate determination of each flow component (e.g. Figure 1, loops B, C and D). The study by [13] further examines this energy transfer determination.

An example of such temperature measurements are shown in Figure 2, for the period 16 July 2020 to 27 July 2020. This illustrates both the daily dynamic nature of the reservoir change (serving as illustration of the importance of consistently measuring a reservoir under investigation at a specific hour), and the temperature recovery slope (5.75˚C to 8.81˚C, over an eleven-day period) of 0.278˚C per day. Note the orange trend-line (for SHT21 Temp) indicating the ambient measured temperature trend, and the blue trend line (for Dam Temp) graphically indicating the system main reservoir temperature recovery slope.

Figure 2. Graphic representation of atmospheric and main reservoir temperatures for the period 16 - 27 July 2020

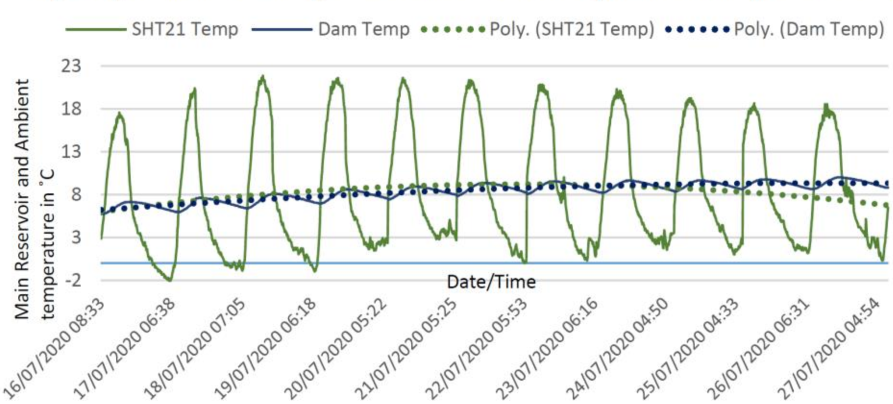

This corresponds very well with the identified recovery slope/buffer temperature criteria previously discussed. Of specific note is that the initial 5.75˚C minimum temperature of the graph is below the identified 7˚C minimum system requirement. Table 1 lists site-specific ambient temperatures for the Bloemfontein district, as obtained from [14]. It illustrates the unusual severity and extended duration of a cold front event. An explanation for this highlights the previous discussion regarding the requirement for a multi-year collated temperature history for the specific site location. The 2020 winter season in Bloemfontein was particularly severe, with below average night-time temperatures, and multiple extended 'extreme' cold weather events [15, 16]. These are typically characterized in Bloemfontein by the passing of a 'cold front' (cold Antarctic weather systems moving across the southern tip of Africa). The datum subset selected and presented was specifically chosen to highlight and show this 'worst-case' scenario. Both the temperature recovery slope and the temperature buffer establishment time are as intended by the design method, and indicates that the system recovery behaviour matches the supplementation criteria established. The chosen buffer establishment, extrapolating from the period-specific 0.278˚C per day temperature recovery slope, would take approximately another 4.3 days (15.3 days total).

Table 1 - Site Temperature Data for the Period 14-27 July 2020, as obtained from (AccuWeather)

	14th	**15th**	**16th**	**17th**	**18th**	**19th**	**20th**	**21st**	**22nd**	**23rd**	**24th**	**25th**	**26th**	**27th**
Max ℃	9	15	21	23	23	24	23	22	22	21	20	19	19	19
Min ℃	-6	-9	-10	-9	-7	-7	-6	-6	-6	-6	-6	-5	-5	-3

The further benefit of a monitoring system that reports loop differential temperatures may be seen by examining Figure 3, which depicts the cumulative power change in the main reservoir (in terms of the previously established nomenclature, the energy change with 1 kWh = 3.6 MJ) and loop contributions, for the period 16 to 27 July 2020. Note the black trend line indicating the system temperature recovery slope expressed as a kWh value and MJ value. In Figure 3, which corresponds to the time period in Figure 2, the relative power change (energy change) of the main reservoir and sub-system contributions were shown. Figure 3 depicts a relative cumulative contribution over the period, i.e. starts from a common reference point (0 kWh or 0 MJ). The benefit of this representation immediately becomes clear, as the dynamic weather-dependent energy cost of each sub-system is readily apparent. It allows direct comparison to grid energy purchase costs, and has some further notable implications:

- The grid-cost equivalent allows comparison of potential solutions;
- The dynamic mass-flow evaluation of system improvements or changes allow immediate evaluation;
- The grid-cost depiction allows for visual insight into the potential benefit of system changes (referring to Figures 1 and 3: physically relocating the bio-filter into the grow-bed enclosure would yield immediate benefits: the grow bed thermal solar absorption (the main reservoir kWh energy input via the sump return flow, Figure 3) yields generally positive net daily benefit. The exposed bio-filter loss over the depicted period is ~75kWh);

ISSN: 2237-0722
Vol. 11 No. 4 (2021)
Received: 14.06.2021 – Accepted: 16.07.2021

- Referring to equation (1) and comparing it to Figure 3, the relationship between the various sub-systems and main system temperature is readily understood;
- The method is applicable to various system layouts and types;
- The sub-system analysis via mass-flow power transfer is readily scalable to multi-loop systems; and
- The representation allows visual appreciation of sub-system energy cost contribution and informed decision regarding system energy cost decisions in terms of grid energy cost.

Figure 3 - Graphic Depiction of System Thermal Interaction Represented in Terms of kWh and MJ

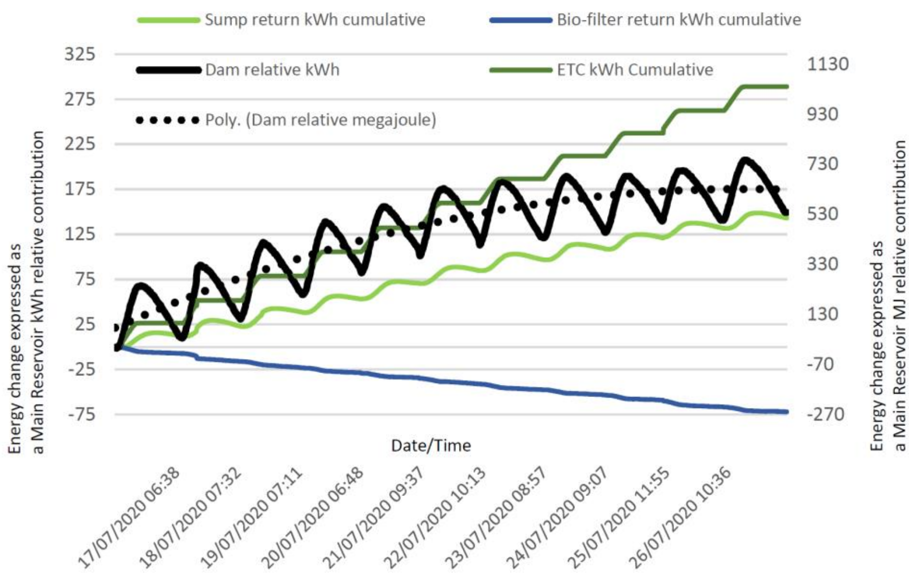

The enclosed grow-bed in the system under investigation [13] acts as a thermal 'battery' during extreme cold weather events, with a net positive influence on the main reservoir, as returned through the sump-return flow. This effect is visually apparent through representation such as in Figure 3, and may only be readily quantified with an electronic monitoring system in place. Note that the grow bed enclosure(s) may differ in size, height, construction, orientation, placement, water flow and surrounding area influence – this will of necessity be a method yielding growing success as more systems are detailed in literature and/or monitored electronically. This would enable increasingly accurate corrective factors for the retrofitted implementation of aquaponics systems to the dams on small holdings in the Bloemfontein area.

The method used to determine a suitable supplementation value is suited to implementation with existing aquaponics systems, and may be used in other topologies such as multiple-loop grow beds. Note that as system topology changes, inherently dynamic sub-system energy transfer to the main reservoir will also proportionally change. This illustrates the importance of implementing an electronic monitoring system, in order to determine the magnitude of these sub-system thermal effects vis-à-vis their mass-flow power-transfer to the main aquaponic reservoir. The implementation of such a monitoring system, with real time online data, promotes the potential adoption into the idea of 'Sustainable Smart Cities'. The studies by [17, 18] further inform the benefit of cloud-based real-time sensor data and IoT aquaponic systems monitoring.

5. Conclusion

The purpose of this paper was to present a simplified baseline approach for determining thermal supplementation for establishing sustainability of a medium sized aquaponics system. The results represented in Figure 2 indicate the expected system thermal recovery and establishment of the temperature buffer. A similar result can be expected when implementing a simple temperature-based supplementation switching scheme (i.e. on/off on-demand based on a thermostat in the main reservoir) or using an ETC supplementation scheme, with, for instance, a simple daylight-switch for supplementation activation.

In order to further refine results and gain insight into the sub-system thermal contribution, via the water-loop mass-flow energy transfer method, an electronic monitoring system is indicated, enabling examination of the results as in Figure 3. The dynamic nature of the sub-system thermal response does not otherwise readily lend itself to manual non-automated measurements.

During winters exhibiting climate such as in the Bloemfontein area, the method described is expected to yield reliable supplementation results in terms of the system biological integrity and avoidance of species mortality. In areas experiencing similar climate challenges, and using the method described as a baseline approach, positive results may be expected. Furthermore, implementing a detailed monitoring system as outlined, targeted system improvements may be made based on the detailed depiction of thermal cost expressed in the same manner as grid energy cost (i.e. kWh grid energy procurement).

Choosing to adopt a similar solar ETC supplementation method results in long-term cost savings and inherently avoids reliance on grid power consistency, at the cost of flexibility in dealing with extreme cold events. However, additional electrical supplementation is certainly readily achievable, in order to assure continued bio-filter micro-biota sustainability. The lure of an increased grow season and improved yield is expected to appeal to commercially minded potential adopters of aquaponics.

Acknowledgements

Of special note is the financial contribution of the Central University of Technology, towards both the physical installation of the system and student fees, and the Centre for Sustainable Smart Cities, Department of Electrical-, Electronics- and Computer Engineering.

References

S. Goddek, B. Delaide, U. Mankasingh, K.V. Ragnarsdottir, H. Jijakli, & R. Thorarinsdottir. *Challenges of Sustainable and Commercial Aquaponics. Sustainability 7,* 4, (2015), 4199–4224.

"IPCC, 2019: Summary for Policymakers — Special Report on Climate Change and Land." IPCC, 2019.

Y.A. Phillis, N. Chairetis, E. Grigoroudis, F.D. Kanellos and V.S. Kouikoglou. Climate Security Assessment of Countries. *Climatic Change 148,* 1, (2018), 25 - 43.

G. Proksch, A. Ianchenko, and B. Kotzen. *In Aquaponics Food Production Systems: Combined Aquaculture and Hydroponic Production Technologies for the Future,* Edited S. Goddek, A. Joyce, B. Kotzen, G.M. Burnell, Cham: Springer International Publishing (2019), 523–58.

B.C. Walraven. *Aquaponics: Economics and social potential for sustainable food production,* Senior Honors Projects, James Madison University, Harrisonburg, Virginia, (2014).

A. Assisi, R. Banzi, C. Buonocore, F. Capasso, V. Di Muzio, F. Michelacci, D. Renzo, G. Tafuri, F. Trotta, M. Vitocolonna and S. Garattini. Fish Oil and Mental Health: The Role of n-3 Long-Chain Polyunsaturated Fatty Acids in Cognitive Development and Neurological Disorders. *International Clinical Psychopharmacology 21,* 6, (2006), 319–336.

M.C.M. Beveridge, S.H. Thilsted, M.J. Phillips, M. Metian, M. Troell, and S. J. Hall. Meeting the Food and Nutrition Needs of the Poor: The Role of Fish and the Opportunities and Challenges Emerging from the Rise of Aquaculturea. *Journal of Fish Biology 83,* 4 (2013), 1067–84.

H. Sugita, H. Nakamura, and T. Shimada. Microbial Communities Associated with Filter Materials in Recirculating Aquaculture Systems of Freshwater Fish. *Aquaculture 243,* 1, (2005), pp. 403–9.

D. Karimanzira, and T. Rauschenbach. Optimal Utilization of Renewable Energy in Aquaponic Systems. *Energy and Power Engineering 10,* 6, (2018), 279–300.

W.R. Cannon. Concepts, Challenges, and Successes in Modeling Thermodynamics of Metabolism. *Frontiers in Bioengineering and Biotechnology 2* (2014).

C.M. Close, D.K. Frederick, and J.C. Newell. *Modeling and Analysis of Dynamic Systems.* 3rd ed. New York, NY: Wiley (2002).

A. Clarke and N.M. Johnston. Scaling of Metabolic Rate with Body Mass and Temperature in Teleost Fish. *Journal of Animal Ecology 68,* 5 (1999), pp. 893–905.

C.A. van Beukering, P. Hertzog, and A. Swart. Investigating Thermal Supplementation of an Aquaponics System under Severe Climate Conditions. *World Journal of Engineering ahead-of-print* (January 25, 2021).

AccuWeather. https://www.accuweather.com/

"3 Cold Fronts to Hit South Africa - Lesotho to See Heaviest Snowfall of All - AfriWX." 2021. https://weatherblog.co.za/cold-front/3-cold-fronts-to-hit-south-africa-lesotho-to-see-heaviest-snowfall-of-all/.

"Mammoth Cold Front Approaches Southern Africa - Biggest in Years - AfriWX." 22, 2021. https://weatherblog.co.za/snow/mammoth-cold-front-approaches-southern-africa-biggest-in-decades/.

W. Vernandhes, N.S. Salahuddin, A. Kowanda, and Sri Poernomo Sari. Smart Aquaponic with Monitoring and Control System Based on IoT. *Proceedings of the 2017 Second International Conference on Informatics and Computing (ICIC)* (2017), Jayapura, Papua, Indonesia, pp. 1–6.

A. Alamri, W.S. Ansari, M.M. Hassan, M.S. Hossain, A. Alelaiwi, and M.A. Hossain. A Survey on Sensor-Cloud: Architecture, Applications, and Approaches. *International Journal of Distributed Sensor Networks 9,* 2, (2013), pp. 917923.

Authors

Chris Van Beukering

Pursuant of qualification MEng: Electrical: Engineering degree and currently enrolled at the Central University of Technology. He is an entrepreneur with his own embedded design and consulting business that was established in 2009, providing solutions to various industry sectors in Southern- and Central Africa.

Pierre Hertzog

Received his DTech: Electrical: Engineering degree in 2004 from the Central University of Technology. His research interests include engineering education and alternative energy. He is currently an Associate Professor at the Central University of Technology.

James Swart

James worked for Telkom SA and De Beers Namaqualand Mines for 4 years and then joined the Vaal University of Technology in 1995 and progressed from a technician to a senior lecturer in 2007. He completed a MEd in 2007 and a DTech in 2011. James loves teaching and has a keen passion for research. One of his mottos relates to life-long learning and states "Live to Learn and you will Learn to Live".

ISSN: 2237-0722
Vol. 11 No. 4 (2021)
Received: 14.06.2021 – Accepted: 16.07.2021